

# Accepted Manuscript

Novel pyrimidine-2,4-dione-1,2,3-triazole and furo[2,3-*d*]pyrimidine-2-one-1,2,3-triazole hybrids as potential anti-cancer agents: Synthesis, computational and X-ray analysis and biological evaluation

Tomislav Gregorić, Mirela Sedić, Petra Grbčić, Andrea Tomljenović Paravić, Sandra Kraljević Pavelić, Mario Cetina, Robert Vianello, Silvana Raić-Malić

PII: S0223-5234(16)30966-7

DOI: [10.1016/j.ejmech.2016.11.028](https://doi.org/10.1016/j.ejmech.2016.11.028)

Reference: EJMECH 9061

To appear in: *European Journal of Medicinal Chemistry*

Received Date: 26 July 2016

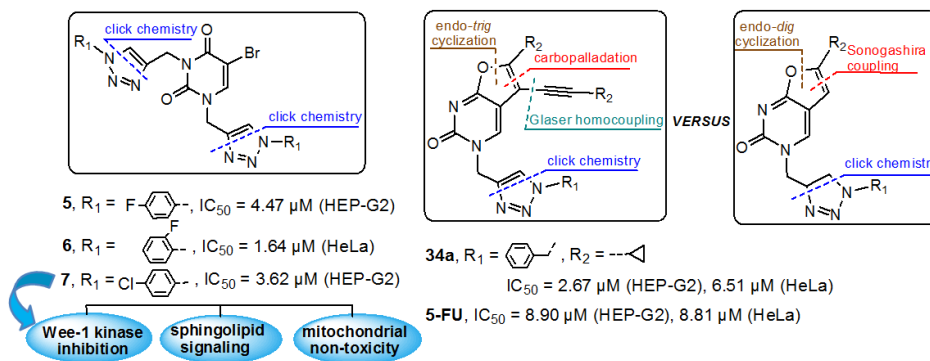
Revised Date: 10 November 2016

Accepted Date: 12 November 2016

Please cite this article as: T. Gregorić, M. Sedić, P. Grbčić, A.T. Paravić, S.K. Pavelić, M. Cetina, R. Vianello, S. Raić-Malić, Novel pyrimidine-2,4-dione-1,2,3-triazole and furo[2,3-*d*]pyrimidine-2-one-1,2,3-triazole hybrids as potential anti-cancer agents: Synthesis, computational and X-ray analysis and biological evaluation, *European Journal of Medicinal Chemistry* (2016), doi: 10.1016/j.ejmech.2016.11.028.

This is a PDF file of an unedited manuscript that has been accepted for publication. As a service to our customers we are providing this early version of the manuscript. The manuscript will undergo copyediting, typesetting, and review of the resulting proof before it is published in its final form. Please note that during the production process errors may be discovered which could affect the content, and all legal disclaimers that apply to the journal pertain.





**Novel pyrimidine-2,4-dione-1,2,3-triazole and furo[2,3-*d*]pyrimidine-2-one-1,2,3-triazole hybrids as potential anti-cancer agents: synthesis, computational and X-ray analysis and biological evaluation**

Tomislav Gregorić,<sup>a</sup> Mirela Sedić,<sup>\*bc</sup> Petra Grbčić,<sup>b</sup> Andrea Tomljenović Paravić,<sup>b</sup> Sandra Kraljević Pavelić,<sup>bc</sup> Mario Cetina,<sup>d</sup> Robert Vianello<sup>\*e</sup> and Silvana Raić-Malić<sup>\*a</sup>

<sup>a</sup> University of Zagreb, Faculty of Chemical Engineering and Technology, Department of Organic Chemistry, Marulićev trg 20, HR-10000 Zagreb, Croatia. Email: sraic@fkit.hr

<sup>b</sup> University of Rijeka, Department of Biotechnology, Radmile Matejčić 2, HR-51000 Rijeka, Croatia. Email: msedic@biotech.uniri.hr

<sup>c</sup> University of Rijeka, Centre for high-throughput technologies, Radmile Matejčić 2, HR-51000 Rijeka, Croatia

<sup>d</sup> University of Zagreb, Faculty of Textile Technology, Department of Applied Chemistry, Prilaz baruna Filipovića 28a, HR-10000 Zagreb, Croatia

<sup>e</sup> Computational Organic Chemistry and Biochemistry Group, Ruđer Bošković Institute, Bijenička 54, HR-10000 Zagreb, Croatia. Email: robert.vianello@irb.hr

**Abstract.** Regioselective 1,4-disubstituted 1,2,3-triazole tethered pyrimidine-2,4-dione derivatives (**5–23**) were successfully prepared by the copper(I)-catalyzed click chemistry. While known palladium/copper-cocatalyzed method based on Sonogashira cross-coupling followed by the intramolecular 5-*endo*-dig ring closure generated novel 6-alkylfuro[2,3-*d*]pyrimidine-2-one-1,2,3-triazole hybrids (**24b–37b**), a small library of their 5-alkylethynyl analogs (**24a–37a**) was synthesized and described for the first time by tandem terminal alkyne dimerization and subsequent 5-*endo*-trig cyclization, which was additionally corroborated with computational and X-ray crystal structure analysis. The nature of substituents on alkynes and thereof homocoupled 1,3-diynes predominantly influenced the ratio of the formed products in both pathways. *In vitro* antiproliferative activity of prepared compounds evaluated on five human cancer cell lines revealed that *N,N*-1,3-bis-(1,2,3-triazole)-5-bromouracil (**5–7**) and 5,6-disubstituted furo[2,3-*d*]pyrimidine-2-one-1,2,3-triazole **34a** hybrids exhibited the most pronounced cytostatic activities against hepatocellular carcinoma (HepG2) and cervical carcinoma (HeLa) cells with higher potencies than the reference drug 5-fluorouracil. Cytostatic effect of pyrimidine-2,4-dione-1,2,3-triazole hybrid **7** in HepG2 cells could be attributed to the Wee-1 kinase inhibition and abolishment of sphingolipid signaling mediated by acid ceramidase and sphingosine kinase 1. Importantly, this compound proved to be a non-mitochondrial toxicant, which makes it a promising candidate for further lead optimization and development of a new and more efficient agent for the treatment of hepatocellular carcinoma.

**Keywords:** furo[2,3-*d*]pyrimidine-2-one; 5-*endo*-trig cyclization; computational chemistry; X-ray analysis; sphingolipid signaling; Wee-1 kinase

## 1. Introduction

Cancer is a multifaceted disease that represents one of the leading causes of mortality in developed countries. One in eight deaths worldwide is due to cancer, and it is the second most common cause of death exceeded only by heart diseases [1]. In spite of continuous advancements in treatment and prevention strategies, the successful treatment of cancer, in particular metastases, still remains a challenge. Discovery of new and safer anticancer agents with improved cytotoxicity in cancer cells will improve the management of cancer [2].

Molecular hybridization, which covalently combines two or more drug pharmacophores into a single molecule, proved to be an effective tool for designing novel entities as potent antitumor agents [3]. Thus, the pyrimidine moiety, as one of the most prominent structures found in nucleic acid chemistry, is a component of a number of useful drugs and is associated with many biological, pharmaceutical and therapeutic activities [4]. Modified pyrimidine nucleosides were among the first chemotherapeutic agents introduced into the medical treatment of cancer [5]. Furthermore, the fusion of pyrimidine moiety with different heterocycle scaffolds gives rise to a new class of hybrid heterocycles exerting improved biological activity [3]. Various five-membered heteroaromatic ring-fused pyrimidines, furopyrimidines in particular, were studied and found to possess remarkable pharmacological properties [6]. Moreover, some 4,5,6-trisubstituted furo[2,3-*d*]pyrimidin-4-amines were discovered as non-receptor tyrosine kinase ACK1 (activated Cdc42-associated tyrosine kinase 1) inhibitors [7], while 4,5-disubstituted furo[2,3-*d*]pyrimidine was potent receptor tyrosine kinase c-Met inhibitor [8]. We found that among bicyclic furo[2,3-*d*]pyrimidine series, 6-butyl- and 6-*p*-bromophenylfuro[2,3-*d*]pyrimidines showed the highest cytostatic activity, particularly in malignant leukemia (L1210) and T-lymphocyte (Molt4/C8 and CEM) cells [9]. Previous studies also demonstrated that some pyrimidine [10] and heteroaromatic ring fused-pyrimidine [11] derivatives have the ability to inhibit key metabolic enzymes that regulate intracellular levels of tumor-suppressor lipids ceramide and sphingosine, which elicit antiproliferative and apoptotic responses in various cancer cells. The same compounds were also shown to interfere with the metabolism of pro-survival lipid sphingosine-1-phosphate (S1P), whose major role is to regulate proliferation, inflammation, angiogenesis and resistance to apoptotic cell death. In addition, clinically approved drug imatinib, *N*-(5-amino-2-methylphenyl)-4-(3-pyridyl)-2-

pyrimidineamine, down-regulates the activity of sphingosine kinase 1 (SK1), an enzyme that catalyzes the phosphorylation of sphingosine to S1P in imatinib-sensitive chronic myeloid leukemia cells, which precedes the onset of apoptosis [12]. Furthermore, the antineoplastic drug carmofur, as the representative of the *N*-acyclic 5-fluorouracil class, was shown to be a potent inhibitor of acid ceramidase (ASAH), an enzyme that catalyzes the lysosomal degradation of ceramide, which contributes to the antiproliferative effects of carmofur [13].

Despite the biological importance of furopyrimidine derivatives, the synthetic methodology used for the *O*-heteroannulation process is limited. Therefore, the need persists for more versatile and efficient procedure. Palladium-catalyzed annulation of functionalized aryl halides and alkynes is the most common method to access a wide variety of carbo- and hetero-cycles [14]. Instead of using copper, application of other catalysts, such as AgNO<sub>3</sub>, Zn(Cl)<sub>2</sub> or Zn<sub>4</sub>(OCOFCF<sub>3</sub>)<sub>6</sub>O cluster, also enabled the cyclization of alkynylated nucleosides to furopyrimidines [15]. Moreover, having in mind the development of environmentally friendly synthetic tools, one-pot protocol to directly access various furopyrimidines under the aqueous conditions with low catalyst loading was applied [16]. In the last decade, 1,2,3-triazole and its derivatives have attracted a great deal of interest due to their synthetic accessibility by click chemistry and wide application in drug discovery, particularly in the early discovery phase and the lead optimization processes [17]. The favorable features of 1,2,3-triazole ring, such as moderate dipole character, hydrogen bonding capability, rigidity and stability under *in vivo* conditions, are clearly responsible for their enhanced biological activities [18]. Moreover, the incorporation of 1,2,3-triazoles between two pharmacophores to give bifunctional drugs is increasingly becoming useful and important in constructing bioactive molecules [19]. Thus, it was found that some 1,2,3-triazole tethered pyrimidine nucleosides [20], 1,2,3-triazole pyrimidine nucleoside conjugates with the 1,2,3-triazole as a substituent at either the pyrimidine ring [21], sugar moiety [22] or sugar mimic [23] were endowed with pronounced cytostatic activity. Taking into consideration the aforementioned data and in continuation of our recent efforts towards the synthesis of 1,2,3-triazole-appended *N*-heterocycle pharmacophores [24], we envisaged that pyrimidine, furo[2,3-*d*]pyrimidine and 1,2,3-triazole pharmacophores, if linked together, would generate novel molecular entities which are likely to exhibit promising biological properties. To the best of our knowledge, this is the first report on

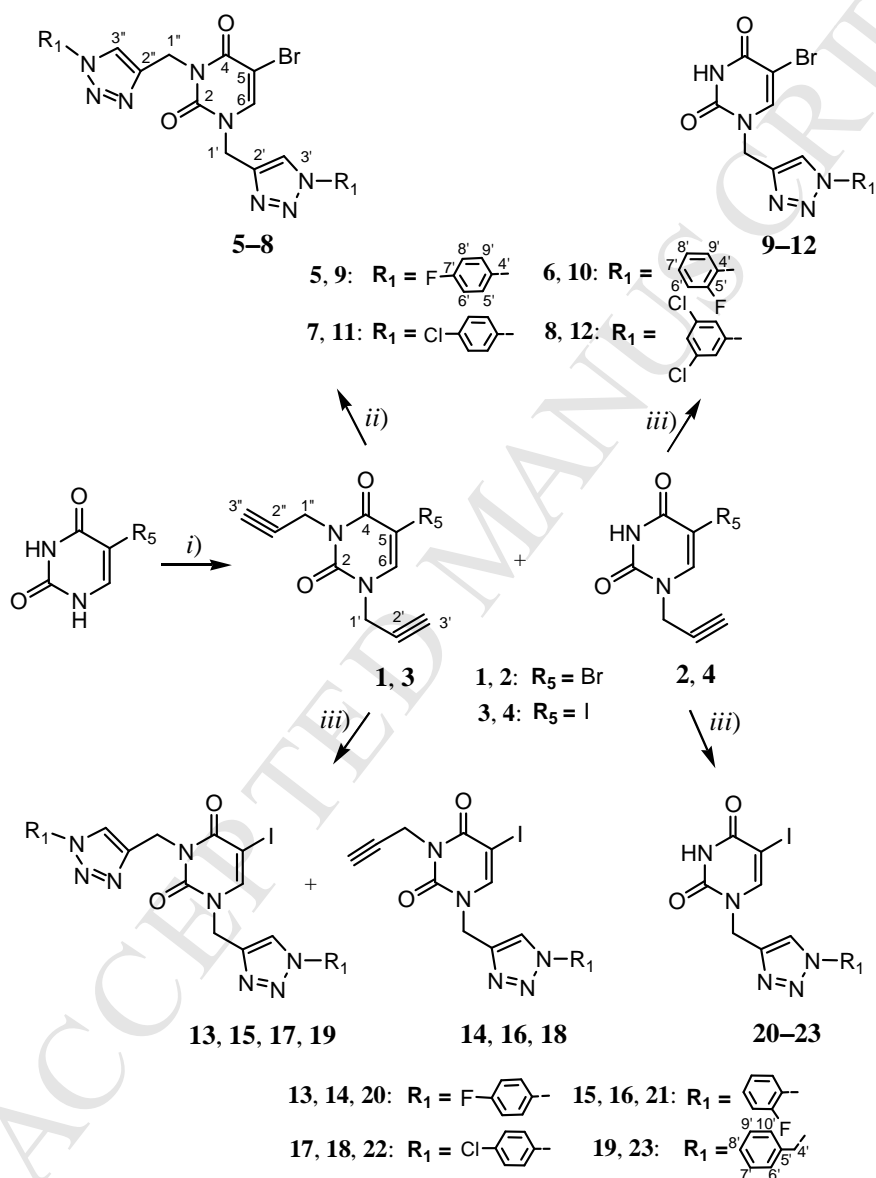
1,2,3-triazole-appended furo[2,3-*d*]pyrimidines. Although the synthetic method to provide 6-substituted furo[2,3-*d*]pyrimidines is well-documented [9,14a,b], the synthesis of their 5-alkylethynyl analogs is still elusive. Herein, we describe for the first time synthetic methodology that enables an access to the construction of furo[2,3-*d*]pyrimidine-2-one (**24a–37a**) with 5-alkylethynyl-6-alkyl substituents through palladium/copper-cocatalyzed symmetrical diyne formation and 5-*endo*-trig cyclization sequence. Precise reaction mechanisms leading to both sets of compounds were rationalized with the aid of computational chemistry methods at the DFT level with implicit solvation. Moreover, the apoptosis induction and mitochondrial toxicity were analyzed for the selected 1,2,3-triazole–pyrimidine hybrids. Additional biological studies were carried out to investigate their inhibitory effects on cell proliferation, growth and survival mechanisms governed by sphingolipid metabolic enzymes acid ceramidase (ASAH) and sphingosine kinase 1 (SK1), as well as those mediated by the cell cycle regulatory enzyme Wee-1 tyrosine kinase which controls the G2 checkpoint in response to DNA damage.

## 2. Results and discussion

### 2.1. Chemistry

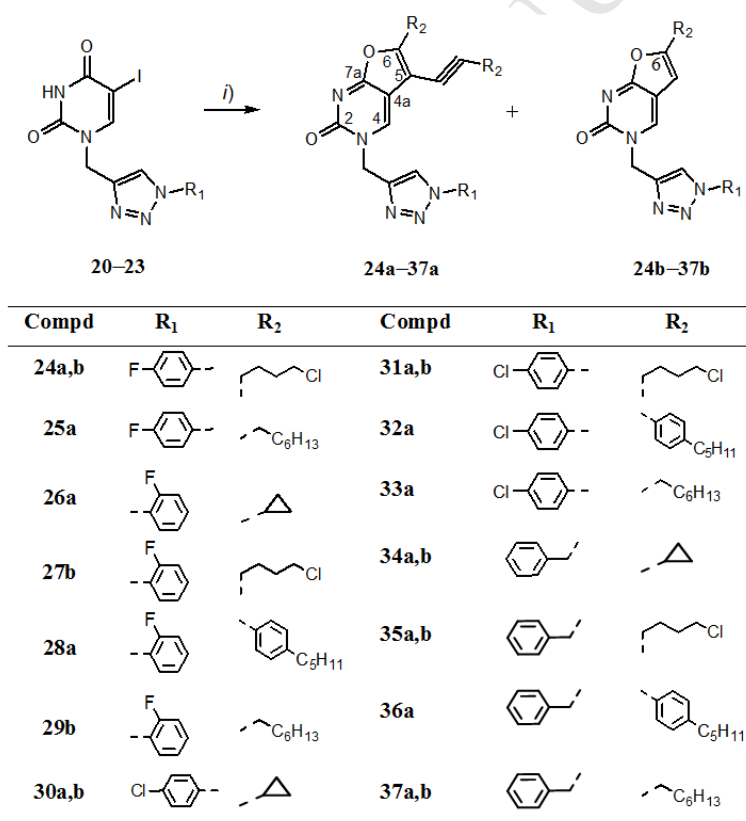
*N*-Propargylation of 5-bromo- and 5-iodouracil with propargyl bromide and sodium hydride gave a mixture of *N,N*-1,3-disubstituted (**1** and **3**) and *N*-1-substituted (**2** and **4**) prop-2-ynyl uracil derivatives (Scheme 1). *N,N*-1,3-Disubstituted (**5–8**) and *N*-1-monosubstituted (**9–12**) 1,2,3-triazole derivatives of 5-bromouracil were subsequently prepared by copper(I)-catalyzed Huisgen 1,3-dipolar cycloaddition reaction of terminal alkyne with corresponding azide (Scheme 1). The synthesis of *N,N*-1,3-disubstituted 1,2,3-triazole–5-bromouracil hybrids (**5–8**) was performed using copper(II) sulfate, sodium ascorbate as a reducing agent, and various azides, including *p*-flouropheryl, *o*-flouropheryl, *p*-chlorophenyl and 3,5-dichlorophenyl azide, in the yield ranging from 30–58%. The 1,3-dipolar cycloaddition of *N*-1-propargyl 5-bromouracil derivative (**2**) and aromatic azides was carried out using copper(II) sulfate and metallic copper as a reducing agent under the microwave irradiation to give *N*-1-monosubstituted 1,2,3-triazole–5-bromouracil hybrids (**9–12**) in higher yield (75–84%) relative to their *N,N*-1,3-disubstituted analogs. Click reaction of 5-iodo-*N,N*-1,3-di(prop-2-ynyl)pyrimidine-2,4-dione (**3**) and aromatic azides afforded *N,N*-1,3-

disubstituted 1,2,3-triazole-5-iodouracil hybrids (**13**, **15**, **17** and **19**) and *N*-1-(1,2,3-triazole)-substituted uracils (**14**, **16** and **18**) bearing prop-2-ynyl side chain at *N*-3 of the uracil ring, as minor products. Reaction of *N*-1-propargyl 5-iodouracil (**4**) with aromatic azides gave 1,2,3-triazole-5-iodouracil hybrids (**20–23**) (Scheme 1).



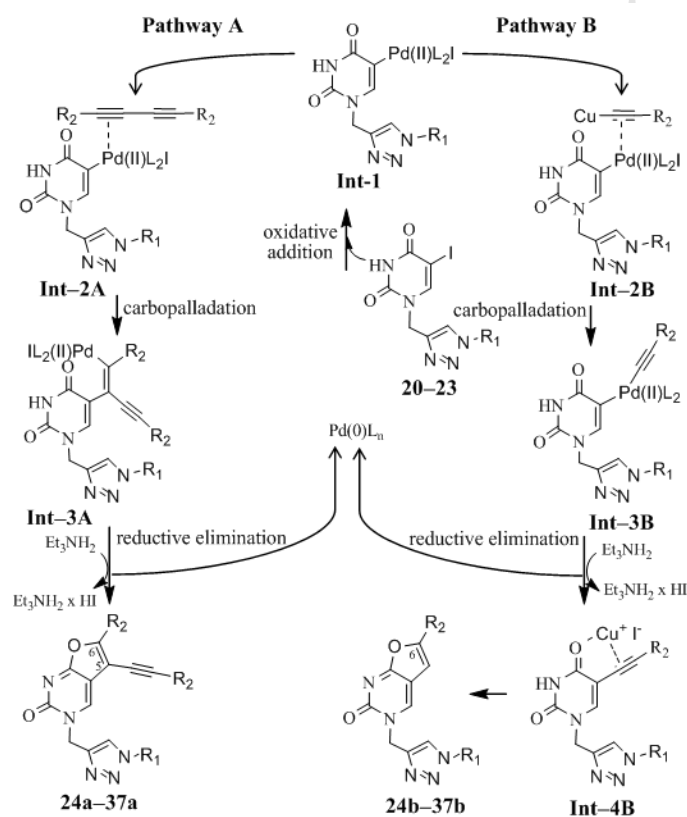
**Scheme 1.** Reagents and conditions: (i) propargyl bromide, NaH, DMF, Ar atmosphere, r.t., 24 h; (ii) azide, sodium ascorbate,  $\text{CuSO}_4 \times 5 \text{H}_2\text{O}$ , DMF, r.t., 24 h. (iii) azide, Cu, 1M  $\text{CuSO}_4$  solution, *tert*-butanol :  $\text{H}_2\text{O} = 1 : 1$ , MW 300 W, 80 °C, 45 min.

In connection with our previous findings on bioactive bicyclic pyrimidine nucleosides [9], we further investigated the feasibility of the terminal alkyne dimerization and subsequent transition copper-mediated intramolecular cyclization for the synthesis of the 5-alkylethynyl-6-alkylfuro[2,3-*d*]pyrimidine-2-one derivatives (Scheme 2). Therefore, the coupling of 1,2,3-triazole-5-iodouracil hybrids (**20–23**) with terminal alkynes including cyclopropylethyne, 5-chloropent-1-yne, 1-ethynyl-4-pentylbenzene and oct-1-yne and the presence of palladium catalyst tetrakis(triphenylphosphine)palladium(0) [Pd(PPh<sub>3</sub>)<sub>4</sub>], *N,N*-diisopropylethylamine (*N,N*-DIPEA) and Cu(I) iodide as cocatalyst afforded target 5-alkylethynyl-6-alkylfuro[2,3-*d*]pyrimidine-2-one derivatives (**24a–37a**) and their 6-substituted analogs (**24b–37b**) (Scheme 2).



**Scheme 2.** Reagents and conditions: (i) corresponding terminal alkyne, CuI, (PPh<sub>3</sub>)<sub>4</sub>Pd, *N,N*-DIPEA, toluene, 80 °C, 24 h.

Generally, an excess amount of alkyne (3 equiv) and *N,N*-DIPEA base (6 equiv) in copper-cocatalyzed conditions under heating provided 5,6-disubstituted furo[2,3-*d*]pyrimidine-2-ones (**24a–37a**), as the major or sole product. The only exceptions were reactions of 4-(2-fluorophenyl)-1,2,3-triazole appended 5-iodouracil (**21**) with 5-chloroprop-1-yne and oct-1-yne, which gave only 6-substituted furo[2,3-*d*]pyrimidine-2-ones **27b** and **29b**. Possible synthetic pathways A and B for the formation of both furopyrimidine rings in **24a–37a** and **24b–37b** series from pyrimidine-2,4-dione–1,2,3-triazole hybrids **20–23** presumably started *via* oxidative addition of 5-iodouracil derivatives **20–23** to Pd(0) (**Int-1**), as depicted in Scheme 3.



**Scheme 3.** Proposed mechanism for the formation of 5,6-disubstituted **24a–37a** and 6-substituted **24b–37b** furopyrimidine–1,2,3-triazole hybrids.

The presence of Cu(I) salt is generally believed to facilitate the transfer of the alkynyl group to the Pd(II) catalyst in **Int-2B** by the *in situ* generation of copper acetylide species and the subsequent trans-metalation of this group to Pd(II) in **Int-3B**. Finally, reductive elimination of **Int-3B** gave 5-alkynyluracil derivatives, which subsequently underwent 5-*endo*-dig cyclization to afford 6-substituted furopyrimidine

series **24b–37b** by copper-promoted reaction. Several studies have already shown that in the typical Sonogashira protocol employing cocatalytic Cu(I) salts, copper increased the reaction rate, but also *in situ* generation of copper acetylides induced Glaser-type oxidative homocoupling of the terminal acetylene to yield symmetrical 1,3-diynes [25]. Therefore, instead of coordination of copper acetylide that occurred in pathway B, symmetrical head-to-head diynes can be anticipated to be involved, as an intermediate, in an alternative pathway A. Thus, coordination of the internal diyne to the metal center of the uracil palladium intermediate **Int-2A** and subsequent insertion into the uracil-Pd bond to give enyne palladium complex **Int-3A** might occur in pathway A. Next step was reductive elimination and intramolecular 5-*endo*-trig cyclization to form 5,6-disubstituted furopyrimidine series **24a–37a** and regenerate Pd(0) (Scheme 3). So far, 5-*endo*-trig cyclization has been rarely explored, due to its disfavored cyclization pattern according to Baldwin's rules [26]. Therefore, our interest was further focused on the elucidation of the proposed mechanism (Scheme 3) with the aid of computations at the DFT level.

## 2.2. Computational analysis

To examine the reaction pathways leading to the formation of target 6-substituted furo[2,3-*d*]pyrimidine-2-ones and their unexpected 5-alkylethynyl derivatives, we performed a computational analysis using the B97D DFT functional in conjunction with the 6-31+G(d) basis set for carbon, nitrogen, oxygen and hydrogen atoms and the SDD pseudopotentials for iodine and copper atoms, all immersed in the implicit SMD solvation corresponding to pure toluene. The molecules studied computationally are presented in Fig. 1.

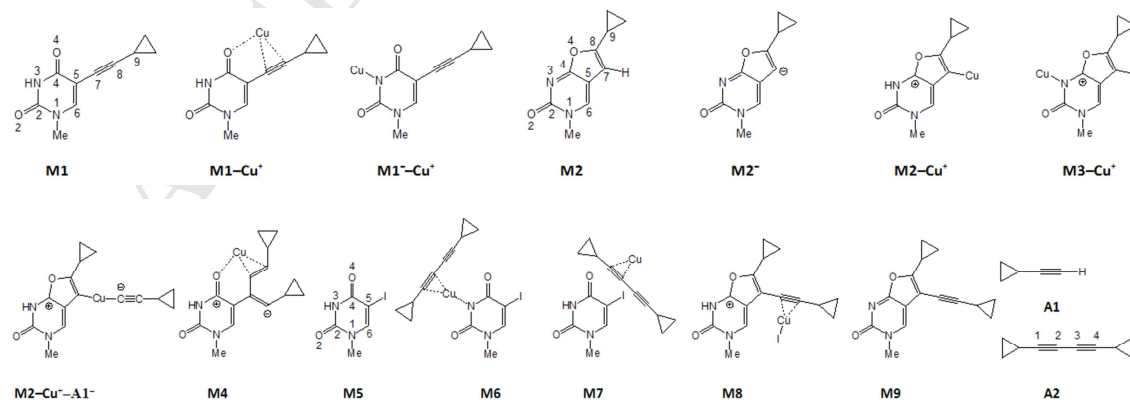


**Fig. 1.** Structure and atom numbering of relevant molecules studied computationally.

We initiated our analysis with the system **M1**, since the mechanism of its formation from the corresponding 5-iodide **M5** is known and well described in the literature [14]. **M1** is a model system for a class of compounds **Int-4B** (Scheme 3), where the substituent on the N1 atom has been truncated to the methyl group, since the length of the alkyl chain at this position does not significantly influence the kind of reactivity investigated in this work. N3–H tautomer is the most stable form of **M1** (**M1-t1**, Fig. S1, Supplementary information). Both O–H tautomers are 13.9 (**M1-t2**) and 20.8 kcal mol<sup>-1</sup> (**M1-t3**) less stable than **M1-t1**. Interestingly, a system in which N–H group tautomerizes to the C7 atom of the acetylene group, **M1-t4**, spontaneously rearranges to the target product **M2**. However, our calculations reveal the barrier to transfer a proton from **M1-t1** to **M1-t4** exceeds 160 kcal mol<sup>-1</sup> making this process highly unfavorable. Therefore, a simple tautomerization of **M1** could not rationalize the **M2** formation.

The cyclization of neutral **M1** is not feasible as during the approach of the O4 atom towards C8, the energy of the system only increases without any indication for transition states or stable intermediates. N3–H deprotonation gives **M1**<sup>-</sup>, which could undergo the mentioned cyclization to give the anionic **M2**<sup>-</sup>; however the calculated barrier for this process appears too high ( $\Delta G^\ddagger = 23.8$  kcal mol<sup>-1</sup>), while the reaction free energy of  $\Delta G_R = 23.0$  kcal mol<sup>-1</sup> is too endergonic for this reaction to be feasible. This goes along with the fact that the calculated pK<sub>a</sub> value for the necessary N3–H deprotonation in toluene assumes pK<sub>a</sub>(**M1**)<sub>N3</sub> = 59.7, being too high to occur under normal conditions. Therefore, we can conclude that the formation of the cyclic product **M2** from either **M1** or deprotonated **M1**<sup>-</sup> is very unlikely.

The presence of Cu(I) ions changes the reactivity of **M1**. Cu(I) ion most preferentially binds between the carbonyl oxygen O4 and the C7–C8 triple bond (**M1**–**Cu**<sup>+</sup>) with the corresponding Cu–O4, Cu–C7 and Cu–C8 distances of 2.114, 2.037 and 2.172 Å, respectively, and the binding free energy of  $\Delta G_{\text{BIND}} = -29.9$  kcal mol<sup>-1</sup>. The cyclization of **M1**–**Cu**<sup>+</sup> follows the mechanism depicted in Fig. 2. It requires 13.8 kcal mol<sup>-1</sup> to arrive at transition state structure characterized with one imaginary frequency of  $\nu_{\text{IMAG}} = 196i$  cm<sup>-1</sup>. During that process, Cu(I) ion moves to the other side of the acetylene bond and is predominantly bonded to C7 with the distance of 1.895 Å. This twists the angle C8–C7–C5 to 116.0° bringing the C8 atom close to O4 at 2.057 Å. Following the O4–C8 bond formation, the system relaxes to monocationic **M2**–**Cu**<sup>+</sup> with the O4–C8 and Cu–C7 bonds assuming 1.490 and 1.885 Å, respectively. The

latter bond is crucial for the stability of  $\mathbf{M2-Cu}^+$ , since the removal of the Cu(I) ion or even placing it to alternative binding positions, including N1, N3, O2, and O4 atoms, restores the system back to the acyclic form  $\mathbf{M1}$ . Interestingly, the rearrangement of  $\mathbf{M2-Cu}^+$  involving the N3 proton and the Cu(I) ions gives  $\mathbf{M3-Cu}^+$  that is by 18.3 kcal mol<sup>-1</sup> more stable than  $\mathbf{M2-Cu}^+$  (Fig. 2).

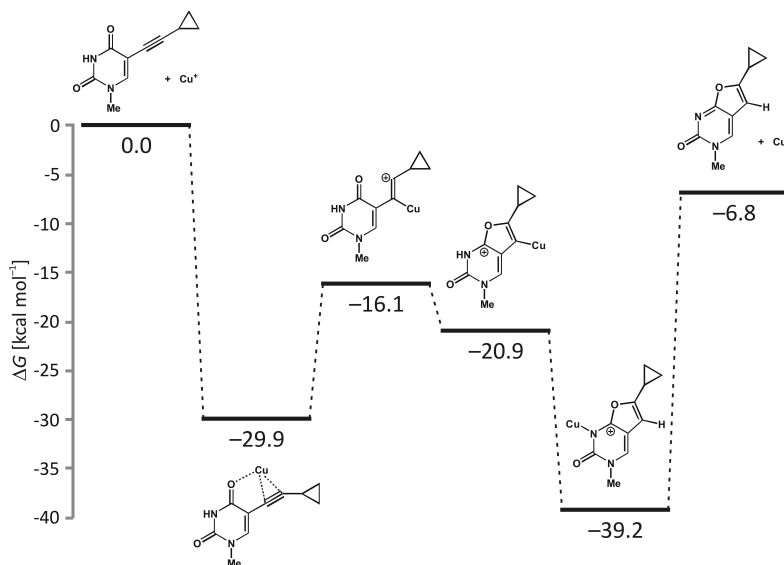


**Fig. 2.** Free energy profile for the Cu(I)-catalyzed cyclization of 5-alkylethynyl uracils towards 6-substituted furo[2,3-*d*]pyrimidine-2-ones.

This rearrangement is facilitated by the fact that the calculated  $pK_a$  value for  $\mathbf{M2-Cu}^+$  is 19.2. To put this number in the proper context, we estimated the influence of Cu(I) on  $\mathbf{A1}$  acetylene deprotonation (Fig. 1), which occurs in toluene during the Sonogashira coupling reaction.  $pK_a$  for isolated  $\mathbf{A1}$  is 77.4 clearly indicating the predominance of the unionized form. Nevertheless, following Cu(I) binding, the  $pK_a$  value drops to 19.1, which could be taken as the acidity constant corresponding to a feasible process in toluene under our reaction conditions. Therefore, the calculated  $pK_a(\mathbf{M2-Cu}^+)_{N3} = 19.2$  indicates a large amount of deprotonated  $\mathbf{M2}^- - \mathbf{Cu}^+$ , which facilitates the rearrangement to  $\mathbf{M3-Cu}^+$ , where the calculated binding free energy of Cu(I) ions is  $\Delta G_{\text{BIND}} = -32.4$  kcal mol<sup>-1</sup>. Therefore, it requires 32.4 kcal mol<sup>-1</sup> to arrive at the first type of products  $\mathbf{M2}$ , being the target 6-substituted furo[2,3-*d*]pyrimidine-2-ones. Still, the overall change in the reaction free energy is  $\Delta G_R = -6.8$  kcal mol<sup>-1</sup>, which, together with the rate limiting cyclization step associated with  $\Delta G^\ddagger = 13.8$  kcal mol<sup>-1</sup> makes this the most likely pathway.

If we consider the formation of the unexpected 5-alkylethynyl derivatives of **M2** from any stationary point on the pathway depicted in Fig. 2, the results would reveal unfeasible processes. Essentially, we would need to substitute the hydrogen atom on C7 in **M2** with another acetylide anion, which would introduce two negative charges into **M2** to give di-anionic molecule, unless the mentioned C7 hydrogen atom is abstracted as the hydride anion, which is something we did not observe. This limitation is what renders most of the investigated mechanisms highly improbable as being associated with either high barriers or unfavorable endergonicities of the overall reaction. For example, the approach of deprotonated **A1**<sup>-</sup> to the C7 atom in **M2** does not produce stable intermediates. Even positively charged **M3**-Cu<sup>+</sup>, with Cu(I) bound to the N3 site, is not electrophilic enough to bind **A1**<sup>-</sup> to the stable C7 intermediate. If we consider **M2**-Cu<sup>+</sup>, it can efficiently bind **A1**<sup>-</sup> to **M2**-Cu<sup>+</sup>-**A1**<sup>-</sup> with the binding free energy as high as  $\Delta G_{\text{BIND}} = -77.7 \text{ kcal mol}^{-1}$ . From there, it takes  $\Delta G^{\ddagger} = 28.2 \text{ kcal mol}^{-1}$  to arrive at the transition state for the C-C bond formation ( $\nu_{\text{IMAG}} = 343i \text{ cm}^{-1}$ ), which appears too high for the feasible process, on top of the fact that the reaction is both highly endergonic,  $\Delta G_{\text{R}} = 10.6 \text{ kcal mol}^{-1}$  and reverts the product back to the acyclic **M4**. The only potentially chemically feasible pathway is when one considers the acyclic **M1**<sup>-</sup>-Cu<sup>+</sup> (Fig. S2, Supplementary information), where Cu(I) is bound with  $\Delta G_{\text{BIND}} = -78.3 \text{ kcal mol}^{-1}$ . The approach of the acetylide anion **A1**<sup>-</sup> is endergonic ( $\Delta G = 5.8 \text{ kcal mol}^{-1}$ ) from which the nucleophilic attack to C7 is associated with the barrier of  $\Delta G^{\ddagger} = 20.2 \text{ kcal mol}^{-1}$  ( $\nu_{\text{IMAG}} = 267i \text{ cm}^{-1}$ ) and  $\Delta G_{\text{R}} = -4.3 \text{ kcal mol}^{-1}$ . This gives anionic intermediate, which increases the Cu<sup>+</sup> binding ( $\Delta G_{\text{BIND}} = -103.5 \text{ kcal mol}^{-1}$ ). Subsequent cyclization requires  $\Delta G^{\ddagger} = 21.8 \text{ kcal mol}^{-1}$  ( $\nu_{\text{IMAG}} = 325i \text{ cm}^{-1}$ ) producing the unexpected 5-alkylethynyl derivative with copper ion bound to N3 with  $\Delta G_{\text{BIND}} = -128.2 \text{ kcal mol}^{-1}$ . However, if one removes the Cu(I) ion from the product, it leaves a dianion (Fig. S2, Supplementary information), which is not what we observed in our experiment or spectroscopic measurements including the crystal structure analysis. In addition, the overall pathway in Fig. S2 is highly unfavorable, as the rate-limiting first step has a large total barrier ( $\Delta G^{\ddagger} = 26.0 \text{ kcal mol}^{-1}$ ) and very unfavorable endergonicity ( $\Delta G_{\text{R}} = 51.3 \text{ kcal mol}^{-1}$ ) rendering this mechanism very unlikely. Therefore, we can conclude that the unexpected 5-alkylethynyl derivatives **M9** cannot be obtained within the same pathway as the expected **M2** shown in Fig. 2.

In order to elucidate the precise mechanistic scenario that would give bicyclic 5-alkylethynyl derivatives, we must recall that Pd(0), instead of catalyzing hetero-coupling among alkyne **A1** and 5-iodouracil **M5** to give **M1**, could facilitate the homo-coupling of two **A1** molecules to yield symmetrical 1,3-diyne **A2** (Fig. 1) [27], which can, as our results will show, enter the reaction with **M5** to give target products **M9**. Still, the reaction of neutral 5-iodouracil **M5** with **A2** is feasible, but unlikely. The transition state for the C2(**A2**)–C5(**M5**) bond formation is 42.6 kcal mol<sup>-1</sup> above the reactants ( $\nu_{\text{IMAG}} = 455i \text{ cm}^{-1}$ ) with C2(**A2**)–C5(**M5**) and C5(**M5**)–I bonds of 1.928 and 2.527 Å, respectively. This very high barrier is slightly reduced in N3-deprotonated **M5**<sup>-</sup> to  $\Delta G^\ddagger = 38.7 \text{ kcal mol}^{-1}$  ( $\nu_{\text{IMAG}} = 334i \text{ cm}^{-1}$ ) and the transition state becomes more compact with C2(**A2**)–C5(**M5**) and C5(**M5**)–I bonds of 1.742 and 2.344 Å, respectively. However, the calculated barrier is still too high for the efficient process. This goes along with the calculated high  $\text{p}K_{\text{a}}(\text{M5})_{\text{N3}} = 56.8$ . We note in passing that any attempts to model the reaction starting with the C1(**A2**)–O4 bond formation in either **M5** or **M5**<sup>-</sup> did not give any stable intermediates or the corresponding transition state structures. The presence of Cu(I) ions reduces the  $\text{p}K_{\text{a}}$  value of **M5** to 16.4 with Cu(I) bound to the deprotonated N3 atom at 1.907 Å and  $\Delta G_{\text{BIND}} = -80.9 \text{ kcal mol}^{-1}$ . This would suggest that, under reaction conditions, **M5** deprotonation is very feasible process when Cu(I) ions are present. However, when Cu(I) is bound to the deprotonated **M5**<sup>-</sup>, it deprives the electron density from 5-iodouracil making the whole system less reactive towards **A2**, in addition to the fact that the most stable reactant complex involves Cu(I) binding the 1,3-diyne **A2** to the opposite site of **M5**<sup>-</sup> (as in **M6**, Fig. 1). This makes the subsequent reaction between the two systems highly unlikely. For example, from **M6** it requires  $\Delta G^\ddagger = 61.5 \text{ kcal mol}^{-1}$  ( $\nu_{\text{IMAG}} = 455i \text{ cm}^{-1}$ ) to reach the transition state for the C2(**A2**)–C5(**M5**<sup>-</sup>) bond formation, which is way too high. Therefore, one must look into the reactivity of neutral **M5**, which allows **M7** as the most stable reactant complex, where Cu(I) is bonded to C1 and C2 atoms of **A2** at 1.945 and 2.317 Å, respectively, with Cu(I)–C1–C2 plane being practically parallel to the plane of the six-membered ring of **M5**. With this, the Cu(I) ion activates C1–C2 triple bond for the nucleophilic attack and two scenarios are possible: the approach of the carbonyl O4(**M5**) atom towards the C1(**A2**) atom (Fig. S3, Supplementary information), and the C5(**M5**) atom towards the C2(**A2**) atom (Fig. 3). As our results demonstrate, the first option is less feasible because of the following. The O4(**M5**)–C1(**A2**) bond formation is associated with a barrier of  $\Delta G^\ddagger = 15.3 \text{ kcal mol}^{-1}$  ( $\nu_{\text{IMAG}} =$

268i cm<sup>-1</sup>) to give the adduct with Cu(I) bound to the C2(A2) atom at 1.902 Å, from which all attempts to model the subsequent ring closure failed and resulted in the formation of CuI and separated M5 and A2. For the latter reaction to be possible, an intramolecular rearrangement must occur, involving a shift of Cu<sup>+</sup> from C2 to C4 in A2, but this gives 4.6 kcal mol<sup>-1</sup> less stable isomer. The subsequent barrier is high,  $\Delta G^\ddagger = 24.8$  kcal mol<sup>-1</sup> ( $\nu_{\text{IMAG}} = 313i$  cm<sup>-1</sup>), and although the reaction is highly exothermic, the overall barrier for this process assumes  $\Delta G^\ddagger = 42.3$  kcal mol<sup>-1</sup> (Fig. 3), rendering this process unlikely. After the formation of M8, the system needs to lose the CuI molecule and be deprotonated at the N3-H position to give the final M9. Collectively, this requires 26.1 kcal mol<sup>-1</sup>, and the details of that will be presented in the next section describing feasible mechanism, where the same requirements exist.

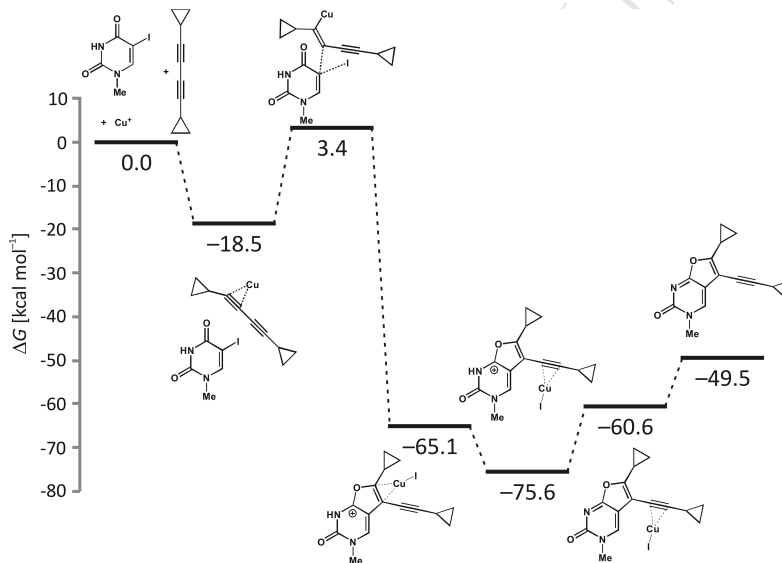


**Fig. 3.** Free energy profile for the formation of the 5-alkylethynyl-6-alkyl-furo[2,3-d]pyrimidine-2-ones initiated by the carbon–carbon bond formation.

The most feasible mechanism producing M9 from M5 and A2 is Cu(I)-catalyzed process depicted in Fig. 3, which is initiated with the C5(M5)–C2(A2) bond formation. Bringing all three components to M7 in favorable (18.5 kcal mol<sup>-1</sup>), with the C5(M5)–C2(A2) distance of 3.602 Å. In the transition state, the latter is reduced to 1.999 Å, while the C5(M5)–I bond elongates from 2.134 to 2.191 Å, and the Cu(I) ion is bound to C1(A2) at 1.925 Å. The barrier for this is 21.9 kcal mol<sup>-1</sup> ( $\nu_{\text{IMAG}} = 405i$  cm<sup>-1</sup>). Interestingly, after the transition state, the system relaxes through a series of events occurring in a concerted manner, involving the C5(M5)–C2(A2) bond

formation, abstraction of the  $\Gamma$  leaving group by the Cu(I) ion to give CuI, and the five-membered ring closure through the O4(**M5**)–C1(**A2**) bond formation. This highly exergonic sequence ( $\Delta G = -68.5 \text{ kcal mol}^{-1}$ ) produces bicyclic compound with CuI bound to the C7–C8 double bond, which is further stabilized to **M8** by the intramolecular rearrangement of the CuI molecule. In order to evaluate whether **M8** is first deprotonated or loses CuI to afford the final **M9**, one needs to consider the corresponding  $pK_a$  values and CuI binding free energies. For **M8**, these assume  $pK_a(\mathbf{M8}) = 11.0$  and  $\Delta G_{\text{BIND}} = -8.3 \text{ kcal mol}^{-1}$ . On the other hand, if one deprotonates **M8**, the binding of CuI changes to  $\Delta G_{\text{BIND}} = -11.1 \text{ kcal mol}^{-1}$ , while if one removes CuI from **M8**, the  $pK_a$  is increased to  $pK_a(\mathbf{M8}) = 14.1$ . This analysis indicates the  $pK_a$  values undergo larger change in a direction of increasing the energy requirements for these processes to occur, thus suggesting **M8** is first deprotonated and then loses CuI. Since no measured autoprotolysis constant of toluene exists in the literature, we followed observations by Kocaoba and co-worker [28] who suggested it is close to zero. Therefore, from the value of  $pK_a(\mathbf{M8}) = 11.0$  we estimated that it requires  $15.0 \text{ kcal mol}^{-1}$  for deprotonating **M8** in toluene leading to a system requiring further  $11.1 \text{ kcal mol}^{-1}$  to remove CuI (Fig. 3) to give the unexpected 5-alkylethynyl-6-substituted furo[2,3-*d*]pyrimidine-2-ones **M9**. On the overall, this mechanism is associated with a barrier of  $\Delta G^\ddagger = 21.9 \text{ kcal mol}^{-1}$  and very favorable exergonicity of  $\Delta G_{\text{R}} = -49.5 \text{ kcal mol}^{-1}$ , both making it highly probable. Comparing it to the process leading to the expected **M2** derivatives (Fig. 2), we conclude that the formation of unexpected **M9** is related with  $8.1 \text{ kcal mol}^{-1}$  higher activation free energy, meaning that it is around six orders of magnitude slower process, being a predominant factor affecting the distribution of **M2** and **M9** products. Still, with a particular choice of substituents on the reacting alkynes **A1** and thereof homocoupled 1,3-diynes **A2**, more favored exergonicity of the pathway producing systems of the **M9**-type could compensate or even overcome differences in the kinetic parameters of both processes and lead to a different ratio of final products.

### 2.3. X-ray crystal structure analysis

The formation of the 5,6-disubstituted furo[2,3-*d*]pyrimidine-2-one was unambiguously confirmed by the X-ray structure of **34a** (Fig. 4a), where two cyclopropane rings are bonded to bicyclic furo[2,3-*d*]pyrimidine-2-one scaffold. One ring is directly bonded to the C6 atom of the bicyclic ring, while the second one is

bonded to the C5 atom *via* the ethynyl linker. The third substituent of the furopyrimidine, (1-benzyl-1,2,3-triazol-4-yl)methyl moiety, is connected to the N3 atom. Search of Cambridge Structural Database [29] revealed that this is the first structure comprising three main structural elements, furo[2,3-*d*]pyrimidine-2-one, cyclopropane and triazole rings. The cyclopropane C9–C11 ring and five-membered O2/C5/C6/C7/C8 ring are almost perpendicular to each other. The dihedral angle between the mean planes of the rings is 84.6(2)°. Furo[2,3-*d*]pyrimidine-2-one ring is planar, with the largest ring atom deviation from the mean plane of 0.019(2) Å. Because of bicyclic ring formation, the N1–C7–C8 bond angle in the six-membered N1/C2/N3/C4/C7/C8 ring is significantly widened and amounts 128.92(18)°.

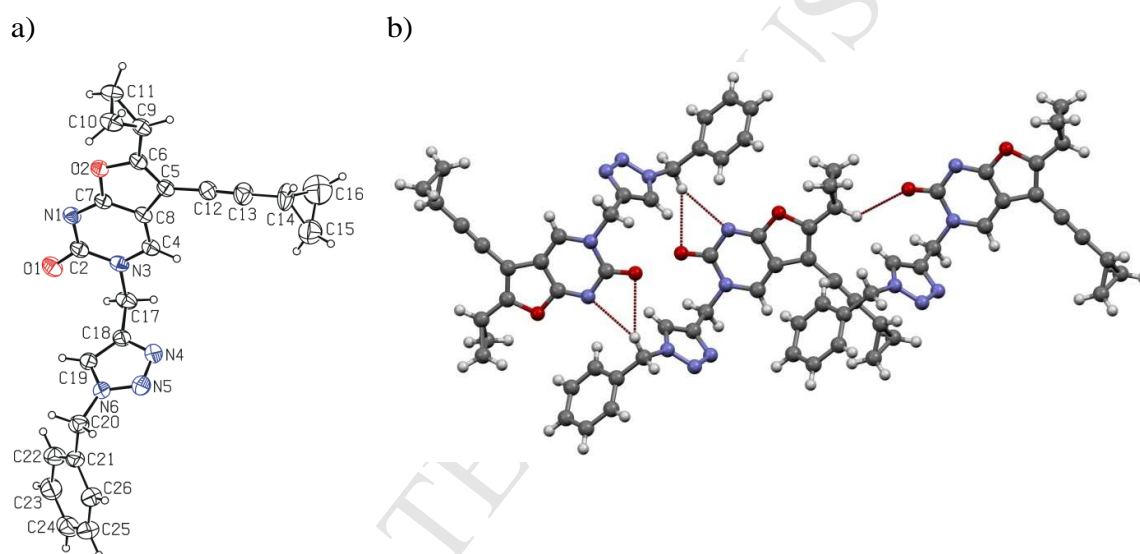


**Fig. 4.** (a) Molecular structure of **34a**, with the atom-numbering scheme. Displacement ellipsoids for non-hydrogen atoms are drawn at the 30% probability level. (b) A part of the crystal structure of **34a**, showing C–H···O and C–H···N intermolecular hydrogen bonds. Only major component of disordered atoms is presented in both figures.

However, the sum of all endocyclic bond angles in the ring is *ca.* 720°, as expected for the six-membered aromatic ring. As strong hydrogen-bonding donors are absent in this compound, the molecules of **34a** are linked only by weak interactions, two C–H···O hydrogen bonds, one C–H···N hydrogen bond, one C–H··· $\pi$  and one  $\pi$ ··· $\pi$  interaction (Table S1, Supplementary information). Two of the abovementioned interactions, the C20···N1 and C20···O1 hydrogen bonds form dimers (Fig. 4b), which are further linked by the C9···O1

hydrogen bond and one C–H $\cdots\pi$  interaction into two-dimensional sheets (Fig. S4 and S5, Supplementary information). One  $\pi\cdots\pi$  interaction extends two-dimensional sheets into three-dimensional network (Fig. S6; for more detailed description of intermolecular interactions see Supplementary information).

#### 2.4. *In vitro* antiproliferative activity screening

The results of antiproliferative evaluations of **5–37a,b** carried out in human tumor cell lines including lung adenocarcinoma (A549), hepatocellular carcinoma (HepG2), ductal pancreatic adenocarcinoma (CFPAC-1), cervical carcinoma (HeLa) and metastatic colorectal adenocarcinoma (SW620), as well as in normal human lung fibroblasts (WI38) and mouse embryonic fibroblasts (3T3), are presented in Table 1.

**Table 1**

The growth-inhibition effects *in vitro* of **5–37a,b** on selected tumor cell lines and normal fibroblasts.

Compound	IC <sub>50</sub> <sup>a</sup> (μM)						logP <sup>c</sup>
	A549	Hep-G2	CFPAC-1	HeLa	SW620	WI38/NIH 3T3	
<b>5</b>	25.45	4.47	6.87	12.58	9.82	0.07 <sup>b</sup>	3.67
<b>6</b>	5.33	7.11	4.53	1.64	7.86	0.59 <sup>b</sup>	3.67
<b>7</b>	7.41	3.62	5.92	6.13	5.63	0.37 <sup>b</sup>	4.48
<b>8</b>	95.79	42.73	>100	>100	>100	4.30 <sup>b</sup>	5.59
<b>9</b>	64.00	68.93	>100	72.90	>100	50.79 <sup>b</sup>	1.52
<b>10</b>	>100	>100	>100	93.86	≥100	59.34 <sup>b</sup>	1.52
<b>11</b>	40.93	19.14	39.54	33.28	>100	6.70 <sup>b</sup>	1.92
<b>12</b>	80.68	7.66	5.51	8.42	9.87	1.16 <sup>b</sup>	2.48
<b>13</b>	78.65	53.49	51.19	41.89	94.82	<0.01	4.20
<b>14</b>	3.06	5.11	4.21	4.50	6.63	<0.01	2.50
<b>15</b>	53.35	36.10	55.94	49.75	>100	2.22	4.20
<b>16</b>	56.16	>100	>100	>100	>100	0.16	2.50
<b>17</b>	71.07	>100	>100	96.49	>100	0.03	5.00
<b>18</b>	4.69	13.12	5.53	4.74	18.29	0.04	2.90
<b>19</b>	41.31	5.77	>100	15.07	>100	<0.01	4.03
<b>20</b>	78.82	>100	83.74	7.20	>100	3.78	2.05

<b>21</b>	95.12	>100	>100	>100	>100	73.12	2.05
<b>22</b>	50.60	>100	77.15	6.79	34.56	<0.01	2.45
<b>23</b>	>100	>100	>100	>100	>100	55.25	1.96
<b>24a</b>	39.43	36.94	95.79	41.83	69.59	0.07	4.17
<b>24b</b>	68.39	14.58	6.49	6.99	>100	<0.01	2.15
<b>25a</b>	>100	>100	>100	>100	>100	>100	6.62
<b>26a</b>	38.28	39.06	54.47	51.20	49.14	45.92	3.02
<b>27b</b>	69.79	79.78	81.75	66.45	>100	76.46	2.87
<b>28a</b>	38.65	72.48	>100	9.00	57.09	7.34	9.96
<b>29b</b>	>100	>100	>100	>100	>100	69.20	4.09
<b>30a</b>	39.01	39.17	35.44	16.07	36.93	3.15	3.42
<b>30b</b>	60.95	>100	>100	>100	>100	>100	2.73
<b>31a</b>	>100	72.53	>100	>100	>100	>100	4.57
<b>31b</b>	51.98	89.83	>100	60.22	>100	72.54	3.27
<b>32a</b>	>100	>100	>100	>100	>100	>100	10.36
<b>33a</b>	>100	>100	>100	>100	>100	>100	7.02
<b>34a</b>	4.81	2.67	4.59	6.51	9.72	0.29	2.93
<b>34b</b>	45.00	49.06	48.45	49.98	54.73	29.66	2.24
<b>35a</b>	26.85	25.54	32.83	25.35	33.86	17.60	4.09
<b>35b</b>	27.94	27.62	23.47	9.58	75.52	5.20	2.78
<b>36a</b>	>100	>100	>100	73.03	>100	2.65	9.87
<b>37a</b>	21.94	25.84	27.30	23.39	32.60	23.39	6.54
<b>37b</b>	51.04	68.70	67.03	59.36	93.47	62.78	4.01
<b>5-FU</b>	2.80	8.90	0.14	8.81	0.08	0.94	-0.9

<sup>a</sup>50% inhibitory concentration or compound concentration required to inhibit tumor cell proliferation by 50%. <sup>b</sup>**5–12** were tested on 3T3 cell line. <sup>c</sup>Values of n-octanol/water partition coefficients logP for synthesized compounds were calculated by two algorithms with their default settings: ChemAxon algorithm available within MarvinView Ver. 5.2.6.

5-Fluorouracil was used as the reference drug. From tested *N,N*-1,3-bis(1-aryl-substituted-1,2,3-triazole)-5-bromouracil hybrids, compounds containing *p*-fluoro- (**5**), *o*-fluoro- (**6**), *p*-chlorophenyl-substituted 1,2,3-triazole (**7**) exhibited marked cytostatic activities against all evaluated tumor cell lines. Among these, the most potent growth inhibitory activity was observed with **6** in HeLa cells (IC<sub>50</sub> = 1.64 μM). Compounds **5** and **7** proved to be selective towards HepG2 cells with IC<sub>50</sub> values of 4.47 and 3.62 μM, respectively. Notably,

introduction of 3,5-dichlorophenyl-substituted 1,2,3-triazole in **8** led to a decrease in potency. On the contrary, within the *N*-1-(1-aryl-substituted-1,2,3-triazole)-5-bromouracil hybrids, compound bearing 3,5-dichlorophenyl-substituted 1,2,3-triazole (**12**) displayed strong cytostatic effects, particularly in CFPAC-1 cells with  $IC_{50} = 5.51 \mu\text{M}$ . Furthermore, 1,2,3-triazole-5-iodouracil hybrids **14**, **18**, **20** and **22** containing *p*-fluoro- and *p*-chlorophenyl-substituted 1,2,3-triazole exhibited strong inhibitory activities ( $IC_{50} = 4.50\text{--}7.20 \mu\text{M}$ ) against HeLa cell line. Additionally, 3-propargylpyrimidine-1,2,3-triazole hybrids **14** and **18** showed marked cytostatic effects (**14**:  $IC_{50} = 3.06 \mu\text{M}$ ; **18**:  $IC_{50} = 4.69 \mu\text{M}$ ) in A549 cells. Amongst the *N,N*-1,3-*bis*(1,2,3-triazole)-substituted 5-iodouracils, only 1-benzyl-substituted 1,2,3-triazole-pyrimidine-2,4-dione hybrid (**19**) inhibited the growth of Hep-G2 cells ( $IC_{50} = 5.77 \mu\text{M}$ ). Among the furopyrimidine-1,2,3-triazole series, **34a** with 5-cyclopropylethynyl and 6-cyclopropyl substituents at bicyclic moiety showed to be the most potent, displaying the highest cytostatic effect ( $IC_{50} = 2.67 \mu\text{M}$ ) against HepG2 cells. Both bicyclic furo[2,3-*d*]pyrimidine congeners **34a** and **34b** had better antiproliferative effects than their 5-iodouracil-1,2,3-triazole analog **23** that showed poor antitumor activity in all evaluated cancer cell lines. Importantly, our data revealed that the formation of bicyclic furopyrimidine scaffold in **24**, **26–28**, **30**, **34**, **35**, **37** led to the improvement in activities relative to corresponding 5-iodouracil analogs **20–23**. Besides, comparison of cytostatic effects for 5,6-disubstituted and 6-substituted furopyrimidines revealed that symmetrical 5-alkylethynyl-6-alkyl-substituted compounds (**30a**, **34a**, **37a**) had better antiproliferative activities than those with 6-alkyl substituent (**30b**, **34b**, **37b**). Thus, the activity of 5,6-disubstituted furopyrimidine **34a** was ~ 10-fold higher than that of 6-substituted analog **34b**. On the other hand, 6-(3-chloropropyl)-substituted furo[2,3-*d*]pyrimidines (**24b** and **35b**) were more potent against CFPAC-1 and HeLa cell lines than corresponding 5,6-disubstituted **24a** and **35a**. However, compounds showing cytostatic activity against cancer cells were also cytotoxic to normal human lung (WI38) and mouse embryonic (3T3) fibroblasts. Calculated octanol/water partition coefficients, logPs take values between 2.5 and 4.7 for the most active compounds. It can be observed that 5,6-disubstituted furopyrimidines had higher lipophilic properties than corresponding 6-substituted analogs that may contribute to their enhanced activity.

### 2.5. The prediction of activity spectra for substances (PASS) analysis

We applied the Prediction of Activity Spectra for Substances (PASS) to explore the biological potential of selected compounds and to prioritize them for further *in vitro* studies. The PASS is an *in silico* tool used for predicting biological activity spectra for natural and

synthetic substances, which is based on the structure-activity relationships knowledgebase for more than 260 000 compounds with known biological activities including drugs, drug candidates, pharmaceutical leads and toxic systems [30]. The PASS predicts the probable biological potential of the compound based on its structure and reveals the predicted activities as the probability of activity (Pa) and inactivity (Pi). The higher Pa value, the lower is the predicted probability of obtaining false positives in biological testing. The PASS analysis of compounds with the most potent antiproliferative activities across the panel of tested tumor cell lines showed high activity score for Wee-1 tyrosine kinase inhibitory effect of **5–7** with Pa values of 0.56, 0.53 and 0.52, respectively (Table S2, Supplementary information). The obtained *in silico* results were further confirmed *in vitro* by Western blot method to validate the probable protein target of selected compounds, as described in the following section.

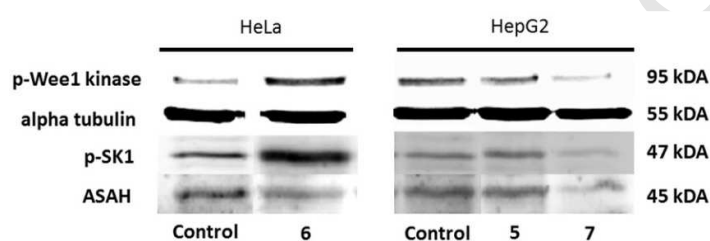
#### 2.6. Western blot validation of potential protein targets

Results of the PASS prediction prompted us to examine *in vitro* inhibitory effect of **5–7** on the activity of Wee-1 tyrosine kinase, an enzyme belonging to the Ser/Thr family of protein kinases and a negative regulator of the G2/M checkpoint that averts mitotic progression by inhibiting the activity of cycle-dependent kinase 1 (CDK1) [31]. It was found that small molecule compounds with anticancer activities based on pyrimidine and heteroaromatic ring fused-pyrimidine moiety inhibited Wee-1 kinase at nanomolar concentrations, *e.g.* pyrido[2,3-*d*]pyrimidine (PD0166285) [32] and pyrazolo-pyrimidine derivative (MK-1775) [33], the latter being investigated in clinical studies either as monotherapy or in combination with standard chemotherapeutics. Since the most potent cytostatic effects of **5–7** were detected in HepG2 and HeLa cells, these cell lines were used for Western blot analyses of Wee-1 kinase activity. Obtained results clearly showed that **7** significantly ( $p < 0.05$ ) reduced the expression level of phospho-Wee-1 kinase indicating strong inhibition of its activity (Fig. 5).

The same trend, although to a lesser extent, was also evident with **5**. Surprisingly, **6** elicited quite the opposite effect on Wee-1 kinase activity as deduced from marked elevation of its phospho-form. These results could be ascribed to the type of halogen substituent and its position at phenyl-substituted 1,2,3-triazole subunit in **5–7**. Thus, *p*-chlorophenyl substituent at the N-1 position of 1,2,3-triazole ring is critical for the inhibitory activity of *N,N*-1,3-disubstituted 1,2,3-triazole–5-bromouracil hybrids towards Wee-1 kinase. Interestingly, *o*-fluoro-substitution in **6** was detrimental for inhibitory activity of Wee-1 tyrosine kinase. A

study carried out by Palmer *et al.* [34] describing Wee-1 inhibitors based on 4-phenylpyrrolo[3,4-*c*]carbazole-1,3-dione template demonstrated that Wee-1 potency and selectivity were improved by the incorporation of lipophilic functionality at the 2'-position of the 4-phenyl ring. Similarly, correlation between lipophilicity and inhibitory activity towards Wee-1 kinase could be observed for tested **5–7**. Thus, *p*-chlorophenyl-substituted 1,2,3-triazole scaffold in **7**, which led to the improvement of its inhibitory activity, also increased the lipophilicity ( $\log P = 4.48$ ) in comparison to *p*-fluoro- and *o*-fluoro-substituted ( $\log P = 3.67$ ) 1,2,3-triazole counterparts **5** and **6**, respectively.

a)



b)

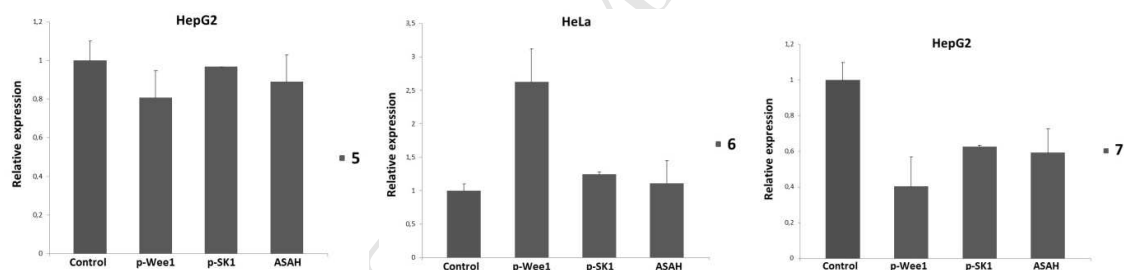


**Fig. 5.** Western blot analysis of predicted protein targets of **5–7**. a) Representative Western blots are shown detecting the cellular levels of phospho-Wee1 kinase, phospho-Sphingosine kinase 1 (SK1) and acid ceramidase (ASAH) before and after treatment of HepG2 and HeLa cells with indicated compounds at their  $2 \times IC_{50}$  values for 48 h. Approximate molecular weights (kDa) are indicated. b) Relative protein expressions, as determined by densitometric analysis of protein bands and normalized to the alpha-tubulin loading control. Two independent experiments were performed with similar results. Data are presented as mean values  $\pm$  SD.

Based on these observations, it is plausible that mechanism other than Wee-1 kinase inhibition accounts for cytostatic effect of **6** in HeLa cells. Previous studies have

demonstrated that enzymes regulating sphingolipid synthesis and turnover are important mediators of G2/M transition and thereby mitotic entry and progression. For example, down-regulation of sphingosine kinase 1 in MDA-MB-231 breast carcinoma cells is associated with mitotic defects characterized by compromised function of spindle checkpoint and cytokinesis failure [35]. Similarly, antiproliferative effects of ceramide kinase inhibitor NVP-231 in breast and lung cancer cells could be attributed to induction of M phase arrest, which was associated with down-regulation of Wee-1 kinase [36]. In order to ascertain whether alterations in the Wee-1 kinase activity induced by tested compounds are linked with perturbations in sphingolipid metabolism, we examined the activity of sphingosine kinase 1 (SK1) and acid ceramidase (ASAH) in HeLa and HepG2 cells. Interestingly, **7**, which proved to be potent Wee-1 kinase inhibitor, interferes with sphingolipid metabolism in HepG2 cells, as this compound was able to induce a significant decline in the expression levels of both phospho-SK1 and ASAH pointing to abrogation of their activities (Fig. 5). On the contrary, **5** and **6** did not exert notable effects on the expression levels of phospho-SK1 and ASAH in HepG2 and HeLa cells, respectively, which suggests that these two enzymes are not the key mediators of cellular response to **5** and **6**. Altogether, obtained results suggest that Wee-1 kinase inhibition by **7** could be correlated with the impairment in sphingolipid metabolism mirrored by negative regulation of SK1 and ASAH activity, whereas **5** and **6** lacking strong inhibitory activity towards Wee-1 did not have impact on critical regulatory points in sphingolipid pathway. Consistent with the results obtained for inhibitory activity of Wee-1 tyrosine kinase of **5–7**, replacement of *p*-fluoro and *o*-fluoro substituent in **5** and **6** with *p*-chloro substituent at the 1-phenyl-1,2,3-triazole subunit in **7** was crucial to achieve abrogation of SK1 and ASAH activities.

### 2.7. Apoptosis detection

Recent study demonstrated that Wee-1 kinase inhibitor pyrido[2,3-*d*]pyrimidine (PD166285) induced apoptosis in human hepatocellular carcinoma cells in a concentration-dependent manner [37]. In order to investigate whether antiproliferative effects of **7**, identified as the Wee-1 kinase inhibitor, as well as the effects of **5** and **6** could be associated with induction of apoptosis, Annexin V assay was performed as previously described [10]. **7** exerted a profound effect in the induction of apoptosis in HepG2 cells in comparison with untreated cells as evidenced from marked reduction in the viable cell population by 44.2% with concomitant increase in early apoptotic and secondary necrotic cells by 34.2% and 10%,

respectively (Table 2, Fig. 6). **5** had weaker pro-apoptotic effect in the same cells as evidenced by a moderate decline in viable cells by 21.3% accompanied by the increase of early apoptotic cells by 26% as compared to control cells (Table 2).

**Table 2**

Results of Annexin V assays for apoptosis detection of **5–7**.

	HepG2 cells (%) <sup>a</sup>			HeLa cells (%) <sup>a</sup>	
	Control	<b>5</b>	<b>7</b>	Control	<b>6</b>
Late apoptotic/primary necrotic cells	0	0	0	2.3	1.8
Viable cells	94.2	72.9	50	75	71.3
Early apoptotic cells	0.6	26.6	34.8	20.4	23.9
Secondary necrotic cells	5.2	0.5	15.2	2.3	3

<sup>a</sup>The percentages of viable cells (PI-/Ann V-), early apoptotic cells (PI-/Ann V+), late apoptotic/primary necrotic cells (PI+/Ann V+) and secondary necrotic cells (PI+) after 48 h treatment with **5–7** at their 2 x IC<sub>50</sub> values.

a) Untreated HepG2 cells

b) HepG2 cells treated with **7**

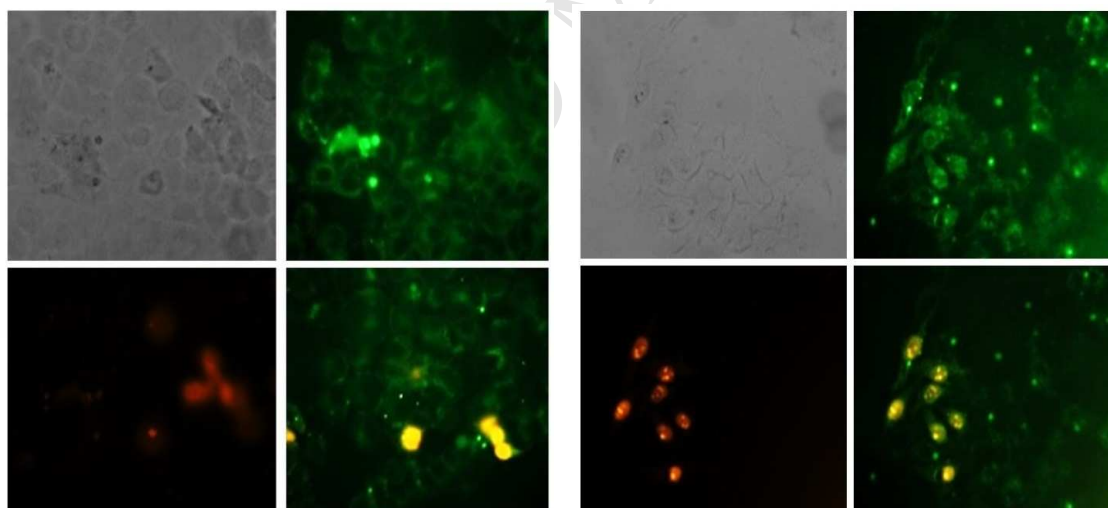


**Fig. 6.** Detection of apoptosis induced by **7** in HepG2 cells using Annexin V-FITC assay. Cells were visualized by fluorescence microscope at 40x magnification before and after treatment with 2 x IC<sub>50</sub> value of **7** for 48 h. PI staining was used as a nuclear marker. Shown here are bright-field images (upper left micrographs), early apoptotic cells (PI-/Ann V+, upper right micrographs), secondary necrotic cells (PI+, lower left micrographs) and late apoptotic/primary necrotic cells (PI+/Ann V+, lower right micrographs).

In HeLa cells, **6** did not induce dramatic changes in cell death response. Thus, we observed slight decline in viable cell population by 3.7% related with an increase in early

apoptotic and secondary necrotic cells by 3.5% and 0.7%, respectively. This weak anti-apoptotic effect of **6** is in agreement with Western blot results showing an absence of its inhibitory activity towards enzymes involved in the regulation of cell growth and survival. Obtained results suggest that apoptosis is not a major cell death mechanism with **6**, and that probably some other modes of cell death mediate cytostatic effects of this system in HeLa cells.

### 2.8. Mitochondrial toxicity

Drug-induced mitochondrial impairment is associated with severe toxicities in mammals, especially those associated with the liver, skeletal and cardiac muscle and the central nervous system [38]. Several drugs withdrawn from the market such as cerivastatin (Baycol), troglitazone (Rezulin) and nefazodone (Serzone) have been shown to severely interfere with mitochondrial function. Therefore, identification of mitochondrial toxicants early in the drug discovery process is highly desirable as to avoid potential adverse effects that may not be obvious in the preclinical and clinical studies due to absence of specific histopathologic changes, and to prevent financial loss that may arise from post-market withdrawal. In the present study, we investigated potential mitochondrial toxicity of **5–7** using previously established protocol [39]. This method relies on the inherent feature of highly proliferative cells such as HepG2 cells to use glycolysis for ATP production when grown in the presence of glucose rather than mitochondrial oxidative phosphorylation despite abundant oxygen and functional mitochondria. When glucose in cell culture media is replaced with galactose, cancer cells are forced to revert back to mitochondrial oxidative phosphorylation to survive because oxidation of galactose to pyruvate *via* glycolysis yields no net ATP. Thus, cells grown in galactose become more susceptible to drugs that cause mitochondrial insult. Our results clearly showed that there were no striking differences in the response between HepG2 cells grown in glucose *versus* those grown in galactose for all three tested compounds, in particular there was not a significant reduction in IC<sub>50</sub> values for galactose-grown cells indicative of mitochondrial toxicity (Table 3). This implies that mitochondrial dysfunction is not a primary mechanism leading to cell death induced by **5–7**, *i.e.* apoptosis and necrosis induced by these compounds could be triggered by some other cellular events that do not involve mitochondrial dysfunction directly.

**Table 3**

Mitochondrial toxicity testing in HepG2 cells grown in the media containing either glucose or galactose.

Compound	IC <sub>50</sub> (μM) glucose <sup>a</sup>	IC <sub>50</sub> (μM) galactose <sup>a</sup>
<b>5</b>	4.78	4.57
<b>6</b>	7.11	4.67
<b>7</b>	3.82	7.10

<sup>a</sup>Decreased IC<sub>50</sub> values in galactose- versus glucose-containing media represent a compound with properties of potential mitochondrial toxicant.

### 3. Conclusions

Both *N,N*-1,3- (**5–8**, **13**, **15**, **17** and **19**) and *N*-1-(1,2,3-triazole) tethered pyrimidine-2,4-diones (**9–12**, **14**, **16**, **18** and **20–23**) containing halogen-substituted and nonsubstituted aromatic subunits were synthesized by copper(I)-catalyzed Huisgen 1,3-dipolar cycloaddition, among which microwave-assisted click reactions proved to be more efficient than conventional ones. Furthermore, we have applied palladium-catalyzed cross-coupling of 5-iodouracil–1,2,3-triazole hybrids (**20–23**) with alkyne in the presence of the CuI catalyst and heteroannulation method to generate furo[2,3-*d*]pyrimidine series **24a,b–37a,b**. The stereostructure of 5-cyclopropylethynyl-6-cyclopropyl-substituted furo[2,3-*d*]pyrimidine derivative (**34a**) was unambiguously confirmed by X-ray crystal structure analysis. The results of the computational analysis revealed that the 6-substituted bicyclic series (**24b–37b**) was produced through the Cu(I)-catalyzed cyclization of the corresponding 5-alkynyluracils associated with a barrier of  $\Delta G^\ddagger = 13.8 \text{ kcal mol}^{-1}$  and a reaction energy of  $\Delta G_R = -13.8 \text{ kcal mol}^{-1}$ , whereas the 5-alkylethynyl analogs (**24a–37a**) were linked with a higher barrier of  $\Delta G^\ddagger = 21.9 \text{ kcal mol}^{-1}$ , yet much favorable change in the reaction energy of  $\Delta G_R = -49.5 \text{ kcal mol}^{-1}$ . Among the 1,2,3-triazole tethered pyrimidine-2,4-dione derivatives (**5–23**), *N,N*-1,3-*bis*(1-phenyl-substituted-1,2,3-triazole)–5-bromouracil hybrids containing *p*-fluoro- (**5**), *o*-fluoro- (**6**) and *p*-chlorophenyl (**7**) moiety exhibited the most pronounced cytostatic activities against hepatocellular and cervical carcinoma cells with potencies better than those of the reference drug 5-fluorouracil. Strong growth inhibitory activity of **7** against HepG2 cells could be associated with induction of early apoptosis and secondary necrosis in these cells. Cell death induced by **7** was triggered by cellular events other than mitochondrial dysfunction, as this compound was not

shown to be mitochondrial toxicant. Major cytostatic effects of **7** could be attributed to inhibition of Wee-1 kinase as well as sphingosine kinase 1 and acid ceramidase that regulate the balance between pro-apoptotic and pro-survival sphingolipids. Taking into account strong antitumor activity and no mitochondrial liabilities detected with **7**, it represents a good starting point for the development of new and more efficient drugs for treating hepatocellular carcinoma.

## 4. Experimentals

### 4.1. Materials and methods

All solvents were dried/purified following recommended drying agents and/or distilled over 3 Å molecular sieves. For monitoring the progress of a reaction and for comparison purpose, thin layer chromatography (TLC) was performed on pre-coated *Merck* silica gel 60F-254 plates using an appropriate solvent system and the spots were detected under UV light (254 nm). For column chromatography silica gel (*Fluka*, 0.063-0.2 mm) was employed, glass column was slurry-packed under gravity. Melting points (uncorrected) were determined with *Kofler* micro hot-stage (*Reichert*, Wien). Microwave-assisted syntheses were performed in a Milestone start S microwave oven using glass cuvettes at 80 °C and 300 W under the pressure of 1 bar. Elemental analyses were performed in the Central Analytic Service, Ruđer Bošković Institute, Zagreb. All elemental compositions were within the 0.4% of the calculated values. <sup>1</sup>H and <sup>13</sup>C NMR spectra were acquired on a *Bruker* 300 and 600 MHz NMR spectrometer. All data were recorded in DMSO-*d*<sub>6</sub> at 298 K. Chemical shifts were referenced to the residual solvent signal of DMSO at δ 2.50 ppm for <sup>1</sup>H and δ 39.50 ppm for <sup>13</sup>C. Individual resonances were assigned based on their chemical shifts, signal intensities, multiplicity of resonances and H–H coupling constants.

### 4.2. Procedures for the preparation of compounds

#### 4.2.1. 5-Bromo-*N*-1,*N*-3-di(prop-2-yn-1-yl)pyrimidine-2,4-dione (**1**) and 5-bromo-*N*-1-(prop-2-yn-1-yl)pyrimidine-2,4-dione (**2**)

To the solution of 5-bromouracil (1 g, 5.2 mmol) in dimethylformamide (DMF) (20 mL), NaH (125.6 mg, 5.2 mmol) were added and reaction mixture was stirred for 2h. Then 3-bromopropyne (0.71 mL, 6.3 mmol) was added and the mixture was stirred for

24 h at room temperature. After 24 h solvent was evaporated and residue was purified by column chromatography on silica gel using  $\text{CH}_2\text{Cl}_2 : \text{CH}_3\text{OH} = 150 : 1$ , as an eluent. **1** (215 mg, 15%, m.p. = 129–130 °C) and **2** (453 mg, 38%, m.p. = 199–200 °C) were isolated as white powder. **1**:  $^1\text{H-NMR}$  (300 MHz, DMSO) ( $\delta/\text{ppm}$ ): 8.4 (1H, s, H-6), 4.6 (4H, dd, H-1', H-1'',  $J = 2.7 \text{ Hz}$ ,  $J = 2.4 \text{ Hz}$ ), 3.5 (1H, t, H-3',  $J = 2.4 \text{ Hz}$ ), 3.2 (1H, t, H-3'',  $J = 2.4 \text{ Hz}$ ) ppm.  $^{13}\text{C-NMR}$  (75 MHz, DMSO) ( $\delta/\text{ppm}$ ): 158.4 (C-4), 149.6 (C-2), 143.8 (C-6), 94.9 (C-5), 78.9 (C-2'), 78.4 (C-2''), 77.0 (C-3'), 74.0 (C-3''), 38.9 (C-1'), 31.9 (C-1'') ppm. Anal. calcd. for  $\text{C}_{10}\text{H}_7\text{BrN}_2\text{O}_2$ : C, 44.97; H, 2.64; N, 10.49%. Found: C, 44.89; H, 2.65; N, 10.51%. **2**:  $^1\text{H-NMR}$  (300 MHz, DMSO) ( $\delta/\text{ppm}$ ): 11.9 (1H, s, N-H), 8.3 (1H, s, H-6), 4.5 (2H, d, H-1',  $J = 2.7 \text{ Hz}$ ), 3.5 (1H, t, H-3',  $J = 2.5 \text{ Hz}$ ) ppm.  $^{13}\text{C-NMR}$  (75 MHz, DMSO) ( $\delta/\text{ppm}$ ): 159.5 (C-4), 149.7 (C-2), 144.1 (C-6), 95.3 (C-5), 78.2 (C-2'), 76.1 (C-3'), 37.1 (C-1') ppm. Anal. calcd. for  $\text{C}_7\text{H}_5\text{BrN}_2\text{O}_2$ : C, 36.71; H, 2.20; N, 12.23%. Found: C, 36.77; H, 2.21; N, 12.26%.

#### 4.2.2. 5-Iodo-N-1,N-3-di(prop-2-yn-1-yl)pyrimidine-2,4-dione (**3**) and 5-iodo-N-1-(prop-2-yn-1-yl)pyrimidine-2,4-dione (**4**)

**3** and **4** were synthesized following the procedure for the preparation of **1** and **2**. Reagents: 5-iodouracil (5 g, 21 mmol), NaH (483 mg, 21 mmol) 3-bromopropyne (2.8 mL, 25 mmol), DMF (40 mL). After column chromatography using  $\text{CH}_2\text{Cl}_2 : \text{CH}_3\text{OH} = 70 : 1$ , as an eluent compounds **3** (3 g, 46%, m.p. = 199–200 °C) and **4** (924 mg, 16%, m.p. = 129–130 °C) were isolated as white powder. **3**:  $^1\text{H-NMR}$  (300 MHz, DMSO) ( $\delta/\text{ppm}$ ): 8.4 (1H, s, H-6), 4.6 (4H, t, H-1', H-1'',  $J = 1.8 \text{ Hz}$ ), 3.5 (1H, t, H-3',  $J = 2.4 \text{ Hz}$ ), 3.2 (1H, t, H-3'',  $J = 2.4 \text{ Hz}$ ) ppm.  $^{13}\text{C-NMR}$  (150 MHz, DMSO) ( $\delta/\text{ppm}$ ): 159.0 (C-4), 149.5 (C-2), 147.8 (C-6), 78.6 (C-2'), 78.1 (C-2''), 76.3 (C-3'), 73.4 (C-3''), 67.5 (C-5), 38.2 (C-1'), 31.4 (C-1'') ppm. Anal. calcd. for  $\text{C}_{10}\text{H}_7\text{IN}_2\text{O}_2$ : C, 38.24; H, 2.25; N, 8.92%. Found: C, 38.18; H, 2.25; N, 8.95%. **4**:  $^1\text{H-NMR}$  (300 MHz, DMSO) ( $\delta/\text{ppm}$ ): 11.7 (1H, s, NH), 8.2 (1H, s, H-6), 4.5 (2H, d, H-1',  $J = 2.4 \text{ Hz}$ ), 3.4 (1H, t, H-3',  $J = 2.4 \text{ Hz}$ ) ppm.  $^{13}\text{C-NMR}$  (150 MHz, DMSO) ( $\delta/\text{ppm}$ ): 160.9 (C-4), 150 (C-2), 148.7 (C-6), 78.3 (C-2'), 75.9 (C-3'), 68.9 (C-5), 36.9 (C-1') ppm. Anal. calcd. for  $\text{C}_7\text{H}_5\text{IN}_2\text{O}_2$ : C, 30.46; H, 1.83; N, 10.15%. Found: C, 30.40; H, 1.82; N, 10.20%.

#### 4.2.3. General procedure for the synthesis of 5-bromo-N-1,N-3-di[4-(1-aryl-1,2,3-triazol-4-yl)methyl]pyrimidine-2,4-dione derivatives (**5–8**)

**1** was dissolved in DMF and corresponding aromatic azide (2.1 eq), water solution (1 mL) of sodium ascorbate (0.3 eq) and water solution (1 mL) of CuSO<sub>4</sub> x 5 H<sub>2</sub>O (0.03 eq) were added. The reaction mixture was stirred for 24 h at room temperature. The progress of the reaction was monitored by TLC. Upon completion, the solvent was removed under reduced pressure and the residue was purified by column chromatography.

4.2.3.1. 5-Bromo-N-1,N-3-di{4-[1-(4-fluorophenyl)-1,2,3-triazol-4-yl]methyl}pyrimidine-2,4-dione (**5**)

**5** was synthesized according to the general procedure from **1** (40 mg, 0.15 mmol) using 1-azido-4-fluorobenzene (0.62 mL, 0.31 mmol), sodium ascorbate (9.9 mg, 0.05 mmol), CuSO<sub>4</sub> x 5 H<sub>2</sub>O (1.1 mg, 4.5 x 10<sup>-3</sup> mmol) and DMF (4 mL). Purification by column chromatography (CH<sub>2</sub>Cl<sub>2</sub> : CH<sub>3</sub>OH = 120 : 1) afforded **5** (42 mg, 52%, m.p. = 180–181 °C) as yellow powder. <sup>1</sup>H-NMR (300 MHz, DMSO) (δ/ppm): 8.8 (1H, s, H-3'), 8.5 (1H, H-3''), 8.5 (1H, H-6), 7.9 (4H, m, H-6',8', H-6'',8''), 7.5 (4H, m, H-5',9', H-5'',9''), 5.2 (4H, m, H-1', H-1'') ppm. <sup>13</sup>C-NMR (150 MHz, DMSO) (δ/ppm): 162.5 (C-7', d, *J* = 245.7 Hz, C-F), 162.4 (C-7'', d, 232.5 Hz, C-F), 158 (C-4), 150.1 (C-2), 144.2 (C-6), 143.5 (C-2'), 143.1 (C-2''), 133.1 (C-4', C-4'', d, *J* = 2.7 Hz, C-F), 122.4 (C-3'), 122.3 (C-3''), 122.2 (C-5',9', C-5'',9'', d, *J* = 9.2 Hz, C-F), 116.7 (C-6',8', C-6'',8'', d, *J* = 24.1 Hz, C-F), 94.5 (C-5), 44.0 (C-1'), 31.4 (C-1'') ppm. Anal. calcd. for C<sub>22</sub>H<sub>15</sub>BrF<sub>2</sub>N<sub>8</sub>O<sub>2</sub>: C, 48.81; H, 2.79; N, 20.70%. Found: C, 48.87; H, 2.78; N, 20.68%.

4.2.3.2. 5-Bromo-N-1,N-3-di{4-[1-(2-fluorophenyl)-1,2,3-triazol-4-yl]methyl}pyrimidine-2,4-dione (**6**)

**6** was synthesized according to the general procedure using **1** (70 mg, 0.26 mmol), 1-azido-2-fluorobenzene (1.08 mL, 0.54 mmol), sodium ascorbate (15.8 mg, 0.08 mmol) and CuSO<sub>4</sub> x 5 H<sub>2</sub>O (1.9 mg, 7.8 x 10<sup>-3</sup> mmol) in DMF (5 mL). Purification by column chromatography (CH<sub>2</sub>Cl<sub>2</sub> : CH<sub>3</sub>OH = 70 : 1) afforded **6** (82 mg, 58%, m.p. = 165–166 °C) as yellow powder. <sup>1</sup>H-NMR (300 MHz, DMSO) (δ/ppm): 8.9 (1H, s, H-3'), 8.7 (1H, s, H-3''), 8.6 (1H, s, H-6), 7.9–7.7 (4H, m, Ph-H), 7.7 (2H, m, Ph-H), 7.4–7.2 (2H, m, Ph-H), 5.2 (4H, H-1', H-1'') ppm. <sup>13</sup>C-NMR (75 MHz, DMSO) (δ/ppm): 162.9 (C-5', C-5'', d, *J* = 243.75 Hz, C-F), 159.1 (C-4), 150.6 (C-2), 144.6 (C-6), 144.2 (C-2'), 144.0 (C-2''), 138.2 (C-4', C-4'', d, *J* = 21 Hz), 132.3 (C-8', C-8'', d, *J* = 5.7 Hz, C-F),

122.5 (C-3'), 122.1 (C-3''), 116.4 (C-9', C-9''), 115.9 (C-7', C-7''), d,  $J = 4.6$  Hz, C-F), 107.9 (C-6', C-6''), d,  $J = 26.6$  Hz, C-F), 95.0 (C-5), 44.7 (C-1'), 37.7 (C-1'') ppm. Anal. calcd. for  $C_{22}H_{15}BrF_2N_8O_2$ : C, 48.81; H, 2.79; N, 20.70%. Found: C, 48.89; H, 2.78; N, 20.75%.

4.2.3.3. 5-Bromo-N-1,N-3-di{4-[1-(4-chlorophenyl)-1,2,3-triazol-4-yl]methyl}pyrimidine-2,4-dione (**7**)

**7** was synthesized according to the general procedure using **1** (70 mg, 0.26 mmol), 1-azido-4-chlorobenzene (1.08 mL, 0.54 mmol), sodium ascorbate (15.8 mg, 0.08 mmol) and  $CuSO_4 \times 5 H_2O$  (1.9 mg,  $7.8 \times 10^{-3}$  mmol) in DMF (5 mL). Purification by column chromatography ( $CH_2Cl_2 : CH_3OH = 80 : 1$ ) afforded **7** (64 mg, 43%, m.p. = > 200 °C) as yellow powder.  $^1H$ -NMR (300 MHz, DMSO) ( $\delta$ /ppm): 8.8 (1H, s, H-3'), 8.7 (1H, s, H-3''), 8.6 (1H, s, H-6), 7.9 (4H, m, H-6',8', H-6'',8''), 7.7 (4H, m, H-5',9', H-5'',9''), 5.2 (4H, d, H-1', H-1''),  $J = 6.0$  Hz) ppm.  $^{13}C$ -NMR (75 MHz, DMSO) ( $\delta$ /ppm): 159.1 (C-4), 150.5 (C-2), 144.6 (C-6), 144.2 (C-2'), 144.0 (C-2''), 135.8 (C-4'), 135.7 (C-4''), 133.5 (C-7'), 133.4 (C-7''), 130.3 (C-6',8'), 130.2 (C-6'',8''), 122.4 (C-3', C-3''), 122.2 (C-5',9'), 122.1 (C-5'',9''), 95.0 (C-5), 44.7 (C-1'), 37.8 (C-1'') ppm. Anal. calcd. for  $C_{22}H_{15}BrCl_2N_8O_2$ : C, 46.02; H, 2.63; N, 19.51%. Found: C, 46.10; H, 2.62; N, 19.48%.

4.2.3.4. 5-Bromo-N-1,N-3-di{4-[1-(3,5-dichlorophenyl)-1,2,3-triazol-4-yl]methyl}pyrimidine-2,4-dione (**8**)

**8** was synthesized according to the general procedure using **1** (100 mg, 0.37 mmol), 1-azido-3,5-dichlorobenzene (140.8 mg, 0.83 mmol), sodium ascorbate (22.8 mg, 0.11 mmol) and  $CuSO_4 \times 5 H_2O$  (2.5 mg, 0.01 mmol) in DMF (6 mL). Purification by column chromatography (n-hexane : ethyl-acetate = 80 : 1) afforded **8** (70 mg, 30%, m.p. = 109–110 °C) as yellow powder.  $^1H$ -NMR (300 MHz, DMSO) ( $\delta$ /ppm): 8.9 (1H, s, H-3'), 8.5 (2H, s, H-3'', H-6), 8.0 (4H, H-5',9', H-5'',9''), 7.8 (2H, t, H-7', H-7''),  $J = 3.0$  Hz), 5.1 (4H, H-1', H-1'') ppm.  $^{13}C$ -NMR (75 MHz, DMSO) ( $\delta$ /ppm): 158.5 (C-4), 150 (C-2), 144.8 (C-6), 144.3 (C-2'), 144.0 (C-2''), 138.5 (C-4', C-4''), 135.7 (C-6',8', C-6'',8''), 128.6 (C-7', C-7''), 122.8 (C-3', C-3''), 119.1 (C-5',9', C-5'',9''), 94.7 (C-5), 44.6 (C-1'), 31.9 (C-1'') ppm. Anal. calcd. for  $C_{22}H_{13}BrCl_4N_8O_2$ : C, 41.09; H, 2.04; N, 17.42%. Found: C, 40.98; H, 2.04; N, 17.45%.

#### 4.2.4. General procedure for the synthesis of 5-bromo-N-1-[4-(1-aryl-1,2,3-triazol-4-yl)methyl]pyrimidine-2,4-dione derivatives (**9–12**)

To a solution of **2** in *tert*-butanol : water (1 : 1) and DMF corresponding aromatic azide (1.2 eq), Cu(0) (0.82 eq), 1M CuSO<sub>4</sub> (0.2 eq) were added. The reaction mixture was then stirred under microwave irradiation (300 W) at 80 °C during 45 min. The progress of the reaction was monitored by TLC. Upon completion, the solvent was removed under reduced pressure and residue was purified by column chromatography.

##### 4.2.4.1. 5-Bromo-N-1-{4-[1-(4-fluorophenyl)-1,2,3-triazol-4-yl]methyl}pyrimidine-2,4-dione (**9**)

**9** was synthesized according to the general procedure using **2** (50 mg, 0.22 mmol), *tert*-butanol : water (1 : 1) (7 mL), 1-azido-4-fluorobenzene (0.52 mL, 0.26 mmol), Cu(0) (11.4 mg, 0.18 mmol) and 1M CuSO<sub>4</sub> (0.04 mL, 0.04 mmol) in DMF (2 mL). Purification by column chromatography (CH<sub>2</sub>Cl<sub>2</sub> : CH<sub>3</sub>OH = 70 : 1) afforded **9** (66 mg, 81%, m.p. = > 200 °C) as yellow powder. <sup>1</sup>H-NMR (300 MHz, DMSO) (δ/ppm): 11.8 (1H, s, NH), 8.8 (1H, s, H-3'), 8.4 (1H, s, H-6), 8.1–7.8 (2H, m, H-5',9'), 7.6–7.2 (2H, m, H-6',8'), 5.1 (2H, s, H-1') ppm. <sup>13</sup>C-NMR (150 MHz, DMSO) (δ/ppm): 162.4 (C-7', d, *J* = 246.1 Hz, C-F), 160.5 (C-4), 150.9 (C-2), 145.9 (C-6), 144.3 (C-2'), 133.8 (C-4', d, *J* = 3.0 Hz), 123.2 (C-5',9', d, *J* = 9.1 Hz, C-F), 122.8 (C-3'), 117.5 (C-6',8', d, *J* = 22.6 Hz, C-F), 95.9 (C-5), 43.7 (C-1') ppm. Anal. calcd. for C<sub>13</sub>H<sub>9</sub>BrFN<sub>5</sub>O<sub>2</sub>: C, 42.64; H, 2.48; N, 19.13%. Found: C, 42.70; H, 2.47; N, 19.16%.

##### 4.2.4.2. 5-Bromo-N-1-{4-[1-(2-fluorophenyl)-1,2,3-triazol-4-yl]methyl}pyrimidine-2,4-dione (**10**)

**10** was synthesized according to the general procedure using **2** (50 mg, 0.22 mmol), *tert*-butanol : water (1 : 1) (8 mL), 1-azido-2-fluorobenzene (0.52 mL, 0.26 mmol), Cu(0) (11.4 mg, 0.18 mmol) and 1M CuSO<sub>4</sub> (0.04 mL, 0.04 mmol) in DMF (2 mL). Purification by column chromatography (CH<sub>2</sub>Cl<sub>2</sub> : CH<sub>3</sub>OH = 60 : 1) afforded **10** (63 mg, 78%, m.p. = > 200 °C) as yellow powder. <sup>1</sup>H-NMR (300 MHz, DMSO) (δ/ppm): 11.8 (1H, s, NH), 8.9 (1H, s, H-3'), 8.4 (1H, s, H-6), 7.9 (2H, m, Ph-H), 7.7 (1H, m, Ph-H), 7.4 (1H, m, Ph-H), 5.1 (2H, s, H-1') ppm. <sup>13</sup>C-NMR (150 MHz, DMSO) (δ/ppm): 162.7 (C-5', d, *J* = 245.3 Hz, C-F), 159.7 (C-4), 150.1 (C-2), 145.1 (C-6), 143.7 (C-2'), 137.7 (C-4', d, *J* = 26.6 Hz, C-F), 131.8 (C-8', d, *J* = 9.2 Hz, C-F), 121.9 (C-3'), 115.9 (C-9'), 115.4 (C-6', d, *J* = 21.0 Hz, C-F), 107.5 (C-7', d, *J* = 10.6 Hz, C-

F), 95.1 (C-5), 42.9 (C-1') ppm. Anal. calcd. for  $C_{13}H_9BrFN_5O_2$ : C, 42.64; H, 2.48; N, 19.13%. Found: C, 42.67; H, 2.48; N, 19.12%.

#### 4.2.4.3. 5-Bromo-N-1-{4-[1-(4-chlorophenyl)-1,2,3-triazol-4-yl]methyl}pyrimidine-2,4-dione (**11**)

**11** was synthesized according to the general procedure using **2** (50 mg, 0.22 mmol), *tert*-butanol : water (1 : 1) (8 mL), 1-azido-4-chlorobenzene (0.52 mL, 0.26 mmol), Cu(0) (11.4 mg, 0.18 mmol) and 1M  $CuSO_4$  (0.04 mL, 0.04 mmol) in DMF (2 mL). Purification by column chromatography ( $CH_2Cl_2$  :  $CH_3OH$  = 70 : 1) afforded **11** (71 mg, 84%, m.p. = > 200 °C) as yellow power.  $^1H$ -NMR (600 MHz, DMSO) ( $\delta$ /ppm): 11.8 (1H, s, NH), 8.8 (1H, s, H-3'), 8.4 (1H, s, H-6), 7.9 (2H, s, H-5',9'), 7.7 (2H, s, H-6',8'), 5.1 (2H, s, H-1') ppm.  $^{13}C$ -NMR (75 MHz, DMSO) ( $\delta$ /ppm): 160.2 (C-4), 150.6 (C-2), 145.6 (C-6), 144.2 (C-2'), 135.8 (C-4'), 133.5 (C-7'), 130.3 (C-5',9'), 122.3 (C-3'), 122.2 (C-6',8'), 95.6 (C-5), 43.4 (C-1') ppm. Anal. calcd. for  $C_{13}H_9BrClN_5O_2$ : C, 40.81; H, 2.37; N, 18.30%. Found: C, 40.88; H, 2.36; N, 18.33%.

#### 4.2.4.4. 5-Bromo-N-1-{4-[1-(3,5-dichlorophenyl)-1,2,3-triazol-4-yl]methyl}pyrimidine-2,4-dione (**12**)

**12** was synthesized according to the general procedure using **2** (50 mg, 0.22 mmol), *tert*-butanol : water (1 : 1) (8 mL), 1-azido-3,5-dichlorobenzene (82.1 mg, 0.44 mmol), Cu(0) (11.4 mg, 0.18 mmol) and 1M  $CuSO_4$  (0.04 mL, 0.04 mmol) in DMF (2 mL). Purification by column chromatography ( $CH_2Cl_2$  :  $CH_3OH$  = 70 : 1) afforded **12** (69 mg, 75%, m.p. = > 200 °C) as white powder.  $^1H$ -NMR (300 MHz, DMSO) ( $\delta$ /ppm): 11.9 (1H, s, NH), 8.9 (1H, s, H-3'), 8.4 (1H, s, H-6), 8.1 (2H, d, H-5',9'), 7.8 (1H, t, H-7',  $J$  = 1.8 Hz), 5.1 (2H, s, H-1') ppm.  $^{13}C$ -NMR (150 MHz, DMSO) ( $\delta$ /ppm): 159.6 (C-4), 150.1 (C-2), 145.0 (C-6), 143.9 (C-2'), 138.1 (C-4'), 135.2 (C-6',8'), 128.1 (C-7'), 122.1 (C-3'), 118.7 (C-5',9'), 95.2 (C-5), 42.9 (C-1') ppm. Anal. calcd. for  $C_{13}H_8BrCl_2N_5O_2$ : C, 37.44; H, 1.93; N, 16.79%. Found: C, 37.40; H, 1.93; N, 16.81%.

#### 4.2.5. General procedure for the synthesis of 5-iodo-N-1,N-3-di{4-[1-aryl-1,2,3-triazol-4-yl]methyl}pyrimidine-2,4-dione derivatives (**13–19**)

To a solution of **3** in *tert*-butanol : water (1 : 1) and DMF corresponding aromatic azide (2.2 eq), Cu(0) (0.82 eq), 1M  $CuSO_4$  (0.2 eq) were added. The reaction mixture was

then stirred under microwave irradiation (300 W) at 80 °C during 45 min. The solvent was removed under reduced pressure and the residue was purified by column chromatography. The progress of the reaction was monitored by TLC.

4.2.5.1. 5-iodo-*N*-1,*N*-3-di{4-[1-(4-fluorofenil)-1,2,3-triazol-4-yl]methyl}pyrimidine-2,4-dione (**13**) 5-iodo-*N*-1-{4-[1-(4-fluorophenyl)-1,2,3-triazol-4-yl]methyl}-*N*-3-(prop-2-yn-1-yl) pyrimidine-2,4-dione (**14**)

**13** and **14** were synthesized according to the general procedure using **3** (400 mg, 1.27 mmol), *tert*-butanol : water (1 : 1) (3 mL), DMF (5 mL), 1-azido-4-fluorobenzene (5.61 mL, 2.80 mmol), Cu(0) (66 mg, 1.04 mmol) and 1M CuSO<sub>4</sub> (0.26 mL, 0.26 mmol). Purification by column chromatography (CH<sub>2</sub>Cl<sub>2</sub> : CH<sub>3</sub>OH = 100 : 1) afforded **13** (146 mg, 24%, m.p. = > 200 °C) and **14** (100 mg, 17%, m.p. = > 200 °C) as white powder. **13**: <sup>1</sup>H-NMR (300 MHz, DMSO) (δ/ppm): 8.8 (1H, s, H-3'), 8.6 (1H, s, H-6), 8.5 (1H, s, H-3''), 8.0 (4H, m, H-6',8', H-6'',8''), 7.5 (4H, m, H-5',9', H-5'',9''), 5.2 (2H, s, H-1'), 5.2 (2H, s, H-1'') ppm. <sup>13</sup>C-NMR (75 MHz, DMSO) (δ/ppm): 162.1 (C-7', d, *J* = 245.7 Hz, C-F), 160.2 (C-4), 150.9 (C-2), 149.1 (C-6), 144.1 (C-2'), 143.9 (C-2''), 133.5 (C-4', C-4''), 122.8 (C-5',9', C-5'',9''), d, *J* = 8.8 Hz), 122.4 (C-3', C-3''), 117.1 (C-6',8', C-6'',8''), d, *J* = 23.2 Hz), 68.2 (C-5), 44.5 (C-1'), 37.9 (C-1'') ppm. Anal. calcd. for C<sub>22</sub>H<sub>15</sub>F<sub>2</sub>IN<sub>8</sub>O<sub>2</sub>: C, 44.91; H, 2.57; N, 19.05%. Found: C, 45.00; H, 2.57; N, 19.03%. **14**: <sup>1</sup>H-NMR (300 MHz, DMSO) (δ/ppm): 8.8 (1H, s, H-3'), 8.5 (1H, s, H-6), 8.0 (2H, m, H-6',8'), 7.5 (2H, m, H-5',9', *J* = 8.8 Hz), 5.1 (2H, s, H-1'), 4.6 (2H, d, H-1'', *J* = 2.3 Hz), 3.1 (1H, t, H-3'', *J* = 2.3 Hz) ppm. <sup>13</sup>C-NMR (75 MHz, DMSO) (δ/ppm): 162.1 (C-7', d, *J* = 245.9 Hz, C-F), 159.7 (C-4), 150.4 (C-2), 149.2 (C-6), 143.7 (C-2'), 133.5 (C-4', d, *J* = 2.9 Hz, C-F), 122.9 (C-5',9', d, *J* = 8.8 Hz), 122.6 (C-3'), 117.2 (C-6',8'), d, *J* = 23.3 Hz), 79.1 (C-2''), 73.9 (C-3''), 67.8 (C-5), 44.4 (C-1'), 31.9 (C-1'') ppm. Anal. calcd. for C<sub>15</sub>H<sub>9</sub>FIN<sub>5</sub>O<sub>2</sub>: C, 41.21; H, 2.08; N, 16.02%. Found: C, 41.29; H, 2.07; N, 16.07%.

4.2.5.2. 5-Iodo-*N*-1,*N*-3-di{4-[1-(2-fluorophenyl)-1,2,3-triazol-4-yl]methyl}pyrimidine-2,4-dione (**15**) and 5-iodo-*N*-1-{4-[1-(2-fluorophenyl)-1,2,3-triazol-4-yl]methyl}-*N*-3-(prop-2-yn-1-yl)pyrimidine-2,4-dione (**16**)

**15** and **16** were synthesized according to the general procedure using **3** (350 mg, 1.11 mmol), *tert*-butanol : water (1 : 1) (3 mL), DMF (5 mL), 1-azido-2-fluorobenzene (4.9

mL, 2.45 mmol), Cu(0) (58 mg, 0.9 mmol) and 1M CuSO<sub>4</sub> (0.23 mL, 0.23 mmol). Purification by column chromatography (CH<sub>2</sub>Cl<sub>2</sub> : CH<sub>3</sub>OH = 100 : 1) afforded **15** (227 mg, 35%, m.p. = > 200 °C) and **16** (188 mg, 29%, m.p. = 177–183 °C) as white powder. **15**: <sup>1</sup>H-NMR (300 MHz, DMSO) (δ/ppm): 8.6 (1H, d, H-3', *J* = 2.0 Hz), 8.5 (1H, s, H-6), 8.4 (1H, d, H-3'', *J* = 2.1 Hz), 7.8 (2H, H-6', H-6''), 7.7–7.3 (6H, H-7',8',9', H-7'',8'',9'', m, Ph-H), 5.2 (4H, H-1', H-1'') ppm. <sup>13</sup>C-NMR (75 MHz, DMSO) (δ/ppm): 161.9 (C-4), 154.2 (C-5', C-5'', d, *J* = 250.6 Hz), 151 (C-2), 149.1 (C-6), 143.5 (C-2'), 143.3 (C-2''), 131.9 (C-9', C-9'', d, *J* = 8.3 Hz, C-F), 126.3 (C-3'), 126.3 (C-8', C-8'', d, *J* = 3.7 Hz, C-F), 125.9 (C-7', C-7'', d, *J* = 5.25 Hz, C-F), 125.5 (C-4', C-4'', d, *J* = 11 Hz, C-F), 117.5 (C-6', C-6'', d, *J* = 19.5 Hz, C-F), 68.1 (C-5), 44.4 (C-1'), 37.8 (C-7'') ppm. Anal. calcd. for C<sub>22</sub>H<sub>15</sub>F<sub>2</sub>IN<sub>8</sub>O<sub>2</sub>: C, 44.91; H, 2.57; N, 19.05%. Found: C, 44.99; H, 2.56; N, 19.09%. **16**: <sup>1</sup>H-NMR (300 MHz, DMSO) (δ/ppm): 8.6 (1H, d, H-3', *J* = 2.1 Hz), 8.5 (1H, s, H-6), 7.8 (1H, dd, H-6', *J* = 7.9 Hz, *J* = 1.6 Hz), 7.6–7.4 (3H, m, H-7',8',9'), 5.1 (2H, s, H-1'), 4.6 (2H, d, H-1'', *J* = 2.4 Hz), 3.1 (1H, t, H-3'', *J* = 2.4 Hz) ppm. <sup>13</sup>C-NMR (75 MHz, DMSO) (δ/ppm): 161.9 (C-4), 156.4 (C-5', d, *J* = 250.5 Hz), 152.6 (C-2), 151.5 (C-6), 145.4 (C-2'), 134.1 (C-9', d, *J* = 7.9 Hz), 128.6 (C-3'), 128.3 (C-8', *J* = 3.8 Hz, C-F), 127.9 (C-7', d, *J* = 4.4 Hz, C-F), 127.1 (C-4', d, *J* = 11 Hz, C-F), 119.8 (C-6', d, *J* = 19.5 Hz, C-F), 81.4 (C-2''), 76.1 (C-3''), 69.9 (C-5), 46.4 (C-1'), 34.1 (C-1'') ppm. Anal. calcd. for C<sub>15</sub>H<sub>9</sub>FIN<sub>5</sub>O<sub>2</sub>: C, 41.21; H, 2.08; N, 16.02%. Found: C, 41.19; H, 2.09; N, 16.04%.

4.2.5.3. 5-Iodo-*N*-1,*N*-3-di{4-[1-(4-chlorophenyl)-1,2,3-triazol-4-yl]methyl}pyrimidine-2,4-dione (**17**) and 5-iodo-*N*-1-{4-[1-(4-chlorophenyl)-1,2,3-triazol-4-yl]methyl}-*N*-(3-prop-2-yn-1-yl)pyrimidine-2,4-dione (**18**)

**17** and **18** were synthesized according to the general procedure using **3** (400 mg, 1.27 mmol), *tert*-butanol : water (1 : 1) (3 mL), DMF (5 mL), 1-azido-4-chlorobenzene (5.61 mL, 2.79 mmol), Cu(0) (66.3 mg, 1.04 mmol) and 1M CuSO<sub>4</sub> (0.26 mL, 0.26 mmol). Purification by column chromatography (CH<sub>2</sub>Cl<sub>2</sub> : CH<sub>3</sub>OH = 100 : 1) afforded **17** (140 mg, 22%, m.p. = > 200 °C) and **18** (75 mg, 13%, m.p. = > 200 °C), as yellow powder. **17**: <sup>1</sup>H-NMR (300 MHz, DMSO) (δ/ppm): 8.8 (1H, s, H-3'), 8.7 (1H, s, H-3''), 8.5 (1H, s, H-6), 7.9 (4H, dd, H-5',9', H-5'',9''), 7.7 (4H, dd, H-6',8', H-6'',8''), 5.2 (4H, s, H-1', H-1'') ppm. <sup>13</sup>C-NMR (150 MHz, DMSO) (δ/ppm): 159.6 (C-4), 150.4 (C-2), 148.5 (C-6), 143.8 (C-2'), 143.5 (C-2''), 135.3 (C-7'), 135.3 (C-7''), 133.0 (C-4'), 132.9

(C-4"), 129.8 (C-6',8'), 129.7 (C-6",8"), 121.9 (C-3'), 121.7 (C-5',9', C-5",9"), 121.6 (C-3"), 67.6 (C-5), 44 (C-1'), 37.4 (C-1") ppm. Anal. calcd. for C<sub>23</sub>H<sub>17</sub>Cl<sub>2</sub>IN<sub>8</sub>O<sub>2</sub>: C, 42.54; H, 2.43; N, 17.64%. Found: C, 42.56; H, 2.43; N, 17.66%. **18**: <sup>1</sup>H-NMR δ: 8.8 (1H, s, H-3'), 8.5 (1H, s, H-6), 7.9 (2H, m, H-5',9'), 7.7 (2H, m, H-6',8'), 5.1 (2H, s, H-1'), 4.6 (2H, d, H-1", *J* = 2.4 Hz), 3.1 (1H, t, H-3", *J* = 2.4 Hz) ppm. <sup>13</sup>C-NMR (75 MHz, DMSO) (δ/ppm): 159.1 (C-4), 149.8 (C-2), 148.7 (C-6), 143.3 (C-2'), 135.2 (C-7'), 132.9 (C-4'), 129.8 (C-6',8'), 121.9 (C-3'), 121.6 (C-5',9'), 78.6 (C-2"), 73.3 (C-3"), 67.3 (C-5), 43.8 (C-1'), 31.3 (C-1") ppm. Anal. calcd. for C<sub>16</sub>H<sub>11</sub>ClIN<sub>5</sub>O<sub>2</sub>: C, 41.09; H, 2.37; N, 14.98%. Found: C, 41.07; H, 2.38; N, 14.99%.

#### 4.2.5.4. 5-Iodo-N-1,N-3-di[4-(1-benzyl-1,2,3-triazol-4-yl)methyl]pyrimidine-2,4-dione (**19**)

**19** was synthesized according to the general procedure using **3** (400 mg, 1.27 mmol), *tert*-butanol : water (1 : 1) (3 mL), DMF (5 mL), 4-benzyl azide (5.61 mL, 2.80 mmol), Cu(0) (66.3 mg, 1.04 mmol) and 1M CuSO<sub>4</sub> (0.26 mL, 0.26 mmol). Purification by column chromatography (CH<sub>2</sub>Cl<sub>2</sub> : CH<sub>3</sub>OH = 100 : 1) afforded **19** (735 mg, 99%, m.p. = > 200 °C) as white powder. <sup>1</sup>H-NMR (300 MHz, DMSO) (δ/ppm): 8.4 (1H, s, H-6), 8.2 (1H, s, H-3'), 8 (1H, s, H-3"), 7.3 (10H, m, 2Ph-H), 5.6 (2H, s, H-4'), 5.5 (2H, s, H-4"), 5.1 (2H, s, H-1'), 5 (2H, s, H-1") ppm. <sup>13</sup>C-NMR (75 MHz, DMSO) (δ/ppm): 160.1 (C-4), 150.8 (C-2), 149.1 (C-6), 142.9 (C-2'), 142.7 (C-2"), 136.5 (C-4'), 136.4 (C-4"), 129.2 (C-6',8', C-6",8"), 128.6 (C-7', C-7"), 128.5 (C-5',8', C-5",8"), 124.4 (C-3'), 124.1 (C-3"), 67.9 (C-5), 44.3 (C-1'), 37.9 (C-1") ppm. Anal. calcd. for C<sub>24</sub>H<sub>21</sub>IN<sub>8</sub>O<sub>2</sub>: C, 49.67; H, 3.65; N, 19.31%. Found: C, 49.62; H, 3.65; N, 19.28%.

#### 4.2.6. General procedure for the synthesis of 5-iodo-N-1-[4-(1-aryl-1,2,3-triazol-4-yl)methyl]pyrimidine-2,4-dione derivatives (**20–23**)

To a solution of **4** in a mixture *tert*-butanol : water (1 : 1) and DMF corresponding aromatic azide (1.2 eq), Cu(0) (0.82 eq), 1M CuSO<sub>4</sub> (0.2 eq) were added. The reaction mixture was then stirred under microwave irradiation (300 W) at 80 °C during 45 min. The progress of the reaction was monitored by TLC. Upon completion, the solvent was removed under reduced pressure and residue was purified by column chromatography.

##### 4.2.6.1. 5-Iodo-N-1-{4-[1-(4-fluorophenyl)-1,2,3-triazol-4-yl]methyl}pyrimidine-2,4-dione (**20**)

**20** was synthesized according to the general procedure using **4** (400 mg, 1.45 mmol), *tert*-butanol : water (1 : 1) (3 mL), DMF (5 mL), 1-azido-4-fluorobenzene (3.48 mL, 1.74 mmol), Cu(0) (75 mg, 1.18 mmol) and 1M CuSO<sub>4</sub> (0.30 mL, 0.30 mmol). Purification by column chromatography (CH<sub>2</sub>Cl<sub>2</sub> : CH<sub>3</sub>OH = 100 : 1) afforded **20** (219 mg, 45%, m.p. = > 200 °C) as a white powder. <sup>1</sup>H-NMR (300 MHz, DMSO) (δ/ppm): 11.7 (1H, s, NH), 8.8 (1H, s, H-3'), 8.4 (1H, s, H-6), 7.9 (2H, dd, H-6',8', *J* = 9.1 Hz, *J* = 4.7 Hz), 7.5 (2H, t, H-5',9', *J* = 8.8 Hz), 5.1 (2H, s, H-1') ppm. <sup>13</sup>C-NMR (75 MHz, DMSO) (δ/ppm): 162.1 (C-7', d, *J* = 245.9 Hz, C-F), 161.6 (C-4), 150.9 (C-2), 150.2 (C-6), 144 (C-2'), 128.6 (C-4'), 122.9 (C-5',9', d, *J* = 8.8 Hz, C-F), 122.5 (C-3'), 117.2 (C-6',8', d, *J* = 23.3 Hz, C-F), 69.2 (C-5), 43.1 (C-1') ppm. Anal. calcd. for C<sub>13</sub>H<sub>9</sub>FIN<sub>5</sub>O<sub>2</sub>: C, 37.79; H, 2.20; N, 16.95%. Found: C, 37.76; H, 2.21; N, 16.97%.

#### 4.2.6.2. 5-Iodo-N-1-{4-[1-(2-fluorophenyl)-1,2,3-triazol-4-yl]methyl}pyrimidine-2,4-dione (**21**)

**21** was synthesized according to the general procedure using **4** (200 mg, 0.72 mmol), *tert*-butanol : water (1 : 1) (8 mL), DMF (2 mL), 1-azido-2-fluorobenzene (1.73 mL, 0.87 mmol), Cu(0) (37.5 mg, 0.60 mmol) and 1M CuSO<sub>4</sub> (0.14 mL, 0.14 mmol). Purification by column chromatography (CH<sub>2</sub>Cl<sub>2</sub> : CH<sub>3</sub>OH = 70 : 1) afforded **21** (189 mg, 30%, m.p. = > 200 °C) as white powder. <sup>1</sup>H-NMR (300 MHz, DMSO) (δ/ppm): 11.7 (1H, s, NH), 8.6 (1H, s, H-3'), 8.4 (1H, s, H-6), 7.9 (1H, m, H-6'), 7.6–7.4 (3H, m, H-7',8',9'), 5.1 (2H, s, H-1') ppm. <sup>13</sup>C-NMR (75 MHz, DMSO) (δ/ppm): 161 (C-4), 157.4 (C-5', d, *J* = 247.5 Hz, C-F), 150.5 (C-2), 149.7 (C-6), 142.9 (C-2'), 136.3 (C-9'), 131.3 (C-8', d, *J* = 1.5 Hz, C-F), 125.9 (C-3'), 125.5 (C-7', d, *J* = 3.8 Hz, C-F), 125.0 (C-4', *J* = 4.5 Hz, C-F), 117 (C-6', d, *J* = 19.3 Hz, C-F), 68.6 (C-5), 42.9 (C-1') ppm. Anal. calcd. for C<sub>13</sub>H<sub>9</sub>FIN<sub>5</sub>O<sub>2</sub>: C, 37.79; H, 2.20; N, 16.95%. Found: C, 37.81; H, 2.20; N, 16.96%.

#### 4.2.6.3. 5-Iodo-N-1-{4-[1-(4-chlorophenyl)-1,2,3-triazol-4-yl]methyl}pyrimidine-2,4-dione (**22**)

**22** was synthesized according to the general procedure using **4** (200 mg, 0.72 mmol), *tert*-butanol : water (1 : 1) (8 mL), DMF (2 mL), 1-azido-4-chlorobenzene 1.73 mL, 0.87 mmol), Cu(0) (37.5 mg, 0.60 mmol) and 1M CuSO<sub>4</sub> (0.14 mL, 0.14 mmol). Purification by column chromatography (CH<sub>2</sub>Cl<sub>2</sub> : CH<sub>3</sub>OH = 70 : 1) afforded **22** (391 mg, 63%, m.p. = > 200 °C) as white powder. <sup>1</sup>H-NMR (300 MHz, DMSO) (δ/ppm):

11.7 (1H, s, NH), 8.8 (1H, s, H-3'), 8.4 (1H, s, H-6), 7.9 (2H, d, H-5',9',  $J = 8.8$  Hz), 7.7 (2H, d, H-6',8',  $J = 8.8$  Hz), 5.1 (2H, s, H-1') ppm.  $^{13}\text{C}$ -NMR (75 MHz, DMSO) ( $\delta/\text{ppm}$ ): 161.6 (C-4), 151 (C-2), 150.1 (C-6), 144.3 (C-2'), 135.8 (C-4'), 133.5 (C-7'), 130.3 (C-5',9'), 122.2 (C-3'), 122.2 (C-6',8'), 69.2 (C-5), 43.2 (C-1') ppm. Anal. calcd. for  $\text{C}_{13}\text{H}_9\text{ClIN}_5\text{O}_2$ : C, 36.35; H, 2.11; N, 16.30%. Found: C, 36.39; H, 2.12; N, 16.27%.

#### 4.2.6.4. 5-Iodo-N-1-[4-(1-benzyl-1,2,3-triazol-4-yl)methyl]pyrimidine-2,4-dione (**23**)

**23** was synthesized according to the general procedure using **4** (200 mg, 0.72 mmol), *tert*-butanol : water (1 : 1) (8 mL), DMF (2 mL), benzyl azide (1.73 mL, 0.87 mmol), Cu(0) (46 mg, 0.60 mmol) and 1M  $\text{CuSO}_4$  (0.15 mL, 0.15 mmol). Purification by column chromatography ( $\text{CH}_2\text{Cl}_2$  :  $\text{CH}_3\text{OH} = 70 : 1$ ) afforded **23** (317 mg, 55%, m.p. =  $> 200$  °C) as white powder.  $^1\text{H}$ -NMR (300 MHz, DMSO) ( $\delta/\text{ppm}$ ): 11.6 (1H, s, NH), 8.3 (1H, s, H-3'), 8.1 (1H, s, H-6), 7.4 (5H, m, Ph-H), 5.5 (2H, s, H-4'), 4.9 (2H, s, H-1') ppm.  $^{13}\text{C}$ -NMR (150 MHz, DMSO) ( $\delta/\text{ppm}$ ): 161 (C-4), 150.4 (C-2), 149.7 (C-6), 142.5 (C-2'), 135.9 (C-5'), 128.7 (C-6',10'), 128.1 (C-8'), 127.9 (C-7',9'), 123.7 (C-3'), 68.4 (C-5), 53.8 (C-4'), 42.7 (C-1') ppm. Anal. calcd. for  $\text{C}_{14}\text{H}_{12}\text{IN}_5\text{O}_2$ : C, 41.09; H, 2.96; N, 17.12%. Found: C, 41.12; H, 2.97; N, 17.10%.

#### 4.2.7. General procedure for the synthesis of furo[2,3-*d*]pyrimidine-2-one derivatives (**24a,b–37a,b**)

To the solution of dry compounds **20–23** in anhydrous toluene, tetrakis(triphenylphosphine)palladium(0) ( $\text{PPh}_3$ ) $_4\text{Pd}$  (0.1 eq), CuI (0.3 eq) and *N,N*-diisopropylethylamine (*N,N*-DIPEA) (6.0 eq) were added under argon atmosphere. Corresponding terminal alkyne (3.0 eq) was added dropwise. The reaction mixture was stirred overnight at 80 °C. Amberlyt IRA 400 and active coal were added and the stirring was continued for 20 min. The solid was filtered off and the filtrate was evaporated. The residue was purified by column chromatography.

##### 4.2.7.1. 5-(5-Chloropent-1-yn-1-yl)-6-(3-chloroprop-1-yl)-N-3- $\{[1-(4\text{-fluorophenyl})-1,2,3\text{-triazol-4-yl}]\text{methyl}\}$ furo[2,3-*d*]pyrimidine-2-one (**24a**) and 6-(3-chloroprop-1-yl)-N-3- $\{[1-(4\text{-fluorophenyl})-1,2,3\text{-triazol-4-yl}]\text{methyl}\}$ furo[2,3-*d*]pyrimidine-2-one (**24b**)

**24a** and **24b** were synthesized following the general procedure for **24a,b–37a,b**. Reagents: **20** (35 mg, 0.08 mmol), anhydrous toluene (5 mL), CuI (3.8 mg, 0.02 mmol), (PPh<sub>3</sub>)<sub>4</sub>Pd (9.2 mg, 0.008 mmol), *N,N*-DIPEA (0.08 mL, 0.48 mmol) and 5-chloropent-1-yne (0.03 mL, 0.24 mmol). Purification by column chromatography (CH<sub>2</sub>Cl<sub>2</sub> : CH<sub>3</sub>OH = 200 : 1) gave **24a** (39 mg, 66%, m.p. > 200 °C) and **24b** (15 mg, 30%, m.p. > 200 °C) as white powder. **24a**: <sup>1</sup>H-NMR (300 MHz, DMSO) (δ/ppm): 8.8 (1H, s, H-3'), 8.8 (1H, s, H-4), 7.9 (2H, m, H-6',8'), 7.5 (2H, m, H-5',9'), 5.3 (2H, s, H-1'), 3.8 (2H, t, H-5''', *J* = 6.4 Hz), 3.7 (2H, t, H-5'', *J* = 6.3 Hz), 2.9 (2H, t, H-3''', *J* = 7.2 Hz), 2.7 (2H, t, H-3'', *J* = 6.9 Hz), 2.1 (2H, m, H-4'''), 2.1 (2H, m, H-4'') ppm. <sup>13</sup>C-NMR (75 MHz, DMSO) (δ/ppm): 170.6 (C-6), 162.1 (C-7', d, *J* = 245.7 Hz, C-F), 159.9 (C-7a), 154.7 (C-2), 144 (C-2'), 143 (C-4), 133.5 (C-4'), 122.8 (C-5',9', d, *J* = 10.9 Hz, C-F), 122.6 (C-3'), 117.2 (C-6',8', d, *J* = 23.2 Hz, C-F), 106.8 (C-4a), 98.4 (C-5), 96.5 (C-2'''), 69.4 (C-1'''), 46.4 (C-1'), 44.7 (C-5'''), 44.6 (C-5''), 31.3 (C-4'''), 29.9 (C-4''), 24.5 (C-3'''), 16.9 (C-3'') ppm. Anal. calcd. for C<sub>21</sub>H<sub>20</sub>C<sub>12</sub>FN<sub>5</sub>O<sub>2</sub>: C, 54.32; H, 4.34; N, 15.08%. Found: C, 54.28; H, 4.35; N, 15.10%. **24b**: <sup>1</sup>H-NMR (300 MHz, DMSO) (δ/ppm): 8.8 (1H, s, H-3'), 8.7 (1H, s, H-4), 8 (2H, m, H-6',8'), 7.5 (2H, m, H-5',9'), 6.6 (1H, s, H-5), 5.3 (2H, s, H-1'), 3.7 (2H, t, H-5'', *J* = 6.4 Hz), 2.8 (2H, t, H-3'', *J* = 7.3 Hz), 2.1 (2H, m, H-4'') ppm. <sup>13</sup>C-NMR (75 MHz, DMSO) (δ/ppm): 172.1 (C-6), 162.1 (C-7', d, *J* = 245.9 Hz, C-F), 157.3 (C-7a), 154.8 (C-2), 143.9 (C-2'), 142.6 (C-4), 133.5 (C-4'), 122.9 (C-5',9', d, *J* = 8.8 Hz, C-F), 122.8 (C-3'), 117.2 (C-6',8', d, *J* = 23.2 Hz, C-F), 107.2 (C-4a), 100.7 (C-5), 46.1 (C-1'), 44.8 (C-5''), 29.9 (C-4''), 25.3 (C-3'') ppm. Anal. calcd. for C<sub>18</sub>H<sub>15</sub>ClFN<sub>5</sub>O<sub>2</sub>: C, 55.75; H, 3.90; N, 18.06%. Found: C, 55.71; H, 3.89; N, 18.04%.

#### 4.2.7.2. *N*-3-[[1-(4-Fluorophenyl)-1,2,3-triazol-4-yl]methyl]-6-(hex-1-yl)-5-(oct-1-yn-1-yl)furo[2,3-*d*]pyrimidine-2-one (**25a**)

**25a** was synthesized following the general procedure for **24a,b–37a,b**. Reagents: **20** (35 mg, 0.08 mmol), anhydrous toluene (5 mL), CuI (3.8 mg, 0.02 mmol), (PPh<sub>3</sub>)<sub>4</sub>Pd (9.2 mg, 0.008 mmol), *N,N*-DIPEA (0.08 mL, 0.48 mmol) and oct-1-yne (0.04 mL, 0.24 mmol). Purification by column chromatography (CH<sub>2</sub>Cl<sub>2</sub> : CH<sub>3</sub>OH = 200 : 1) afforded **25a** (22 mg, 65%, m.p. > 200 °C) as white powder. **25a**: <sup>1</sup>H-NMR (300 MHz, DMSO) (δ/ppm): 8.8 (1H, s, H-3'), 8.8 (1H, s, H-4), 8 (1H, m, H-6',8'), 7.4 (2H, t, H-5',9', *J* = 8.8 Hz), 5.3 (2H, s, H-1'), 2.7 (2H, t, H-3'', *J* = 7.1 Hz), 2.5 (2H, m, H-3'''), 1.7–1.4 (6H, m, H-4''', H-4'', H-5'''), 1.3 (10H, m, H-5''', H-6''', H-7''', H-6'', H-7''), 0.9

(6H, t, H-8''', H-8'') ppm.  $^{13}\text{C}$ -NMR (75 MHz, DMSO) ( $\delta$ /ppm): 170.6 (C-6), 162.1 (C-7', d,  $J = 245.7$  Hz, C-F), 161.2 (C-7a), 154.7 (C-2), 144 (C-2'), 142.7 (C-4), 133.5 (C-4'), 122.9 (C-5',9', d,  $J = 8.8$  Hz), 122.6 (C-3'), 117.2 (C-6',8', d,  $J = 23.3$  Hz), 106.9 (C-4a), 98.1 (C-5), 97.8 (C-2'''), 69 (C-1'''), 46.3 (C-1'), 31.2 (C-6'', C-6'''), 28.4 (C-5'', C-5'''), 28.3 (C-1''), 26.9 (C-4'', C-4'''), 22.5 (C-7'', C-7'''), 19.3 (C-3'''), 14.4 (C-8'', C-8''') ppm. Anal. calcd. for  $\text{C}_{21}\text{H}_{22}\text{FN}_5\text{O}_2$ : C, 63.78; H, 5.61; N, 17.71%. Found: C, 63.79; H, 5.60; N, 17.75%.

4.2.7.3. 6-Cyclopropyl-5-(cyclopropylethyn-1-yl)-N-3- $\{[1-(2\text{-fluorophenyl})-1,2,3\text{-triazol-4-yl]methyl}\}$ furo[2,3-*d*]pyrimidine-2-one (**26a**)

**26a** was synthesized following the general procedure for **24a,b–37a,b**. Reagents: **21** (70 mg, 0.17 mmol), anhydrous toluene (8 mL), CuI (9.7 mg, 0.05 mmol),  $(\text{PPh}_3)_4\text{Pd}$  (23.1 mg, 0.017 mmol), *N,N*-DIPEA (0.2 mL, 1.02 mmol) and cyclopropylethyne (0.04 mL, 0.51 mmol). Purification by column chromatography ( $\text{CH}_2\text{Cl}_2$  :  $\text{CH}_3\text{OH} = 150 : 1$ ) afforded **26a** (25 mg, 40%, m.p. = 105–106 °C) as yellow powder. **26a**:  $^1\text{H}$ -NMR (300 MHz, DMSO) ( $\delta$ /ppm): 8.8 (1H, s, H-3'), 8.6 (1H, s, H-4), 7.8 (1H, t, Ph-H,  $J = 6.3$  Hz), 7.6 (2H, m, Ph-H), 7.4 (1H, t, Ph-H,  $J = 7.8$  Hz), 5.3 (2H, s, H-1'), 2.2 (1H, m, H-3'''), 1.6 (1H, m, H-3''), 1.1–0.8 (8H, m, H-5''', H-5'', H-4''', H-4'') ppm.  $^{13}\text{C}$ -NMR (150 MHz, DMSO) ( $\delta$ /ppm): 169.6 (C-6), 161.1 (C-7a), 154.2 (C-2), 153.8 (C-5', d,  $J = 250.7$  Hz, C-F), 142.9 (C-2'), 141.3 (C-4), 131.3 (C-9', d,  $J = 7.6$  Hz, C-F), 125.9 (C-3'), 125.5 (C-7', d,  $J = 4.5$  Hz, C-F), 125.2 (C-8'), 124.6 (C-4', d,  $J = 10.6$  Hz, C-F), 117.1 (C-6', d,  $J = 19.6$  Hz, C-F), 106.9 (C-4a), 100.4 (C-5), 95.7 (C-2'''), 63.4 (C-1'''), 45.6 (C-1'), 8.9 (C-3'''), 8.6 (C-4''', C-5'''), 7.5 (C-4'', C-5''), 0.1 (C-3'') ppm. Anal. calcd. for  $\text{C}_{23}\text{H}_{18}\text{FN}_5\text{O}_2$ : C, 66.50; H, 4.37; N, 16.86%. Found: C, 66.45; H, 4.38; N, 16.82%.

4.2.7.4. 6-(3-Chloroprop-1-yl)-N-3- $\{[1-(2\text{-fluorophenyl})-1,2,3\text{-triazol-4-yl]methyl}\}$ furo[2,3-*d*]pyrimidine-2-one (**27b**)

**27b** was synthesized following the general procedure for **24a,b–37a,b**. Reagents: **21** (20 mg, 0.05 mmol), anhydrous toluene (5 mL), CuI (1.9 mg, 0.01 mmol),  $(\text{PPh}_3)_4\text{Pd}$  (5.8 mg, 0.005 mmol), *N,N*-DIPEA (0.05 mL, 0.3 mmol) and 5-chloropent-1-yne (0.01 mL, 0.15 mmol). Purification by column chromatography ( $\text{CH}_2\text{Cl}_2$  :  $\text{CH}_3\text{OH} = 150 : 1$ ) afforded **27b** (10 mg, 54%, m.p. = 170–171 °C) as yellow powder. **27b**:  $^1\text{H}$ -NMR (300

MHz, DMSO) ( $\delta$ /ppm): 8.7 (1H, s, H-3'), 8.6 (1H, s, H-4), 7.8–7.6 (1H, m, Ph-H), 7.6 (2H, m, Ph-H), 7.5 (1H, m, Ph-H), 6.6 (1H, s, H-5), 5.3 (2H, s, H-1'), 3.7 (2H, t, H-5",  $J = 6.3$  Hz), 2.8 (2H, t, H-3",  $J = 7.2$  Hz), 2.1 (2H, m, H-4") ppm.  $^{13}\text{C-NMR}$  (75 MHz, DMSO) ( $\delta$ /ppm): 172.1 (C-6), 157.3 (C-7a), 154.7 (C-2), 154.2 (C-5', d,  $J = 249.1$  Hz, C-F), 143.2 (C-2'), 142.7 (C-4), 132.5 (C-9', d,  $J = 2.6$  Hz, C-F), 126.3 (C-8'), 126 (C-7', d,  $J = 3.7$  Hz, C-F), 125.8 (C-3'), 125.1 (C-4', d,  $J = 10.7$  Hz, C-F), 117.7 (C-6', d,  $J = 19.4$  Hz, C-F), 107.1 (C-4a), 100.7 (C-5), 45.9 (C-1'), 44.8 (C-5"), 29.8 (C-3"), 25.3 (C-4") ppm. Anal. calcd. for  $\text{C}_{18}\text{H}_{15}\text{ClFN}_5\text{O}_2$ : C, 55.75; H, 3.90; N, 18.06%. Found: C, 55.79; H, 3.91; N, 18.08%.

4.2.7.5. *N*-3- $\{[1-(2\text{-Fluorophenyl})-1,2,3\text{-triazol-4-yl}]methyl\}$ -6-(4-pentylphenyl)-5-(4-pentylphenyl)ethyn-1-ylfuro[2,3-*d*]pyrimidine-2-one (**28a**)

**28a** was synthesized following the general procedure for **24a,b–37a,b**. Reagents: **21** (20 mg, 0.05 mmol), anhydrous toluene (8 mL), CuI (1.9 mg, 0.01 mmol),  $(\text{PPh}_3)_4\text{Pd}$  (5.8 mg, 0.005 mmol), *N,N*-DIPEA (0.05 mL, 0.3 mmol) and 1-ethynyl-4-pentylbenzene (0.03 mL, 0.15 mmol). Purification by column chromatography ( $\text{CH}_2\text{Cl}_2$  :  $\text{CH}_3\text{OH} = 150 : 1$ ) yielded **28a** (15 mg, 49%, m.p. = 165–166 °C) as yellow powder. **28a**:  $^1\text{H-NMR}$  (600 MHz, DMSO) ( $\delta$ /ppm): 9.1 (1H, s, H-3'), 8.6 (1H, s, H-4), 8.1 (2H, Ph-H), 7.8–7.6 (4H, m, H-6',7',8',9'), 7.6–7.3 (6H, Ph-H), 5.4 (2H, s, H-1'), 2.7–2.6 (4H, m, H-7"', H-7''), 1.6–1.5 (4H, m, H-8"', 8''), 1.3 (8H, m, H-9"', H-9'', H-10"', H-10''), 0.9 (6H, H-11"', H-11'') ppm.  $^{13}\text{C-NMR}$  (75 MHz, DMSO) ( $\delta$ /ppm): 170.3 (C-6), 161.7 (C-7a), 155.9 (C-2), 155.9 (C-5', d,  $J = 212.3$  Hz, C-F), 145.7 (C-2'), 143.2 (C-4), 133.5 (C-3''), 131.9 (C-9'), 131.7 (C-5a"',b"', C-5a'',b''), 129.7 (C-4a"',b"', C-4a'',b''), 129.3 (C-7'), 127.4 (C-3''), 126.4 (C-3'), 126.4 (C-8), 125.9 (C-4', d,  $J = 18.9$  Hz, C-F), 119.3 (C-3''), 117.6 (C-6', d,  $J = 19.5$  Hz, C-F), 107.8 (C-4a), 98.6 (C-5), 95.8 (C-2''), 78.8 (C-1''), 46.6 (C-1'), 35.5 (C-7''', C-7''), 31.3 (C-9''', C-9''), 29.1 (C-8''', C-8''), 22.4 (C-10''', C-10''), 14.4 (C-11''', C-11'') ppm. Anal. calcd. for  $\text{C}_{39}\text{H}_{38}\text{FN}_5\text{O}_2$ : C, 74.62; H, 6.10; N, 11.16; O, 5.10%. Found: C, 74.59; H, 6.11; N, 11.19; O, 5.09%.

4.2.7.6. *N*-3- $\{[1-(2\text{-Fluorophenyl})-1,2,3\text{-triazol-4-yl}]methyl\}$ -(6-hex-1-yl)furo[2,3-*d*]pyrimidine-2-one (**29b**)

**29b** was synthesized following the general procedure for **24a,b–37a,b**. Reagents: **21** (20 mg, 0.05 mmol), dry toluene (5 mL), CuI (1.9 mg, 0.01 mmol),  $(\text{PPh}_3)_4\text{Pd}$  (5.8 mg, 0.005 mmol), *N,N*-DIPEA (0.05 mL, 0.3 mmol) and oct-1-yne (0.02 mL, 0.15 mmol).

Purification by column chromatography (CH<sub>2</sub>Cl<sub>2</sub> : CH<sub>3</sub>OH = 150 : 1) yielded **29b** (15 mg, 78%, m.p. = 145–146 °C) as yellow powder. **29b**: <sup>1</sup>H-NMR (300 MHz, DMSO) (δ/ppm): 8.7 (1H, s, H-3'), 8.6 (1H, s, H-4), 7.8 (1H, m Ph-H), 7.7 (2H, m, Ph-H), 7.5 (1H, m, Ph-H), 6.5 (1H, s, H-5), 5.3 (2H, s, H-1'), 2.7 (2H, t, H-3'', J = 7.5 Hz), 1.7 (2H, m, H-7''), 1.4–1.2 (6H, m, H-4'', H-5'', H-6''), 0.9 (3H, t, H-8'', J = 6.8 Hz) ppm. <sup>13</sup>C-NMR (150 MHz, DMSO) (δ/ppm): 171.6 (C-6), 164.5 (C-7a), 158.4 (C-2), 153.8 (C-5', d, J = 250.3 Hz, C-F), 142.8 (C-2'), 141.8 (C-4), 131.9 (C-9', d, J = 2.5 Hz, C-F), 131.4 (C-7', d, J = 9.7 Hz, C-F), 125.9 (C-3'), 125.5 (C-8'), 124.6 (C-4', d, J = 10.7 Hz, C-F), 117.1 (C-6', d, J = 19.5 Hz, C-F), 106.7 (C-4a), 99.5 (C-5), 45.6 (C-1'), 30.8 (C-3''), 27.9 (C-6''), 27.3 (C-5''), 26.3 (C-4''), 21.9 (C-7''), 13.8 (C-8'') ppm. Anal. calcd. for C<sub>21</sub>H<sub>22</sub>FN<sub>5</sub>O<sub>2</sub>: C, 63.78; H, 5.61; N, 17.71%. Found: C, 63.81; H, 5.62; N, 17.68%.

4.2.7.7. *N*-3-*{*[1-(4-Chlorophenyl)-1,2,3-triazol-4-yl]methyl*}*-6-(cycloprop-1-yl)-5-(cyclopropylethyn-1-yl)furo[2,3-*d*]pyrimidine-2-one (**30a**) and *N*-1-*{*[1-(4-chlorophenyl)-1,2,3-triazol-4-yl]methyl*}*-6-(cyclopropyl)furo[2,3-*d*]pyrimidine-2-one (**30b**)

**30a** and **30b** were synthesized following the general procedure for **24a,b–37a,b**. Reagents: **22** (100 mg, 0.23 mmol), dry toluene (10 mL), CuI (13.3 mg, 0.07 mmol), (PPh<sub>3</sub>)<sub>4</sub>Pd (26.6 mg, 0.023 mmol), *N,N*-DIPEA (0.2 mL, 1.15 mmol) and cyclopropylethyne (0.06 mL, 0.69 mmol). Purification by column chromatography (CH<sub>2</sub>Cl<sub>2</sub> : CH<sub>3</sub>OH = 150 : 1) gave **30a** (38 mg, 34%, m.p. = > 200 °C) and **30b** (11 mg, 13%, m.p. = > 200 °C) as yellow powder. **30a**: <sup>1</sup>H-NMR (300 MHz, DMSO) (δ/ppm): 8.8 (1H, s, H-3'), 8.7 (1H, s, H-4), 8.0 (2H, m, H-6',8'), 7.7 (2H, m, H-5',9'), 5.3 (2H, s, H-1'), 2.2 (1H, m, H-3'''), 1.7 (1H, m, H-3''), 1.1 (4H, m, H-5''', H-5''), 1.0 (2H, m, H-4'''), 0.8 (2H, m, H-4'') ppm. <sup>13</sup>C-NMR (75 MHz, DMSO) (δ/ppm): 170.1 (C-6), 161.6 (C-7a), 154.7 (C-2), 144.2 (C-2'), 141.8 (C-4), 135.8 (C-7'), 133.4 (C-4'), 130.3 (C-5',9'), 122.3 (C-6',8'), 122.2 (C-3'), 107.5 (C-4a), 100.9 (C-5), 96.3 (C-2'''), 63.9 (C-1'''), 46.3 (C-1'), 9.4 (C-3'''), 9.1 (C-4'', C-5''), 8.0 (C-4''', C-5'''), 0.4 (C-3'') ppm. Anal. calcd. for C<sub>23</sub>H<sub>18</sub>ClN<sub>5</sub>O<sub>2</sub>: C, 63.96; H, 4.20; N, 16.22%. Found: C, 63.91; H, 4.20; N, 16.25%. **30b**: <sup>1</sup>H-NMR (600 MHz, DMSO) (δ/ppm): 8.8 (1H, s, H-3'), 8.6 (1H, s, H-4), 7.9 (2H, d, H-6',8'), 7.6 (2H, d, H-5',9'), 6.4 (1H, s, H-5), 5.3 (2H, s, H-1'), 2.0 (1H, m, H-3'''), 1.0 (2H, m, H-5''), 0.9 (2H, m, H-4'') ppm. <sup>13</sup>C-NMR (75 MHz, DMSO) (δ/ppm): 166.1 (C-6), 161.7 (C-7a), 154.3 (C-2), 146.6 (C-2'), 141.7 (C-4), 140.2 (C-

7'), 140.1 (C-4'), 130.3 (C-5',9'), 122.3 (C-3'), 122.2 (C-6',8'), 104.5 (C-7), 98.2 (C-5), 46.1 (C-1'), 9.2 (C-3''), 7.3 (C-4'', C-5'') ppm. Anal. calcd. for C<sub>18</sub>H<sub>14</sub>ClN<sub>5</sub>O<sub>2</sub>: C, 58.78; H, 3.84; N, 19.04%. Found: C, 58.80; H, 3.83; N, 19.02%.

4.2.7.8. 5-(5-Chloropent-1-yn-1-yl)-N-3-*{*[1-(4-chlorophenyl)-1,2,3-triazol-4-yl]methyl*}*-6-(3-chloroprop-1-yl)furo[2,3-*d*]pyrimidine-2-one (**31a**) and N-3-*{*[1-(4-chlorophenyl)-1,2,3-triazol-4-yl]methyl*}*-6-(3-chloroprop-1-yl)furo[2,3-*d*]pyrimidine-2-one (**31b**)

**31a** and **31b** were synthesized following the general procedure for **24a,b–37a,b**. Reagents: **22** (70 mg, 0.17 mmol), dry toluene (8 mL), CuI (9.7 mg, 0.05 mmol), (PPh<sub>3</sub>)<sub>4</sub>Pd (19.6 mg, 0.017 mmol), *N,N*-DIPEA (0.2 mL, 1.15 mmol) and 5-chloropent-1-yne (0.05 mL, 0.51 mmol). Purification by column chromatography (CH<sub>2</sub>Cl<sub>2</sub> : CH<sub>3</sub>OH = 150 : 1) gave **31a** (38 mg, 47%, m.p. = > 200 °C) as white powder and **31b** (13 mg, 20%, m.p. = > 200 °C) as brown powder. **31a**: <sup>1</sup>H-NMR (600 MHz, DMSO) (δ/ppm): 8.8 (1H, s, H-3'), 8.8 (1H, s, H-4), 7.9 (2H, d, H-6',8'), 7.7 (2H, d, H-5',9'), 5.3 (2H, s, H-1'), 3.8 (2H, t, H-5'', *J* = 6.0 Hz), 3.7 (2H, t, H-5'', *J* = 6.0 Hz), 2.9 (2H, t, H-3'', *J* = 7.2 Hz), 2.7 (2H, t, H-3'', *J* = 6.6 Hz), 2.1 (2H, m, H-4'''), 2.1 (2H, m, H-4'') ppm. <sup>13</sup>C-NMR (150 MHz, DMSO) (δ/ppm): 170.1 (C-6), 159.5 (C-7a), 154.2 (C-2), 143.6 (C-2'), 142.5 (C-4), 135.2 (C-7'), 132.9 (C-4'), 129.8 (C-5',9'), 121.9 (C-6',8'), 121.7 (C-3'), 106.3 (C-4a), 97.9 (C-5), 96.0 (C-2'''), 68.9 (C-1'''), 45.5 (C-1'), 40.0 (C-5''), 39.7 (C-5'''), 30.8 (C-4''), 29.5 (C-4'''), 23.9 (C-3''), 16.5 (C-3''') ppm. Anal. calcd. for C<sub>23</sub>H<sub>20</sub>Cl<sub>3</sub>N<sub>5</sub>O<sub>2</sub>: C, 54.72; H, 3.99; N, 13.87%. Found: C, 54.70; H, 4.00; N, 13.89%. **31b**: <sup>1</sup>H-NMR (600 MHz, DMSO) (δ/ppm): 8.8 (1H, s, H-3'), 8.7 (H, s, H-4), 7.9 (2H, d, H-6',8'), 7.7 (2H, d, H-5',9', *J* = 8.4 Hz), 6.5 (1H, s, H-5), 5.3 (2H, s, H-1'), 3.7 (2H, t, H-5'', *J* = 6.0 Hz), 2.8 (2H, t, H-3'', *J* = 7.8 Hz), 2.1 (2H, m, H-4'') ppm. <sup>13</sup>C-NMR (75 MHz, DMSO) (δ/ppm): 172.1 (C-6), 157.3 (C-7a), 154.8 (C-2), 144.1 (C-2'), 142.6 (C-4), 135.8 (C-7'), 133.5 (C-4'), 130.3 (C-5',9'), 122.6 (C-3'), 122.2 (C-6',8'), 107.2 (C-4a), 100.7 (C-5), 46.1 (C-1'), 44.8 (C-5''), 29.9 (C-4''), 25.4 (C-3'') ppm. Anal. calcd. for C<sub>18</sub>H<sub>15</sub>Cl<sub>2</sub>N<sub>5</sub>O<sub>2</sub>: C, 53.48; H, 3.74; N, 17.32%. Found: C, 53.51; H, 3.72; N, 17.30%.

4.2.7.9. N-3-*{*[1-(4-Chlorophenyl)-1,2,3-triazol-1-yl]methyl*}*-6-(4-pentylphenyl)-5-(4-pentylphenyl)ethyn-1-ylfuro[2,3-*d*]pyrimidine-2-one (**32a**)

**32a** was synthesized following the general procedure for **24a,b–37a,b**. Reagents: **22** (70 mg, 0.17 mmol), dry toluene (8 mL), CuI (9.7 mg, 0.05 mmol), (PPh<sub>3</sub>)<sub>4</sub>Pd (19.6 mg, 0.017 mmol), *N,N*-DIPEA (0.2 mL, 1.15 mmol) and 1-ethynyl-4-pentylbenzene (0.1 mL, 0.51 mmol). Purification by column chromatography (CH<sub>2</sub>Cl<sub>2</sub> : CH<sub>3</sub>OH = 150 : 1) yielded **32a** (42 mg, 40%, m.p. = > 200 °C) as yellow powder. **32a**: <sup>1</sup>H-NMR (600 MHz, DMSO) (δ/ppm): 9.1 (1H, s, H-3'), 8.8 (1H, s, H-4), 8.1 (2H, d, Ph-H), 7.9 (2H, d, H-5',9'), 7.7 (2H, d, H-6',8'), 7.6–7.3 (6H, m, Ph-H'), 5.4 (2H, s, H-1'), 2.7 (4H, m, H-7'', H-7'''), 1.6 (4H, m, H-8'', H-8'''), 1.3 (8H, m, H-9'', H-9''', H-10'', H-10'''), 0.9 (6H, t, H-11'', H-11''', *J* = 7.2 Hz) ppm. <sup>13</sup>C-NMR (150 MHz, DMSO) (δ/ppm): 169.8 (C-6), 162.2 (C-7a), 154.3 (C-2), 145.2 (C-3'''), 144.3 (C-3''), 143.6 (C-2'), 143.6 (C-4), 135.3 (C-7'), 131.4 (C-5a'',b'''), 129.8 (C-4a'',b'''), 129.2 (C-5a'',b''), 128.8 (C-3'') 125.4 (C-4a'',b''), 121.6 (C-3'), 118.8 (C-3'''), 107.4 (C-4a), 98.2 (C-5), 95.3 (C-2'''), 78.3 (C-1'''), 46.2 (C-1'), 34.9 (C-7'', C-7'''), 30.8 (C-9''), 30.7 (C-9'''), 30.3 (C-8''), 30.2 (C-8'''), 21.8 (C-10'', C-10'''), 13.6 (C-11'', C-11''') ppm. Anal. calcd. for C<sub>39</sub>H<sub>38</sub>ClN<sub>5</sub>O<sub>2</sub>: C, 72.71; H, 5.95; N, 10.87%. Found: C, 72.76; H, 5.94; N, 10.88%.

4.2.7.10. *N*-3-[[1-(4-Chlorophenyl)-1,2,3-triazol-4-yl]methyl]-6-(hex-1-yl)-5-(oct-1-yn-1-yl)furo[2,3-*d*]pyrimidine-2-one (**33a**)

**33a** was synthesized following the general procedure for **24a,b–37a,b**. Reagents: **22** (70 mg, 0.17 mmol), dry toluene (8 mL), CuI (9.7 mg, 0.05 mmol), (PPh<sub>3</sub>)<sub>4</sub>Pd (19.6 mg, 0.017 mmol), *N,N*-DIPEA (0.2 mL, 1.15 mmol) and oct-1-yne (0.07 mL, 0.51 mmol). Purification by column chromatography (CH<sub>2</sub>Cl<sub>2</sub> : CH<sub>3</sub>OH = 150 : 1) afforded **33a** (39 mg, 47%, m.p. = > 200 °C), as yellow powder. **33a**: <sup>1</sup>H-NMR (600 MHz, DMSO) (δ/ppm): 8.8 (1H, s, H-3'), 8.8 (1H, s, H-4), 7.9 (2H, d, H-6',8'), 7.7 (2H, d, H-5',9'), 5.3 (2H, s, H-1'), 2.7 (2H, t, H-3''', *J* = 7.2 Hz), 2.4 (2H, s, H-3''), 1.7 (2H, m, H-4'''), 1.6 (2H, m, H-4''), 1.4 (12H, m, H-5''', H-5'', H-6''', H-6'', H-7''', H-7''), 0.9–0.8 (6H, m, H-8''', H-8'') ppm. <sup>13</sup>C-NMR (75 MHz, DMSO) (δ/ppm): 170.6 (C-6), 161.2 (C-7a), 154.7 (C-2), 144.2 (C-2'), 142.6 (C-4), 135.7 (C-7'), 133.4 (C-4'), 130.3 (C-5'), 122.4 (C-3'), 122.3 (C-6'), 106.9 (C-4a), 98.1 (C-5), 97.8 (C-2''), 69.0 (C-1'''), 46.3 (C-1'), 31.2 (C-4'', C-4'''), 28.4 (C-3'', C-3'''), 26.9 (C-5'''), 26.8 (C-5''), 22.5 (C-6'''), 22.4 (C-6''), 19.3 (C-7'', C-7'''), 14.3 (C-8'', C-8''') ppm. Anal. calcd. for C<sub>29</sub>H<sub>34</sub>ClN<sub>5</sub>O<sub>2</sub>: C, 66.97; H, 6.59; N, 13.47%. Found: C, 67.00; H, 6.60; N, 13.49%.

4.2.7.11. *N*-3-[1-Benzyl-1,2,3-triazol-4-yl)methyl]-6-(cyclopropyl)-5-(cyclopropylethyn-1-yl)furo[2,3-*d*]pyrimidine-2-one (**34a**) and *N*-3-[(1-benzyl-1,2,3-triazol-4-yl)methyl]-6-(cyclopropyl)furo[2,3-*d*]pyrimidine-2-one (**34b**)

**34a** and **34b** were synthesized following the general procedure for **24a,b–37a,b**. Reagents: **23** (70 mg, 0.17 mmol), dry toluene (8 mL), CuI (9.7 mg, 0.05 mmol), (PPh<sub>3</sub>)<sub>4</sub>Pd (19.6 mg, 0.017 mmol), *N,N*-DIPEA (0.2 mL, 1.15 mmol) and cyclopropylethyne (0.04 mL, 0.51 mmol). Purification by column chromatography (CH<sub>2</sub>Cl<sub>2</sub> : CH<sub>3</sub>OH = 150 : 1) afforded **34a** (39 mg, 54%, m.p. = > 200 °C) and **34b** (6 mg, 10%, m.p. = > 200 °C) as yellow powder. **34a**: <sup>1</sup>H-NMR (300 MHz, DMSO) (δ/ppm): 8.7 (1H, s, H-3'), 8.1 (1H, s, H-4), 7.4 (5H, m, Ph-H), 5.6 (2H, s, H-4'), 5.2 (2H, s, H-1'), 2.1 (1H, m, H-3''), 1.6 (1H, m, H-3'''), 1.0 (8H, m, H-5''', H-5'', H-4''', H-4'') ppm. <sup>13</sup>C-NMR (150 MHz, DMSO) (δ/ppm): 169.5 (C-6), 161.0 (C-7a), 154.1 (C-2), 142.4 (C-2'), 141.1 (C-4), 135.9 (C-5'), 128.7 (C-7',9'), 128.1 (C-3'), 128.0 (C-6',10'), 123.9 (C-8'), 106.8 (C-4a), 100.4 (C-5), 95.7 (C-2''), 63.3 (C-1'''), 52.8 (C-4'), 45.8 (C-1'), 8.9 (C-3'''), 8.6 (C-5''', C-4'''), 7.5 (C-5'', C-4''), 0.1 (C-3'') ppm. Anal. calcd. for C<sub>24</sub>H<sub>21</sub>N<sub>5</sub>O<sub>2</sub>: C, 70.06; H, 5.14; N, 17.02%. Found: C, 70.09; H, 5.13; N, 16.98%. **34b**: <sup>1</sup>H-NMR (300 MHz, DMSO) (δ/ppm): 8.6 (1H, s, H-3'), 8.1 (1H, s, H-4), 7.4 (5H, m, Ph-H), 6.4 (1H, s, H-5), 5.6 (2H, s, H-4'), 5.2 (2H, s, H-1'), 2.1–1.9 (1H, m, H-3''), 1.0 (2H, m, H-4''), 0.9 (2H, m, H-5'') ppm. <sup>13</sup>C-NMR (150 MHz, DMSO) (δ/ppm): 171.2 (C-6), 159.2 (C-7a), 154.2 (C-2), 142.5 (C-2'), 141.2 (C-4), 135.9 (C-5'), 128.7 (C-7',9'), 128.1 (C-6',10'), 127.9 (C-3'), 123.9 (C-8'), 106.8 (C-4a), 97.6 (C-5), 52.8 (C-4'), 45.7 (C-1'), 8.7 (C-3''), 6.8 (C-4'', C-5'') ppm. Anal. calcd. for C<sub>19</sub>H<sub>17</sub>N<sub>5</sub>O<sub>2</sub>: C, 65.69; H, 4.93; N, 20.16%. Found: C, 65.72; H, 4.92; N, 20.19%.

4.2.7.12. *N*-3-[(1-Benzyl-1,2,3-triazol-4-yl)methyl]-5-(5-chloropent-1-yn-1-yl)-6-(3-chloroprop-1-yl)furo[2,3-*d*]pyrimidine-2-one (**35a**) and *N*-3-[(1-benzyl-1,2,3-triazol-4-yl)methyl]-6-(3-chloroprop-1-yl)furo[2,3-*d*]pyrimidine-2-one (**35b**)

**35a** and **35b** were synthesized following the general procedure for **24a,b–37a,b**. Reagents: **23** (70 mg, 0.17 mmol), dry toluene (8 mL), CuI (9.7 mg, 0.05 mmol), (PPh<sub>3</sub>)<sub>4</sub>Pd (19.6 mg, 0.017 mmol), *N,N*-DIPEA (0.2 mL, 1.15 mmol) and 5-chloropent-1-yne (0.05 mL, 0.51 mmol). Purification by column chromatography (CH<sub>2</sub>Cl<sub>2</sub> : CH<sub>3</sub>OH = 150 : 1) gave **35a** (50 mg, 60%), as oil and **35b** (15 mg, 22%, m.p. = > 200 °C), as red-brown powder. **35a**: <sup>1</sup>H-NMR (300 MHz, DMSO) (δ/ppm): 8.8 (1H, s, H-3'), 8.2 (1H, s, H-4), 7.4 (5H, m, Ph-H), 5.6 (2H, s, H-1'), 5.2 (2H, s, H-4'), 3.8 (2H, t,

H-5''',  $J = 6.0$  Hz), 3.7 (2H, t, H-5'',  $J = 6.0$  Hz), 2.9 (2H, t, H-3''',  $J = 6.0$  Hz), 2.6 (2H, t, H-3'',  $J = 6.0$  Hz), 2.1 (4H, m, H-4''', C-4'') ppm.  $^{13}\text{C}$ -NMR (150 MHz, DMSO) ( $\delta$ /ppm): 170.0 (C-6) 159.4 (C-7a), 154.1 (C-2), 142.4 (C-2'), 142.3 (C-4), 135.9 (C-5'), 128.7 (C-7',9'), 128.1 (C-6',10'), 128.0 (C-3'), 124.0 (C-8'), 106.2 (C-4a), 97.9 (C-5), 95.9 (C-2'''), 68.9 (C-1'''), 52.8 (C-4'), 44.2 (C-1'), 44.1 (C-5''', C-5''), 30.8 (C-4'''), 29.5 (C-4''), 23.9 (C-3'''), 16.5 (C-3'') ppm. Anal. calcd. for  $\text{C}_{24}\text{H}_{23}\text{Cl}_2\text{N}_5\text{O}_2$ : C, 59.51; H, 4.79; N, 14.46%. Found: C, 59.48; H, 4.80; N, 14.48%. **35b**:  $^1\text{H}$ -NMR (300 MHz, DMSO) ( $\delta$ /ppm): 8.6 (1H, s, H-3'), 8.2 (1H, s, H-4), 7.4 (5H, m, Ph-H), 6.5 (1H, s, H-5), 5.6 (2H, s, H-4'), 5.2 (2H, s, H-1'), 3.7 (2H, t, H-5'',  $J = 6.0$  Hz), 2.8 (2H, t, H-3'',  $J = 6.0$  Hz), 2.1 (2H, m, H-4'') ppm.  $^{13}\text{C}$ -NMR (150 MHz, DMSO) ( $\delta$ /ppm): 171.5 (C-6), 156.7 (C-7a), 154.2 (C-2), 142.4 (C-2'), 142.1 (C-4), 135.9 (C-5'), 128.7 (C-7',9'), 128.1 (C-6',10'), 127.9 (C-3'), 124.0 (C-8'), 106.5 (C-4a), 100.1 (C-5), 52.8 (C-4'), 45.7 (C-1'), 44.3 (C-5''), 29.3 (C-3''), 24.8 (C-4'') ppm. Anal. calcd. for  $\text{C}_{19}\text{H}_{18}\text{ClN}_5\text{O}_2$ : C, 59.45; H, 4.73; N, 18.25%. Found: C, 59.40; H, 4.74; N, 18.27%.

4.2.7.13. *N*-3-[(1-Benzyl-1,2,3-triazol-4-yl)methyl]-6-(4-pentylphenyl)-5-(4-pentylphenyl)ethyn-1-yl)furo[2,3-*d*]pyrimidine-2-one (**36a**)

**36a** was synthesized following the general procedure for **24a,b–37a,b**. Reagents: **23** (70 mg, 0.17 mmol), dry toluene (8 mL), CuI (9.7 mg, 0.05 mmol), ( $\text{PPh}_3$ ) $_4$ Pd (19.6 mg, 0.017 mmol), *N,N*-DIPEA (0.2 mL, 1.15 mmol) and 1-ethynyl-4-pentylbenzene (0.1 mL, 0.51 mmol). Purification by column chromatography ( $\text{CH}_2\text{Cl}_2$  :  $\text{CH}_3\text{OH} = 150 : 1$ ) afforded **36a** (48 mg, 72%, m.p. = > 200 °C) as yellow powder. **36a**:  $^1\text{H}$ -NMR (600 MHz, DMSO) ( $\delta$ /ppm): 9.0 (1H, s, H-3'), 8.2 (1H, s, H-4), 8.1 (2H, d, Ph-H), 7.6–7.3 (6H, m, Ph-H), 7.2 (5H, m, Ph-H), 5.6 (2H, s, H-4'), 5.3 (2H, s, H-1'), 2.6 (4H, dd, H-7''', H-7'',  $J = 7.2$  Hz,  $J = 7.8$  Hz), 1.6 (4H, m, H-8''), 1.3 (8H, m, H-9''', H-10'', H-9'', H-10''), 0.9 (6H, m, H-11''', 11'') ppm.  $^{13}\text{C}$ -NMR (150 MHz, DMSO) ( $\delta$ /ppm): 169.7 (C-6), 154.3 (C-7a), 154.1 (C-2), 145.2 (C-6'''), 144.2 (C-2'), 143.4 (C-4), 143.4 (C-6'''), 135.9 (C-5'), 131.3 (C-5a''',b'''), 129.2 (C-4a''',b'''), 128.8 (C-7',9'), 128.7 (C-6',10'), 128.1 (C-3'), 127.9 (C-5a'',b''), 125.3 (C-3''), 125.3 (C-8'), 124.1 (C-4a'',b''), 118.8 (C-3'''), 107.3 (C-4a), 98.1 (C-5), 95.2 (C-2'''), 78.3 (C-1'''), 52.8 (C-4'), 46.2 (C-1'), 34.9 (C-7'', C-7'''), 30.8 (C-9'', C-9'''), 30.3 (C-8''), 30.2 (C-8'''), 21.9 (C-10'', C-10'''), 13.9 (C-11''), 13.8 (C-11''') ppm. Anal. calcd. for  $\text{C}_{40}\text{H}_{41}\text{N}_5\text{O}_2$ : C, 77.02; H, 6.62; N, 11.23; O, 5.13%. Found: C, 76.98; H, 6.61; N, 11.25; O, 5.12%.

4.2.7.14. *N*-3-[(1-Benzyl-1,2,3-triazol-4-yl)methyl]-6-(hex-1-yl)-5-(oct-1-yn-1-yl)furo[2,3-*d*]pyrimidine-2-one (**37a**) and *N*-3-[(1-benzyl-1,2,3-triazol-4-yl)methyl]-6-(hex-1-yl)furo[2,3-*d*]pyrimidine-2-one (**37b**)

**37a** and **37b** were synthesized following the general procedure for **24a,b–37a,b**. Reagents: **23** (40 mg, 0.09 mmol), dry toluene (8 mL), CuI (5.7 mg, 0.03 mmol), (PPh<sub>3</sub>)<sub>4</sub>Pd (10.4 mg, 0.009 mmol), *N,N*-DIPEA (0.1 mL, 0.54 mmol) and oct-1-yne (0.04 mL; 0.27 mmol). Purification by column chromatography (CH<sub>2</sub>Cl<sub>2</sub> : CH<sub>3</sub>OH = 150 : 1) yielded **37a** (27 mg, 54%), as oil, and **37b** (4 mg, 9%, m.p. = > 200 °C), as brown powder. **37a**: <sup>1</sup>H-NMR (600 MHz, DMSO) (δ/ppm): 8.7 (1H, s, H-3'), 8.2 (1H, s, H-4), 7.4 (5H, m, Ph-H), 5.6 (2H, s, H-4'), 5.2 (2H, s, H-1'), 2.7 (2H, t, H-3'', *J* = 6.6 Hz), 2.5 (2H, t, H-3''', *J* = 6.6 Hz), 1.7 (2H, m, H-4''), 1.6 (2H, m, H-4'''), 1.5 (2H, m, CH<sub>2</sub>), 1.3 (10H, m, CH<sub>2</sub>), 0.9–0.8 (6H, m, H-8'', H-8''') ppm. <sup>13</sup>C-NMR (75 MHz, DMSO) (δ/ppm): 170.5 (C-6), 161.2 (C-7a), 154.6 (C-2), 142.8 (C-2'), 142.6 (C-4), 136.4 (C-5'), 129.2 (C-7', 9'), 128.6 (C-6', 10'), 128.5 (C-3'), 124.5 (C-8'), 106.7 (C-4a), 98.0 (C-5), 97.8 (C-2'''), 68.9 (C-1'''), 53.3 (C-4'), 46.3 (C-1'), 31.2 (C-5''), 31.1 (C-5'''), 28.4 (C-6''), 28.3 (C-6'''), 26.9 (C-4''), 26.8 (C-4'''), 22.5 (C-7''), 22.4 (C-7'''), 19.3 (C-3'', C-3'''), 14.3 (C-8'', C-8''') ppm. Anal. calcd. for C<sub>30</sub>H<sub>37</sub>N<sub>5</sub>O<sub>2</sub>: C, 72.12; H, 7.46; N, 14.02%. Found: C, 72.10; H, 7.47; N, 14.00%. **37b**: <sup>1</sup>H-NMR (600 MHz, DMSO) (δ/ppm): 8.6 (1H, s, H-3'), 8.2 (H, s, H-4), 7.4 (5H, m, Ph-H), 6.4 (1H, s, H-5), 5.6 (2H, s, H-4'), 5.2 (2H, s, H-1'), 2.6 (2H, t, H-3'', *J* = 7.2 Hz), 1.6 (2H, m, H-4''), 1.3 (6H, m, CH<sub>2</sub>), 0.9 (3H, m, H-8'') ppm. <sup>13</sup>C-NMR (75 MHz, DMSO) (δ/ppm): 169.1 (C-6), 164.4 (C-4), 153.7 (C-2), 142.9 (C-2'), 142.3 (C-4), 136.4 (C-5'), 129.2 (C-7',9'), 128.6 (C-6',10'), 128.5 (C-3'), 127.6 (C-8'), 107.1 (C-4a), 99.9 (C-5), 53.3 (C-4'), 46.3 (C-1'), 35.4 (C-3''), 31.3 (C-5''), 28.4 (C-6''), 26.8 (C-4''), 22.4 (C-7''), 14.4 (C-8'') ppm. Anal. calcd. for C<sub>22</sub>H<sub>25</sub>N<sub>5</sub>O<sub>2</sub>: C, 67.50; H, 6.44; N, 17.89%. Found: C, 67.52; H, 6.43; N, 17.91%.

#### 4.3. Crystal structure determination of **34a**

Single crystal of **34a** suitable for X-ray single crystal analysis was obtained at room temperature by partial evaporation from ethanol solution. Data were collected at 295 K on Oxford Diffraction Xcalibur Nova R diffractometer with Ruby detector using mirror-monochromatized CuK<sub>α</sub> radiation ( $\lambda = 1.54184 \text{ \AA}$ ). The *CrysAlisPro* program [40] was used for the data collection and processing. The intensities were corrected for absorption using the multi-scan absorption correction method [40]. The structure was

solved using direct methods with *SIR-2004* [41] and refined by full-matrix least-squares calculations based on  $F^2$  using *SHELXL-2014* [42] integrated in the *WinGX* program package [43]. All hydrogen atoms were included in calculated positions as riding atoms, with *SHELXL-2014* [42] defaults. The atoms of the C14–C16 cyclopropane ring, as well as of the C21–C26 phenyl ring were severely disordered and were refined with fixed occupancy ratio of 70/30% and 60/40%, respectively. Restraints on anisotropic thermal parameters and geometric restraints were applied in their refinement. High electron residual density of  $0.72 \text{ e}\text{\AA}^{-3}$  was observed  $0.62 \text{ \AA}$  from disordered C15 atom. The *PLATON* [44] and *Mercury* [45] programs were used for structure analysis and molecular and crystal structure drawings preparation. The CCDC 1482369 contain the supplementary crystallographic data for this paper. These data can be obtained free of charge from The Cambridge Crystallographic Data Centre via [www.ccdc.cam.ac.uk/data\\_request/cif](http://www.ccdc.cam.ac.uk/data_request/cif).

Crystal data.  $0.18 \times 0.17 \times 0.14 \text{ mm}^3$ ;  $\text{C}_{24}\text{H}_{21}\text{N}_5\text{O}_2$ ,  $M_r = 411.46$ , triclinic, space group  $P \bar{1}$  (No. 2);  $a = 8.9293(3) \text{ \AA}$ ,  $b = 9.6284(4) \text{ \AA}$ ,  $c = 13.8834(4) \text{ \AA}$ ,  $\alpha = 76.513(3)^\circ$ ,  $\beta = 76.627(3)^\circ$ ,  $\gamma = 66.249(4)^\circ$ ,  $V = 1049.67(7) \text{ \AA}^3$ ,  $T = 295 \text{ K}$ ,  $Z = 2$ ;  $\rho = 1.302 \text{ g cm}^{-3}$ ,  $\mu = 0.694 \text{ mm}^{-1}$ , 8690 reflections ( $\theta_{\text{max}} = 69.996^\circ$ ) measured (3943 unique reflections and 3595 with  $I \geq 2\sigma(I)$ ,  $R_{\text{int}} = 0.0209$ , completeness = 99.3%); Final  $R$  indices [ $I > 2\sigma(I)$ ]:  $R_1 = 0.0673$ ,  $wR_2 = 0.2133$ ,  $R$  indices [all data]:  $R_1 = 0.0713$ ,  $wR_2 = 0.2201$ ,  $S = 1.047$  for 361 parameters and 59 restraints, largest diff. peak and hole  $0.724/-0.409 \text{ e}\text{\AA}^{-3}$ .

#### 4.4. Cell culturing

Human cell lines A549 (lung carcinoma), HeLa (cervical carcinoma), SW620 (colorectal adenocarcinoma, metastatic), HepG2 (hepatocellular carcinoma), CFPAC-1 (pancreatic cancer, derived from metastatic: liver) and WI38 (normal fetal lung fibroblasts) as well as NIH 3T3 (mouse embryo fibroblast) were cultured as monolayers and maintained in Dulbecco's modified Eagle medium (DMEM) supplemented with 10% fetal bovine serum (FBS), 2 mM L-glutamine, 100 U/ml penicillin and 100  $\mu\text{g/mL}$  streptomycin in a humidified atmosphere with 5%  $\text{CO}_2$  at  $37^\circ\text{C}$ .

For mitochondrial toxicity studies, HepG2 cells were cultured in media containing DMEM deprived of glucose supplemented with 10 mM galactose, 2 mM glutamine, 5 mM HEPES, 10% FBS, 1 mM sodium pyruvate, 100 U/ml penicillin and 100  $\mu\text{g/mL}$  streptomycin.

Cells were maintained in the media containing galactose for greater than 5 passages before experiments were conducted.

#### 4.5. Proliferation assays

The panel cell lines were inoculated onto a series of standard 96-well microtiter plates on day 0, at 5000 cells per well according to the doubling times of specific cell line. Test agents were then added in five, 10-fold dilutions (0.01 to 100  $\mu$ M) and incubated for further 72 h. Working dilutions were freshly prepared on the day of testing in the growth medium. The solvent (DMSO) was also tested for eventual inhibitory activity by adjusting its concentration to be the same as in the working concentrations (DMSO concentration never exceeded 0.1%). After 72 h of incubation, the cell growth rate was evaluated by performing the MTT assay: experimentally determined absorbance values were transformed into a cell percentage growth (PG) using the formulas proposed by NIH and described previously [46]. This method directly relies on control cells behaving normally at the day of assay because it compares the growth of treated cells with the growth of untreated cells in control wells on the same plate – the results are therefore a percentile difference from the calculated expected value. The  $IC_{50}$  and  $LC_{50}$  values for each compound were calculated from dose-response curves using linear regression analysis by fitting the mean test concentrations that give PG values above and below the reference value. If, however, all of the tested concentrations produce PGs exceeding the respective reference level of effect (*e.g.* PG value of 50) for a given cell line, the highest tested concentration is assigned as the default value (in the screening data report that default value is preceded by a ">" sign). Each test point was performed in quadruplicate in three individual experiments. The results were statistically analyzed (ANOVA, Tukey post-hoc test at  $p < 0.05$ ). Finally, the effects of the tested substances were evaluated by plotting the mean percentage growth for each cell type in comparison to control on dose response graphs.

#### 4.6. Computational details

As a good compromise between accuracy and feasibility, computational analysis was performed using the B97D functional employing the 6-31+G(d) basis set for carbon, nitrogen, oxygen and hydrogen atoms and the Stuttgart-Dresden (SDD) effective core potentials [47] for the inner electrons of iodine and copper atoms and its associated double- $\zeta$  basis set for the outer ones. Thermal corrections were extracted from the corresponding frequency calculations

without the application of scaling factors to calculate the total free energies reported here. To account for the solvation effects, we included the SMD polarizable continuum model with all parameters corresponding to pure toluene ( $\epsilon = 2.3741$ ), giving rise to (SMD)/B97D/6-31+G(d)/SDD model employed here. The choice of this computational setup was prompted by its success in reproducing kinetic and thermodynamic parameters of various organic and organometallic reactions [48]. All of the transition state structures were verified to have the appropriate imaginary frequency from which the corresponding reactants and products were determined using the Intrinsic Reaction Coordinate (IRC) procedure [49].  $pK_a$  values were calculated in absolute fashion employing experimentally determined value of  $\Delta G_{\text{SOLV}}(\text{H}^+) = -231.45 \text{ kcal mol}^{-1}$  in toluene. All of the calculations were performed using the Gaussian 09 software [50].

#### 4.7. *In silico analysis*

Values of n-octanol/water partition coefficients logP for synthesized compounds were calculated by ChemAxon algorithm available within MarvinView Ver. 5.2.6. Predictions of plausible biological targets and pharmacological activities were made by web-service PASS (<http://www.pharmaexpert.ru/passonline/index.php>) which is based on the identification of substructure features typical for active molecules [30].

#### 4.8. *Apoptosis detection*

Detection and quantification of apoptosis and differentiation from necrosis at single cell level was carried out by Annexin-V-FITC Staining kit (Santa Cruz Biotech) according to the manufacturer's instructions. Briefly, cells were seeded into Lab-tek II Chamber Slide with 8 wells and treated with test compounds at their  $2 \times \text{IC}_{50}$  concentrations for 48 h. The cells were washed with Incubation buffer, and Annexin-V-FITC labelling solution was added. After incubation at room temperature for 15 min, chambers and silicon borders of the chamber slides were removed, the cells were fixed with 20% glycerol and analyzed by fluorescence microscopy.

#### 4.9. *Western blot analysis*

Cells were cultured in 6-well plates at seeding density of 200000 cells/well and subjected to treatment with selected compounds at their  $2 \times \text{IC}_{50}$  concentrations for 48 h. Cells were lysed in RIPA buffer containing 20 mM Tris-HCl (pH 7.5), 150 mM NaCl, 1 mM Na<sub>2</sub>

EDTA, 1 mM EGTA, 1% NP-40 and 1% sodium deoxycholate supplemented with protease inhibitor cocktail (Roche). Total proteins (50 µg) were resolved on 12% Tris-glycine polyacrylamide gels and transferred to PVDF membranes. Subsequently, membranes were blocked for 1 h at room temperature with 4% BSA in TBST [50 mmol/L Tris base, 150 mmol/L NaCl, 0.1% Tween 20 (pH 7.5)] and probed overnight at 4 °C with primary antibody against either p-SK1 (ECM Biosciences), ASAH1 (Abcam) or p-Wee1 kinase (Cell Signaling Technology). Membranes were washed with TBST and incubated with either goat anti-mouse (Santa Cruz Biotechnology) or goat anti-rabbit (Santa Cruz Biotechnology) horseradish peroxidase–conjugated secondary antibody at room temperature for 1 h. Individual proteins were visualized by the BM Chemiluminescence Western Blotting Substrate (POD) (Roche) using ImageQuant LAS 500 (GE Healthcare). Densitometry quantitation was determined using the Quantity One 1-D Analysis Software (Bio-Rad, USA).

### **Acknowledgments**

We greatly appreciate the financial support of the Croatian Science Foundation (grant numbers IP–2013–11–5596 and IP–2014–09–3386), University of Rijeka research grants 13.11.1.1.11. and 13.11.2.1.12., and the access to equipment in the possession of the University of Rijeka within the project RISK “Development of University of Rijeka campus laboratory research infrastructure”, financed by the European Regional Development Fund (ERDF). R.V. wishes to thank the Zagreb University Computing Centre (SRCE) for granting computational resources on the ISABELLA cluster and the CRO–NGI infrastructure.

### **Supplementary data**

Supplementary data associated with this article can be found, in the online version, at XXXX.

**References**

- [1] A. Jemal, R. Siegel, E. Ward, T. Murray, J. Xu, *Cancer Statistics, 2007*, *CA Cancer J. Clin.* 57 (2007) 43–66.
- [2] S. L. Zhu, Y. Wu, C. J. Liu, C. Y. Wei, J. C. Tao, H. M. Liu, Design and stereoselective synthesis of novel isosteviol-fused pyrazolines and pyrazoles as potential anticancer agents, *Eur. J. Med. Chem.* 65 (2013) 70–82.
- [3] (a) K. Nepali, S. Sharma, M. Sharma, P. M. S. Bedi, K. L. Dhar, Rational approaches, design strategies, structure activity relationship and mechanistic insights for anticancer hybrids, *Eur. J. Med. Chem.* 77 (2014) 422–487; (b) L. K. Gediya, V. C. Njar, Promise and challenges in drug discovery and development of hybrid anticancer drugs, *Expert Opinion on Drug Discovery*, 4 (2009) 1099–1111.
- [4] (a) A. Pałasz, D. Ciez, In search of uracil derivatives as bioactive agents. Uracils and fused uracils: Synthesis, biological activity and applications, *Eur. J. Med. Chem.* 97 (2015) 582–611; (b) M. S. Mohamed, M. M. Youns and N. M. Ahmed, Synthesis, antimicrobial, antioxidant activities of novel 6-aryl-5-cyano thiouracil derivatives, *Eur. J. Med. Chem.* 69 (2013) 591–600.
- [5] (a) C. K. Chu, D. C. Baker, *Nucleosides and Nucleotides as Antitumor and Antiviral Agents*, Plenum Press, New York, 1993; (b) J. P. Godefridus, *Deoxynucleoside Analogs in Cancer Therapy*, Humana Press, Totowa, 2006; (c) M. Ferrero and V. Gotor, Biocatalytic Selective Modifications of Conventional Nucleosides, Carbocyclic Nucleosides, and C-Nucleosides, *Chem. Rev.* 100 (2000) 4319–4348; (d) L. B. Townsend, *Chemistry of Nucleosides and Nucleotides*, Plenum Press, New York, 1994; (e) C. M. Galmarini, J. R. Mackey, C. Dumontet, Nucleoside analogues and nucleobases in cancer treatment, *Lancet Oncol.* 3 (2002) 415–424.
- [6] (a) A. Martin-Kohler, J. Widmer, G. Bold, T. Meyer, U. Sequin, P. Traxler, Furo[2,3-*d*]pyrimidines and Oxazolo[5,4-*d*]pyrimidines as inhibitors of receptor tyrosine kinases (RTK), *Helv. Chim. Acta*, 87 (2004) 956–975; (b) Y. H. Peng, H. Y. Shiao, C. H. Tu, P. M. Liu, J. T. A. Hsu, P. K. Amancha, J. S. Wu, M. S. Coumar, C. H. Chen, S. Y. Wang, W. H. Lin, H. Y. Sun, Y. S. Chao, P. C. Lyu, H. P. Hsieh, S. Y. Wu, Protein kinase inhibitor design by targeting the Asp-Phe-Gly (DFG) motif: The role of the DFG motif in the design of epidermal growth factor receptor inhibitors, *J. Med. Chem.* 56 (2013) 3889–3903; (c) L. Zhang, M. Xin, H. Shen, J. Wen, F. Tang, C. Tu, X. Zhao, P. Wei, Five-membered heteroaromatic ring fused-pyrimidine derivatives: Design, synthesis,

- and hedgehog signaling pathway inhibition study, *Bioorg. Med. Chem. Lett.* 24 (2014) 3486–3492; (d) H. Y. Shiao, M. S. Coumar, C. W. Chang, Y. Y. Ke, Y. H. Chi, C. Y. Chu, H. Y. Sun, C. H. Chen, W. H. Lin, K. S. Fung, P. C. Kuo, C. T. Huang, K. Y. Chang, C. T. Lu, J. T. Hsu, C. T. Chen, W. T. Jiaang, Y. S. Chao, H. P. Hsieh, Optimization of ligand and lipophilic efficiency to identify an in vivo active furanopyrimidine aurora kinase inhibitor, *J. Med. Chem.* 56 (2013) 5247–5360.
- [7] X. Jiao, D. J. Kopecky, J. Liu, J. Liu, J. C. Jaen, M. G. Cardozo, R. Sharma, N. Walker, H. Wesche, S. Li, E. Farrelly, S. H. Xiao, Z. Wang, F. Kayser, Synthesis and optimization of substituted furo[2,3-*d*]-pyrimidin-4-amines and 7H-pyrrolo[2,3-*d*]pyrimidin-4-amines as ACK1 inhibitors, *Bioorg. Med. Chem. Lett.* 22 (2012) 6212–6217.
- [8] A. Zhao, X. Gao, Y. Wang, J. Ai, Y. Wang, Y. Chen, M. Geng, A. Zhang, Discovery of novel c-Met kinase inhibitors bearing a thieno[2,3-*d*]pyrimidine or furo[2,3-*d*]pyrimidine scaffold, *Bioorg. Med. Chem.* 19 (2011) 3906–3918.
- [9] T. Gazivoda, M. Šokčević, M. Kralj, L. Šuman, K. Pavelić, E. De Clercq, G. Andre, R. Snoeck, J. Balzarini, M. Mintas, S. Raić-Malić, Synthesis and antiviral and cytostatic evaluations of the new C-5 substituted pyrimidine and furo[2,3-*d*]pyrimidine 4',5'-didehydro-L-ascorbic acid derivatives, *J. Med. Chem.* 50 (2007) 4105–4112.
- [10] A. Meščić, A. Harej, M. Klobučar, D. Glavač, M. Cetina, S. Kraljević Pavelić, S. Raić-Malić, Discovery of new acid ceramidase-targeted acyclic 5-alkynyl and 5-heteroaryl uracil nucleosides, *ACS Med. Chem. Lett.* 6 (2015) 1150–1155.
- [11] (a) B. Ogretmen, Y. A. Hannun, Biologically active sphingolipids in cancer pathogenesis and treatment *Nature Reviews Cancer*, 4 (2004) 604–616; (b) D. Pizzirani, C. Pagliuca, N. Realini, D. Branduardi, G. Bottegoni, M. Mor, F. Bertozzi, R. Scarpelli, D. Piomelli, T. Bandiera, Discovery of a New Class of Highly Potent Inhibitors of Acid Ceramidase: Synthesis and Structure–Activity Relationship (SAR), *J. Med. Chem.* 56 (2013) 3518–3530.
- [12] E. Bonhoure, A. Lauret, D. J. Barnes, C. Martin, B. Malavaud, T. Kohama, J. V. Melo, O. Cuvillier, Sphingosine kinase-1 is a downstream regulator of imatinib-induced apoptosis in chronic myeloid leukemia cells, *Leukemia*, 22 (2008) 971–979.
- [13] N. Realini, C. Solorzano, C. Pagliuca, D. Pizzirani, A. Armirotti, R. Luciani, M. P. Costi, T. Bandiera, D. Piomelli, Discovery of highly potent acid ceramidase inhibitors with in vitro tumor chemosensitizing activity, *Sci. Rep.* 3 (2013) 1035–1042.

- [14] (a) R. Chinchilla, C. Nájera, The Sonogashira reaction: A booming methodology in synthetic organic chemistry, *Chem. Rev.* 107 (2007) 874–922; (b) Z. Janeba, A. Holý, R. Pohl, R. Snoeck, G. Andrei, E. De Clercq, J. Balzarini, Synthesis and biological evaluation of acyclic nucleotide analogues with a furo[2,3-*d*]pyrimidin-2(3H)-one base, *Can. J. Chem.* 88 (2010) 628–638; (c) W. J. Ang, C. H. Tai, L.C. Lo, Y. Lam, Palladium-catalyzed annulation of internal alkynes in aqueous medium, *RSC Adv.* 4 (2014) 4921–4929; (d) L. Mahendar, A. G. K. Reddy, J. Krishn, G. Satyanarayana, [Cu]-Catalyzed domino Sonogashira coupling followed by intramolecular 5-exo-dig cyclization: Synthesis of 1,3-dihydro-2-benzofurans, *J. Org. Chem.* 79 (2014) 8566–8576.
- [15] (a) V. Aucagne, F. Amblard, A. Agrofoglio, Highly efficient AgNO<sub>3</sub>-catalyzed preparation of substituted furano-pyrimidine nucleosides, *Synlett.* (2004) 2406–2408; (b) A. Sniady, A. Durham, M. S. Morreale, A. Marcinek, S. Szafert, T. Lis, K. R. Brzezinska, T. Iwasaki, T. Ohshima, K. Mashima, R. Dembinski, Zinc-catalyzed cycloisomerizations. Synthesis of substituted furans and furopyrimidine nucleosides, *J. Org. Chem.* 73 (2008) 5881–5889.
- [16] N. Fresneau, M. A. Hiebel, L. A. Agrofoglio, S. Berteina Raboin, One-pot Sonogashira-cyclization protocol to obtain substituted furopyrimidine nucleosides in aqueous conditions, *Tetrahedron Lett.* 53 (2012) 1760–1763.
- [17] (a) S. Raić-Malić, A. Meščić, Recent trends in 1,2,3-Triazolo-nucleosides as promising anti-infective and anticancer agents, *Curr. Med. Chem.* 22 (2015) 1462–1499; (b) D. Saftić, R. Vianello, B. Žinić, 5-Triazolyluracils and their N1-sulfonyl derivatives: intriguing reactivity differences in the sulfonation of triazole N1'-substituted and N1'-unsubstituted uracil molecules, *Eur. J. Org. Chem.* 35 (2015) 7695–7704.
- [18] H. C. Kolb, K. B. Sharpless, The growing impact of click chemistry on drug discovery, *Drug Discov. Today*, 8 (2003) 1128–1137.
- [19] (a) J. Zhang, H. Zhang, W. X. Cai, L. P. Yu, X. C. Zhen, A. Zhang, 'Click' D<sub>1</sub> receptor agonists with a 5-HT<sub>1A</sub> receptor pharmacophore producing D<sub>2</sub> receptor activity, *Bioorg. Med. Chem.* 17 (2009) 4873–4880; (b) R. Jagasia, J. M. Holub, M. Bollinger, K. Kirshenbaum, M. G. Finn, Peptide cyclization and cyclodimerization by CuI-mediated azide–alkyne cycloaddition, *J. Org. Chem.* 74 (2009) 2964–2974; (c) D. Huber, H. Hubner, P. Gmeiner, 1,1'-disubstituted ferrocenes as molecular hinges in mono- and bivalent dopamine receptor ligands, *J. Med. Chem.* 52 (2009) 6860–6870.

- [20] I. E. Głowacka, J. Balzarini, A. E. Wróblewski, The synthesis, antiviral, cytostatic and cytotoxic evaluation of a new series of acyclonucleotide analogues with a 1,2,3-triazole linker, *Eur. J. Med. Chem.* 70 (2013) 703–722.
- [21] (a) A. Montagu, V. Roy, J. Balzarini, R. Snoeck, G. Andrei, L. A. Agrofoglio, Synthesis of new C5-(1-substituted-1,2,3-triazol-4 or 5-yl)-2'-deoxyuridines and their antiviral evaluation, *Eur. J. Med. Chem.* 46 (2011) 778–786; (b) Y. S. Lee, S. M. Park, H. M. Kim, S. K. Park, K. Lee, C. W. Lee, B. H. Kim, C5-Modified nucleosides exhibiting anticancer activity, *Bioorg. Med. Chem. Lett.* 19 (2009) 4688–4691; (c) S. M. Park, H. Yang, S. K. Park, H. M. Kim, B. H. Kim, Design, synthesis, and anticancer activities of novel perfluoroalkyltriazole-appended 2'-deoxyuridines, *Bioorg. Med. Chem. Lett.* 20 (2010) 5831–5834.
- [22] (a) J. L. Yu, Q. P. Wu, Q. S. Zhang, X. D. Xi, N. N. Liu, Y. Z. Li, Y. H. Liu, H. Q. Yin, Synthesis and antitumor activity of novel 2',3'-diethanethio-2',3',5'-trideoxy-5'-triazolonucleoside analogues, *Eur. J. Med. Chem.* 45 (2010) 3219–3222; (b) J. M. Kumar, M. M. Idris, G. Srinivas, P. V. Kumar, V. Meghah, M. Kavitha, C. V. Reddy, P. S. Mainkar, B. Pal, S. Chandrasekar, N. Nagesh, Phenyl 1,2,3-triazole-thymidine ligands stabilize G-Quadruplex DNA, inhibit DNA synthesis and potentially reduce tumor cell proliferation over 3'-azido deoxythymidine, *PLoS ONE*, 8 (2013) e70798.
- [23] H. Miyakoshi, S. Miyahara, T. Yokogawa, K. Endoh, T. Muto, W. Yano, T. Wakasa H. Ueno, K. T. Chong, J. Taguchi, M. Nomura, Y. Takao, A. Fujioka, A. Hashimoto, K. Itou, K. Yamamura, S. Shuto, H. Nagasawa, M. Fukuoka, Synthesis and discovery of *N*-carbonylpyrrolidine- or *N*-sulfonylpyrrolidine-containing uracil derivatives as potent human deoxyuridine triphosphatase inhibitors, *J. Med. Chem.* 55 (2012) 6427–6437.
- [24] (a) S. Maračić, T. Gazivoda Kraljević, H. Čipčić Paljetak, M. Perić, M. Matijašić, D. Verbanac, M. Cetina, S. Raić-Malić, 1,2,3-Triazole pharmacophore-based benzofused nitrogen/sulfur heterocycles with potential anti-*Moraxella catarrhalis* activity, *Bioorg. Med. Chem.* 23 (2015) 7448–7463; (b) S. Krištafor, A. Bistrović, J. Plavec, D. Makuc, T. Martinović, S. Kraljević Pavelić, S. Raić-Malić, One-pot click synthesis of 1,2,3-triazole-embedded unsaturated uracil derivatives and hybrids of 1,5- and 2,5-disubstituted tetrazoles and pyrimidines, *Tetrahedron Lett.* 56 (2015) 1222–1228; (c) S. Korunda, S. Krištafor, M. Cetina, S. Raić-Malić, Conjugates of 1,2,3-Triazoles and Acyclic Pyrimidine Nucleoside Analogues: Syntheses and X-ray crystallographic studies, *Curr. Org. Chem.* 17 (2013) 1114–1124.

- [25] A. S. Batsanov, J. C. Collings, I. J. S. Fairlamb, J. P. Holland, J. A. K. Howard, Z. Lin, T. B. Marder, A. C. Parsons, R. M. Ward, J. Zhu, Requirement for an oxidant in Pd/Cu Co-catalyzed terminal alkyne homocoupling to give symmetrical 1,4-disubstituted 1,3-diyne, *J. Org. Chem.* 70 (2005) 703–706.
- [26] (a) C. P. Johnston, A. Kothari, T. Sergeieva, S. I. Okovytyy, K. E. Jackson, R. S. Paton, M. D. Smith, Catalytic enantioselective synthesis of indanes by a cation-directed 5-endo-trig cyclization, *Nature Chemistry*, 7 (2015) 171–177; (b) W. Du, M. N. Zhao, Z. H. Ren, Y. Y. Wang, Z. H. Guan, Copper-catalyzed 5-endo-trig cyclization of ketoxime carboxylates: a facile synthesis of 2-arylpyrroles, *Chem. Commun.* 50 (2014) 7437–7439; (c) I. V. Alabugin, K. Gilmore, Finding the right path: Baldwin “Rules for Ring Closure” and stereoelectronic control of cyclizations, *Chem. Commun.* 49 (2013) 11246–11250.
- [27] (a) M. Kotora, T. Takahashi, *Handbook of Organopalladium Chemistry for Organic Synthesis*; eds. E. I. Negishi and A. de Meijere, Wiley-Interscience, New York, 2002, p. 973; (b) P. Siemsen, R. C. Livingston, F. Diederich, Acetylenic coupling: A powerful tool in molecular construction, *Angew. Chem., Int. Ed.* 39 (2000) 2632–2657.
- [28] (a) S. Kocaoba, F. Aydogan, H. Afsar, Potentiometric titration of some diamino compounds in toluene, *Reviews in Analytical Chemistry*, 27 (2008) 263–271; (b) S. Kocaoba, F. Aydogan, H. Afsar, No-aqueous titrations: potentiometric titration of some primary amines, *Reviews in Analytical Chemistry*, 27 (2008) 123–130.
- [29] F. H. Allen, The Cambridge Structural Database: a quarter of a million crystal structures and rising, *Acta Crystallogr. B* 58 (2002) 380–388.
- [30] (a) K. R. Patil, P. Mohapatra, H. M. Patel, S. N. Goyal, S. Ojha, C. N. Kundu, C. R. Patil, Pentacyclic triterpenoids inhibit IKK $\beta$  mediated activation of NF- $\kappa$ B pathway: in silico and in vitro evidences, *PLoS ONE*, 10 (2015) e0125709; (b) D. A. Filimonov, V. V. Poroikov, *Chemoinformatics Approaches to Virtual Screening*, eds. A. Varnek and A. Tropsha, RSC Publishing, Cambridge, UK, 2008, p. 182–216.
- [31] E. Weisberg, A. Nonami, Z. Chen, F. Liu, J. Zhang, M. Sattler, E. Nelson, K. Cowens, A. L. Christie, C. Mitsiades, K. K. Wong, Q. Liu, N. Gray, J. D. Griffin, Identification of Wee1 as a novel therapeutic target for mutant RAS-driven acute leukemia and other malignancies, *Leukemia*, 29 (2015) 27–37.
- [32] O. Hashimoto, M. Shinkawa, T. Torimura, T. Nakamura, K. Selvendiran, M. Sakamoto, H. Koga, T. Ueno, M. Sata, Cell cycle regulation by the Wee1 inhibitor PD0166285,

- pyrido [2,3-*d*] pyrimidine, in the B16 mouse melanoma cell line, *BMC Cancer*, 19 (2006) 292–303.
- [33] (a) S. Leijen, J. H. Schellens, G. Shapiro, A. C. Pavlick, R. Tibes, T. Demuth, J. Viscusi, J. D. Cheng, Y. Xu, A. M. Oza, A phase I pharmacological and pharmacodynamic study of MK-1775, a Wee1 tyrosine kinase inhibitor, in monotherapy and combination with gemcitabine, cisplatin, or carboplatin in patients with advanced solid tumors, *J. Clin. Oncol.* 28 (2010) 3067; (b) K. Do, D. Wilsker J. Ji, J. Zlott, T. Freshwater, R. J. Kinders, J. Collins, A. P. Chen, J. H. Doroshow, S. Kummar, Phase I study of single-agent AZD1775 (MK-1775), a Wee1 kinase inhibitor, in patients with refractory solid tumors, *J. Clin. Oncol.* 33 (2015) 3409–3415; (c) P. C. De Witt Hamer, S. E. Mir, D. Noske, C. J. Van Noorden, T. Würdinger, WEE1 kinase targeting combined with DNA-damaging cancer therapy catalyzes mitotic catastrophe, *Clin. Cancer. Res.* 17 (2011) 4200–4207.
- [34] B. D. Palmer, A. M. Thompson, R. J. Booth, E. M. Dobrusin, A. J. Kraker, H. H. Lee, E. A. Lunney, L. H. Mitchell, D. F. Ortwine, J. B. Smaill, L. M. Swan, W. A. Denny, 4-Phenylpyrrolo[3,4-*c*]carbazole-1,3(2*H*,6*H*)-dione inhibitors of the checkpoint kinase Wee1. Structure-activity relationships for chromophore modification and phenyl ring substitution, *J. Med. Chem.* 49 (2006) 4896–4911.
- [35] N. Kotelevets, D. Fabbro, A. Huwiler, U. Zangemeister-Wittke, Targeting sphingosine kinase 1 in carcinoma cells decreases proliferation and survival by compromising PKC activity and cytokinesis, *PLoS One*, 7 (2012) e39209.
- [36] O. Pastukhov, S. Schwalm, U. Zangemeister-Wittke, D. Fabbro, F. Bornancin, L. Japtok, B. Kleuser, J. Pfeilschifter, A. Huwiler, The ceramide kinase inhibitor NVP-231 inhibits breast and lung cancer cell proliferation by inducing M phase arrest and subsequent cell death, *Br. J. Pharmacol.* 171 (2014) 5829–5844.
- [37] T. Kogiso, H. Nagahara, E. Hashimoto, S. Ariizumi, M. Yamamoto, K. Shiratori, Efficient Induction of Apoptosis by Wee1 Kinase Inhibition in Hepatocellular Carcinoma Cells, *PLoS ONE*, 9 (2014) e100495.
- [38] D. E. Amacher, Drug-associated mitochondrial toxicity and its detection, *Curr. Med. Chem.* 12 (2005) 1829–1839.
- [39] L. D. Marroquin, J. Hynes, J. A. Dykens, J. D. Jamieson, Y. Will, Circumventing the Crabtree effect: replacing media glucose with galactose increases susceptibility of HepG2 cells to mitochondrial toxicants, *Toxicol Sci.* 97 (2007) 539–547.

- [40] Oxford Diffraction, Xcalibur CCD System. CrysAlisPro, Agilent Technologies, Abingdon, England, 2012.
- [41] M. C. Burla, R. Caliandro, M. Camalli, B. Carrozzini, G. L. Cascarano, L. De Caro, C. Giacovazzo, G. Polidori, R. Spagna, SIR2004: an improved tool for crystal structure determination and refinement, *J. Appl. Crystallogr.* 38 (2005) 381–388.
- [42] G. M. Sheldrick, Crystal structure refinement with SHELXL, *Acta Crystallogr.* C71 (2015) 3–8.
- [43] L. J. Farrugia, WinGX and ORTEP for Windows: an update, *J. Appl. Crystallogr.* 45 (2012) 849–854.
- [44] A. L. Spek, Structure validation in chemical crystallography, *Acta Crystallogr.* D65 (2009) 148–155.
- [45] C. F. Macrae, I. J. Bruno, J. A. Chisholm, P. R. Edgington, P. McCabe, E. Pidcock, L. Rodriguez-Monge, R. Taylor, J. van de Streek, P. A. Wood, Mercury CSD 2.0 – new features for the visualization and investigation of crystal structures, *J. Appl. Crystallogr.* 41 (2008) 466–470.
- [46] T. Gazivoda, S. Raić-Malić, V. Krištafor, D. Makuc, J. Plavec, S. Kraljević-Pavelić, K. Pavelić, L. Naesens, G. Andrei, R. Snoeck, J. Balzarini, M. Mintas, Synthesis, cytostatic and anti-HIV evaluations of the new unsaturated acyclic C-5 pyrimidine nucleoside analogues, *Bioorg. Med. Chem.* 16 (2008) 5624–5634.
- [47] D. Andrae, U. Häussermann, M. Dolg, H. Stoll, H. Preuss, Energy-adjusted ab initio pseudopotentials for the second and third row transition elements. *Theor. Chim. Acta*, 77 (1990) 123–141.
- [48] (a) L. Sikk, J. Tammiku-Taul, P. Burk, Computational study of copper-free sonogashira cross-coupling reaction, *Organometallics*, 30 (2011) 5656–5664; (b) M. García-Melchor, M. C. Pacheco, C. Nájera, A. Lledós, G. Ujaque, Mechanistic exploration of the Pd-catalyzed copper-free Sonogashira reaction, *ACS Catal.* 2 (2012) 135–144; (c) I. Picek, R. Vianello, P. Šket, J. Plavec, B. Foretić, Tandem  $\beta$ -elimination/hetero-Michael addition rearrangement of an *N*-alkylated pyridinium oxime to an *O*-alkylated pyridine oxime ether: an experimental and computational study, *J. Org. Chem.* 80 (2015) 2165–2170.
- [49] K. Fukui, The path of chemical reactions - the IRC approach *Acc. Chem. Res.* 14 (1981) 363–368.

- [50] M. J. Frisch, G. W. Trucks, H. B. Schlegel, G. E. Scuseria, M. A. Robb, J. R. Cheeseman, G. Scalmani, V. Barone, B. Mennucci, G. A. Petersson, H. Nakatsuji, M. Caricato, X. Li, H. P. Hratchian, A. F. Izmaylov, J. Bloino, G. Zheng, J. L. Sonnenberg, M. Hada, M. Ehara, K. Toyota, R. Fukuda, J. Hasegawa, M. Ishida, T. Nakajima, Y. Honda, O. Kitao, H. Nakai, T. Vreven, J. A. Montgomery, Jr., J. E. Peralta, F. Ogliaro, M. Bearpark, J. J. Heyd, E. Brothers, K. N. Kudin, V. N. Staroverov, R. Kobayashi, J. Normand, K. Raghavachari, A. Rendell, J. C. Burant, S. S. Iyengar, J. Tomasi, M. Cossi, N. Rega, J. M. Millam, M. Klene, J. E. Knox, J. B. Cross, V. Bakken, C. Adamo, J. Jaramillo, R. Gomperts, R. E. Stratmann, O. Yazyev, A. J. Austin, R. Cammi, C. Pomelli, J. W. Ochterski, R. L. Martin, K. Morokuma, V. G. Zakrzewski, G. A. Voth, P. Salvador, J. J. Dannenberg, S. Dapprich, A. D. Daniels, Ö. Farkas, J. B. Foresman, J. V. Ortiz, J. Cioslowski, D. J. Fox, GAUSSIAN 09 (Revision A.02), Gaussian Inc., Wallingford CT, 2009.

**Figure captions**

**Fig. 1.** Structure and atom numbering of relevant molecules studied computationally.

**Fig. 2.** Free energy profile for the Cu(I)-catalyzed cyclization of 5-alkylethynyl uracils towards 6-substituted furo[2,3-*d*]pyrimidine-2-ones.

**Fig. 3.** Free energy profile for the formation of the 5-alkylethynyl-6-alkyl-furo[2,3-*d*]pyrimidine-2-ones initiated by the carbon-carbon bond formation.

**Fig. 4.** (a) Molecular structure of **34a**, with the atom-numbering scheme. Displacement ellipsoids for non-hydrogen atoms are drawn at the 30% probability level. (b) A part of the crystal structure of **34a**, showing C-H...O and C-H...N intermolecular hydrogen bonds. Only major component of disordered atoms is presented in both figures.

**Fig. 5.** Western blot analysis of predicted protein targets of **5-7**. a) Representative Western blots are shown detecting the cellular levels of phospho-Wee1 kinase, phospho-Sphingosine kinase 1 (SK1) and acid ceramidase (ASAH) before and after treatment of HepG2 and HeLa cells with indicated compounds at their 2 x IC<sub>50</sub> values for 48 h. Approximate molecular weights (kDa) are indicated. b) Relative protein expressions, as determined by densitometric analysis of protein bands and normalized to the alpha tubulin loading control. Two independent experiments were performed with similar results. Data are presented as mean values ± SD.

**Fig. 6.** Detection of apoptosis induced by **7** in HepG2 cells using Annexin V-FITC assay. Cells were visualized by fluorescence microscope at 40x magnification before and after treatment with 2 x IC<sub>50</sub> value of **7** for 48 h. PI staining was used as a nuclear marker. Shown here are bright-field images (upper left micrographs), early apoptotic cells (PI-/Ann V+, upper right micrographs), secondary necrotic cells (PI+, lower left micrographs) and late apoptotic/primary necrotic cells (PI+/Ann V+, lower right micrographs).

**Research highlights**

- Pd/Cu-catalyzed reactions gave furo[2,3-*d*]pyrimidine-2-one-1,2,3-triazole hybrids
- Tandem terminal alkyne dimerization and 5-*endo*-trig cyclization afforded **24a–37a**
- Precise reaction mechanisms were elucidated by the DFT computational analysis
- Compound **7** did not show mitochondrial toxicity *in vitro*
- **7** in Hep-G2 cells inhibited Wee-1 kinase and abolished sphingolipid signaling